FINAL REPORT

U.F. Project No: 00110686
FDOT Project No: BDV31-977-11

INTERNALLY CURED CONCRETE FOR PAVEMENT AND BRIDGE DECK APPLICATIONS

Mang Tia
Thanachart Subgranon
Kukjoo Kim
Andrea Medina Rodriguez
Abdullah Algazlan

July 2015

Department of Civil and Coastal Engineering
Engineering School of Sustainable Infrastructure and Environment
College of Engineering
University of Florida
Gainesville, Florida 32611-6580

DISCLAIMER

The opinions, findings, and conclusions expressed in this publication are those of the authors and not necessarily those of the State of Florida Department of Transportation or the U.S. Department of Transportation.

Prepared in cooperation with the State of Florida Department of Transportation and the U.S. Department of Transportation.

SI (MODERN METRIC) CONVERSION FACTORS (from FHWA)

APPROXIMATE CONVERSIONS TO SI UNITS

SYMBOL	WHEN YOU KNOW	MULTIPLY BY	TO FIND	SYMBOL
LENGTH				
in	inches	25.4	millimeters	mm
ft	feet	0.305	meters	m
yd	yards	0.914	meters	m
mi	miles	1.61	kilometers	km

SYMBOL	WHEN YOU KNOW	MULTIPLY BY	TO FIND	SYMBOL
AREA				
in^2	square inches	645.2	square millimeters	mm^2
ft^2	square feet	0.093	square meters	m^2
yd^2	square yard	0.836	square meters	m^2
ac	acres	0.405	hectares	ha
mi^2	square miles	2.59	square kilometers	km^2

SYMBOL	WHEN YOU KNOW	MULTIPLY BY	TO FIND	SYMBOL
VOLUME				
fl oz	fluid ounces	29.57	milliliters	mL
gal	gallons	3.785	liters	L
ft^3	cubic feet	0.028	cubic meters	m^3
yd^3	cubic yards	0.765	cubic meters	m^3
NOTE: volumes greater than 1000 L shall be shown in m^3				

SYMBOL	WHEN YOU KNOW	MULTIPLY BY	TO FIND	SYMBOL
MASS				
oz	ounces	28.35	grams	g
lb	pounds	0.454	kilograms	kg
T	short tons (2000 lb)	0.907	megagrams (or "metric ton")	Mg (or "t")

SYMBOL	WHEN YOU KNOW	MULTIPLY BY	TO FIND	SYMBOL
TEMPERATURE (exact degrees)				
ºF	Fahrenheit	5 (F-32)/9 or (F-32)/1.8	Celsius	ºC

SYMBOL	WHEN YOU KNOW	MULTIPLY BY	TO FIND	SYMBOL
ILLUMINATION				
fc	foot-candles	10.76	lux	lx
fl	foot-Lamberts	3.426	candela/m^2	cd/m^2

SYMBOL	WHEN YOU KNOW	MULTIPLY BY	TO FIND	SYMBOL
FORCE and PRESSURE or STRESS				
lbf	poundforce	4.45	newtons	N
kip	kilo poundforce	4.45	kilo newtons	kN
lbf/in^2	poundforce per square inch	6.89	kilopascals	kPa

APPROXIMATE CONVERSIONS TO SI UNITS

SYMBOL	WHEN YOU KNOW	MULTIPLY BY	TO FIND	SYMBOL
LENGTH				
mm	millimeters	0.039	inches	in
m	meters	3.28	feet	ft
m	meters	1.09	yards	yd
km	kilometers	0.621	miles	mi

SYMBOL	WHEN YOU KNOW	MULTIPLY BY	TO FIND	SYMBOL
AREA				
mm^2	square millimeters	0.0016	square inches	in^2
m^2	square meters	10.764	square feet	ft^2
m^2	square meters	1.195	square yards	yd^2
ha	hectares	2.47	acres	ac
km^2	square kilometers	0.386	square miles	mi^2

SYMBOL	WHEN YOU KNOW	MULTIPLY BY	TO FIND	SYMBOL
VOLUME				
mL	milliliters	0.034	fluid ounces	fl oz
L	liters	0.264	gallons	gal
m^3	cubic meters	35.314	cubic feet	ft^3
m^3	cubic meters	1.307	cubic yards	yd^3

SYMBOL	WHEN YOU KNOW	MULTIPLY BY	TO FIND	SYMBOL
MASS				
g	grams	0.035	ounces	oz
kg	kilograms	2.202	pounds	lb
Mg (or "t")	megagrams (or "metric ton")	1.103	short tons (2000 lb)	T

SYMBOL	WHEN YOU KNOW	MULTIPLY BY	TO FIND	SYMBOL
TEMPERATURE (exact degrees)				
ºC	Celsius	1.8C+32	Fahrenheit	ºF

SYMBOL	WHEN YOU KNOW	MULTIPLY BY	TO FIND	SYMBOL
ILLUMINATION				
lx	lux	0.0929	foot-candles	fc
cd/m^2	candela/m^2	0.2919	foot-Lamberts	fl

SYMBOL	WHEN YOU KNOW	MULTIPLY BY	TO FIND	SYMBOL
FORCE and PRESSURE or STRESS				
N	newtons	0.225	poundforce	lbf
kPa	kilopascals	0.145	poundforce per square inch	lbf/in^2

*SI is the symbol for International System of Units. Appropriate rounding should be made to comply with Section 4 of ASTM E380.
(Revised March 2003)

TECHNICAL REPORT DOCUMENTATION PAGE

1. Report No.	2. Government Accession No.	3. Recipient's Catalog No.

4. Title and Subtitle	5. Report Date
Internally Cured Concrete for Pavement and Bridge Deck Applications	July 2015
	6. Performing Organization Code
7. Author(s)	8. Performing Organization Report No.
Mang Tia, Thanachart Subgranon, Kukjoo Kim, Andrea Medina Rodriguez, Abdullah Algazlan	00110686
9. Performing Organization Name and Address	10. Work Unit No. (TRAIS)
Department of Civil and Coastal Engineering Engineering School of Sustainable Infrastructure & Environment University of Florida 365 Weil Hall – P.O. Box 116580 Gainesville, FL 32611-6580	
	11. Contract or Grant No.
	BDV31-977-11
12. Sponsoring Agency Name and Address	13. Type of Report and Period Covered
Florida Department of Transportation 605 Suwannee Street, MS 30 Tallahassee, FL 32399	Final Report 01/7/14 – 7/31/15
	14. Sponsoring Agency Code

15. Supplementary Notes

Prepared in cooperation with the U.S. Department of Transportation and the Federal Highway Administration

16. Abstract

A laboratory and field testing program was conducted to evaluate the performance and usability of internally cured concrete (ICC) using lightweight aggregates for bridge decks and concrete pavement slabs under Florida conditions. The laboratory testing program evaluated three standard mixes (SM) and three corresponding ICC mixes with the same water-cementitious (w/c) ratios and cementitious materials contents. The ICC mixes were produced by replacing a part of the fine aggregate with a pre-wetted lightweight aggregate (LWA). The quantity of LWA used was an amount that would supply 7 lb of absorbed water per 100 lb of cementitious materials used. The amounts of water-reducing admixtures needed for the ICC mixes to achieve the same workability of the fresh concrete were less than those for the standard mixes with the same w/c ratios. The compressive strength, flexural strength, elastic modulus, splitting tensile strength, and coefficient of thermal expansion of the ICC mixes were lower than those of the standard mixes with the same w/c ratio. The ICC mixes showed substantially greater resistance to shrinkage cracking than the standard mixes as observed from the results of the restrained shrinkage ring test.

Two ICC test slabs and one SM test slab were constructed to evaluate the performance of ICC in pavement slabs. The results of the critical stress analysis showed that at a critical loading condition, the computed stress-to-strength ratios for the ICC slabs were lower than that for the SM slab. Visual inspection of the SM slab after heavy vehicle simulator (HVS) loading showed that some hairline cracks could be seen next to the wheel path. These hairline cracks could be caused when micro shrinkage cracks developed into hairline cracks after the slab was loaded repetitively by the HVS wheel load. No visible cracks were observed from the two ICC test slabs.

Based on the results of the critical stress analysis and the visual inspection of the three test slabs, the ICC test slabs appeared to have better performance than the standard-mix slab. A field testing program to further assess the performance and benefits of ICC mixes in bridge deck and pavement applications is recommended.

17. Key Words	18. Distribution Statement
Internally Cured Concrete, Lightweight Aggregate, Bridge Deck, Pavement Slab, Coefficient of Thermal Expansion, Modulus of Elasticity, Shrinkage Cracking, Restraint Ring Test, Heavy Vehicle Simulator, Critical Stress Analysis, Stress-to-Strength Ratio	No restrictions.

19. Security Classif. (of this report)	20. Security Classif. (of this page)	21. No. of Pages	22. Price
Unclassified	Unclassified	175	

Form DOT F 1700.7 (8-72) Reproduction of completed page authorized

ACKNOWLEDGMENTS

A compilation of this nature could not have been completed without the help and support of others. The Florida Department of Transportation (FDOT) is gratefully acknowledged for providing the financial support for this study. The FDOT Materials Office provided the additional testing equipment, materials, and personnel needed for this investigation. Sincere thanks and appreciation are extended to the project manager, Mr. Michael Bergin, for providing his technical coordination and expert advice throughout the project. Sincere gratitude is extended to Harvey DeFord, Richard DeLorenzo, Patrick Carlton, Thomas Frank, and Patrick Gallagher of the FDOT Materials Office for their invaluable expert advice and help on this project. Sincere thanks is also extended to Big River Industry Inc. for providing lightweight aggregate for this project.

EXECUTIVE SUMMARY

Background and Objective of Study

In recent years, high-strength-high-performance concrete has been used in rapid repair of concrete bridge decks and concrete pavement. This type of concrete usually comes with very high early-shrinkage which in turn can cause shrinkage cracking. The concrete also generates more heat, which naturally tends to cause more cracking. These early cracks are one of the primary causes of the concrete structure's deficiencies or even failures.

The Florida Department of Transportation (FDOT) acknowledges this problem and tries to find a solution to the problem. Internally cured concrete (ICC) is one way to mitigate this problem. By incorporating pre-wetted lightweight aggregates (LWAs) into a normal concrete, they help to reduce the cracking tendency of the concrete at the early age. The key to this effect is that LWA is a very porous material. When saturated, each LWA particle acts like a small reservoir inside the concrete, which will give out water to the surrounding cement paste during its hydrating period. This mechanism helps to reduce the self-desiccation phenomenon and promotes hydration of the cement in the concrete. ICC could produce a bridge deck or pavement with increased service life and reduced life cycle cost. In order to be able to use ICC in bridge decks and concrete pavements in Florida effectively, there was a great need to study the performance and usability of ICC in these applications under Florida conditions.

To address this need, a laboratory and field testing program was conducted to evaluate the performance and usability of ICC using lightweight aggregates for bridge decks and concrete pavement slabs under Florida conditions.

Findings from Laboratory Testing Program

A laboratory testing program was conducted to evaluate the properties of three standard concrete mixes and three corresponding ICC mixes with the same water-cementitious (w/c)

ratios and cementitious materials contents. These three sets of concrete mixes met the requirements for Florida Class II (Bridge Deck), IV, and V concretes, had w/c ratios of 0.40, 0.36, and 0.32, and had total cementitious materials contents of 687, 780, and 860 lb/yd^3, respectively. The cementitious materials consisted of 80% Type I/II Portland cement and 20% Class F fly ash. The ICC mixes were produced by replacing a part of the fine aggregate with a pre-wetted LWA. The quantity of LWA used was an amount that would supply 7 lb of absorbed water per 100 lb of cementitious materials used. The LWA used was a manufactured expanded clay with a dry bulk specific gravity of 1.23 and water absorption of 25.2%.

The main findings from the laboratory testing program can be summarized as follows:

(1) The amounts of water-reducing admixture needed for the ICC mixes to achieve the same workability of the fresh concrete are less than the amounts for the standard mixes with the same w/c ratios.

(2) The average compressive strength of the ICC mixes was lower than that of the standard mixes with the same w/c ratio by about 11%.

(3) The average flexural strength of the ICC mixes was lower than that of the standard mixes with the same w/c ratio by about 6%.

(4) The average elastic modulus of the ICC mixes was lower than that of the standard mixes with the same w/c ratio by about 18%.

(5) The splitting tensile strength of the ICC mixes was lower than that of the standard mixes with the same w/c ratio by about 10%.

(6) The ICC mixes showed substantially greater resistance to shrinkage cracking than the standard mixes. The average cracking age of all ICC mixes, as measured by the restrained shrinkage ring test, was 2.7 times that of the standard mixes.

(7) The average drying shrinkage of the ICC mixes was higher than that of the standard mixes by about 24%.

(8) The average coefficient of thermal expansion of the ICC mixes was lower than that of the standard mixes with the same w/c ratios by about 10%.

Findings from Evaluation of Test Slabs

Three test slabs were constructed to evaluate the performance of ICC in pavement slabs. They were constructed respectively with (1) a standard mixture with 0.40 w/c ratio, (2) an ICC mixture with 0.40 w/c ratio, and (3) an ICC mixture with 0.32 w/c ratio. Samples of the concrete used were collected and evaluated for their fresh concrete properties and hardened concrete properties. The falling weight deflectometer (FWD) tests were performed on the test slabs to characterize their structural behavior. Repetitive wheel loads by the heavy vehicle simulator (HVS) were applied to the test slabs to evaluate their structural performance and to measure the load-induced strains in the concrete slabs.

Using the measured properties of the hardened concrete, the measured FWD deflections, and the measured HVS load-induced strains, 3-D finite element models were developed and calibrated for the test slabs. The calibrated models were then used to calculate the maximum stresses in these test slabs under the critical temperature-load condition when a 22-kip axle load was applied to the mid-edge of the pavement slab with a temperature differential of +20 °F. The maximum computed stresses for the test slab were then divided by the flexural strength of the respective concrete to determine the stress-to-strength ratios, which were used to evaluate the potential performance of the test slabs.

The results of the critical stress analysis showed that, at this critical loading condition, the computed stress-to-strength ratios for the ICC slab with 0.40 w/c ratio and the ICC slab with 0.32

w/c ratio were 0.55 and 0.60, respectively, as compared with a stress-to-strength ratio of 0.62 for the standard-mix slab.

The flexural strength of the sampled ICC with 0.32 w/c ratio was noted to be much lower than a similar ICC with the same w/c ratio in the laboratory study. When the flexural strength from the laboratory study was used to compute the stress-to-strength ratio for this ICC slab, the stress-to-strength ratio was reduced to 0.48, which is substantially lower than that for the standard-mix slab.

Visual inspection of the standard-mix slab after HVS loading and at three months after placement showed that some hairline cracks could be seen next to the wheel path. These hairline cracks could be caused when micro shrinkage cracks developed into hairline cracks after the slab was loaded repetitively by the HVS wheel load. No visible crack was observed from the two ICC test slabs. From the visual observation of these three test slabs, the ICC slabs appeared to have better performance than the standard-mix slab.

Based on the results of the critical stress analysis and the visual inspection of the three test slabs, the ICC test slabs appeared to have better performance than the standard-mix slab.

Recommended Field Implementation Plan

Based on the results from the laboratory testing program and the evaluation of the ICC test slabs, it is recommended that a field testing program be implemented to further assess the performance and benefits of ICC mixes in bridge deck and pavement applications. It is recommended that three sets of experimental bridge decks and three sets of pavement test slabs be constructed for evaluation. The recommended plans for concrete mix designs, quality control, instrumentation, monitoring, and evaluation of these experimental bridge decks and pavement test slabs are presented in Chapter 6 of this report.

TABLE OF CONTENTS

page

LIST OF TABLES

LIST OF FIGURES

CHAPTER 1
INTRODUCTION

1.1 Background

In recent years, high-strength-high-performance concrete has been used in rapid repair of concrete bridge decks and concrete pavement. This type of concrete usually comes with very high early chemical shrinkage -- called "self-desiccation" -- which in turn can cause shrinkage cracking. The concrete also generates more heat, which naturally tends to cause more cracking. These early cracks are one of the primary causes of the concrete structure's deficiencies or even failures.

The Florida Department of Transportation (FDOT) acknowledges this problem and tries to find a solution to the problem. Internally cured concrete (ICC) is one way to mitigate this problem. By incorporating lightweight aggregates (LWAs) into a normal concrete, they help to reduce the cracking tendency of the concrete at the early age. The key to this effect is that LWA is a very porous material. When saturated, each LWA particle acts like a small reservoir inside the concrete, which will give out water to the surrounding cement paste during its hydrating period. This mechanism helps to reduce the self-desiccation phenomenon and promotes hydration of the cement in the concrete. In some instances, the ICC has a higher strength and lower elastic modulus than a conventional concrete, which makes the concrete even more resistant to cracking at its later age.

As generally accepted, when there is less cracking in the concrete, the concrete structure would last longer. Therefore, from the economic standpoint, ICC could produce a bridge deck or pavement with increased service life and reduced life cycle cost. In order to be able to use ICC in bridge decks and concrete pavements in Florida effectively, there was a great need to study the performance and usability of ICC in these applications under Florida conditions.

1.2 Objectives

The main purpose of this study was to conduct a laboratory and field testing program to evaluate performance and usability of internally cured concrete using lightweight aggregates for bridge decks and concrete pavement slabs under Florida conditions.

1.3 Scope of Study

The study objective was accomplished through the conductance of five main tasks which are presented in Chapters 2 through 6 of this report. Chapter 2 presents a literature review on the properties of ICC and special tests for evaluation of ICC mixtures as reported by other researchers. Chapter 3 presents the development of the experimental design for the laboratory study of ICC mixtures which are applicable to Florida conditions. Chapter 4 presents the performance of the laboratory testing program and analysis of results. Based on the results of the laboratory testing program, three full-size pavement slabs were constructed and tested by the heavy vehicle simulator (HVS) at the FDOT accelerated pavement testing (APT) facility. This work is presented in Chapter 5. Based on the results from the laboratory testing program and the APT evaluation of the ICC test slabs, recommendations were made to implement a field testing program to further assess the performance and benefits of ICC mixes in bridge deck and pavement applications. The recommended field implementation plan is presented in Chapter 6. Finally, the summary of findings and recommendations from this study are presented in Chapter 7.

CHAPTER 2
LITERATURE REVIEW

2.1 Properties of Internally Cured Concrete

2.1.1 Plastic Shrinkage

Plastic shrinkage occurs after the concrete is placed, while it is still in a plastic state, and before it develops any strength. It occurs when plastic concrete loses its moisture by evaporation of water through the surface or by means of absorption of water by aggregates or sub-base. A high rate of evaporation during concrete placement usually leads to cracking in concrete, allowing aggressive particles to attack the concrete and diminishing its service life. In concrete pavements, the area exposed to the environment is larger than other structures; consequently, the larger area of the slab is exposed to sun and wind, leading to plastic shrinkage [Mindess et al., 2002].

After placement, cement and aggregate particles tend to settle and the water moves up to the surface. The bleeding water is the thin layer of water that is created by the movement of the water to the top and it evaporates at a constant rate because the concrete is exposed to the environment. This period is known as the drying period. In this phase, the concrete settles on the surface and the system consolidates. Then, the falling period is reached when the reduction in the accessible water causes the rate of evaporation to slow down. Plastic shrinkage can occur when the water is driven off and the concrete reaches the falling rate period, causing capillary stresses [Lura, Pease, Mazzotta, Rajabipour, & Weiss, 2007].

Researchers Henkensiefken, Briatka, Bentz, Nantung, and Weiss conducted a study to evaluate concretes with different percentages of LWA replacement, ranging from 0% to 18% of LWA. The data showed that, in mixtures containing 18% of LWA replacement, there was a significant reduction in potential cracking and the width of the cracks generated by plastic

shrinkage were relatively smaller. Meanwhile, the standard mix with 0% LWA showed earlier shrinkage and larger crack widths. The results indicate that the presence of a high percentage of LWA replacement could improve plastic shrinkage [Henkensiefken, Briatka, Bentz, Nantung, & Weiss, 2010].

When LWA is used, the water stored in the LWA pores can be transferred into the cement paste. The cement paste maintains its saturation, the capillary stresses are reduced, and subsequently plastic shrinkage is reduced too. It can be deduced that plastic shrinkage cracking may decrease or be eradicated if the right amount of LWA is used in the concrete [Henkensiefken et al., 2010]. LWA is beneficial to reducing shrinkage cracking, but it is also necessary to understand that any water consumed during shrinkage will not be available later to reduce autogenous and/or drying shrinkage [Bentz & Weiss, 2011].

2.1.2 Autogenous Shrinkage

Autogenous shrinkage occurs inside the concrete paste and without any loss of water from evaporation. The loss of volume is caused by a chemical reaction between water and cement, called hydration. Hydration involves several chemical reactions. For this reason, this phenomenon is also known as self-desiccation shrinkage or chemical shrinkage [Kosmatka, Kerkhoff & Panarese, 2003].

Autogenous shrinkage could be evaluated through its several phases. The first phase is known as the liquid phase, where contraction is caused by a chemical reaction which generates products with less volume. Then, skeleton-formation phase is reached when the paste starts to have some stiffness. Stresses are generated from the restraint movement of the rigid skeleton when the paste shrinks. Finally, the hardening phase autogenous shrinkage is induced by self-desiccation. This phase is usually not evaluated because the high availability of humidity makes

the effects of self-desiccation on the autogenous shrinkage insignificant [Ji, Zhang, Zhuang, & Wu, 2015].

To evaluate autogenous deformation in pastes and mortars, a corrugated polymeric tube is often used. The deformation of a sample is measured and the expansion or shrinkage is calculated [Pease, Hossain, & Weiss, 2004]. Previous research studies evaluated internal curing using mortars with blended cement, w/cm of 0.35, and LWA [8% and 20% replacement]. The results showed a significant reduction in the autogenous shrinkage with a replacement level of 8% of LWA, and an almost complete elimination of autogenous shrinkage with 20% substitution of LWA [Geiker, Bentz, and Jensen, LWA 2004].

Recent studies to evaluate autogenous shrinkage used an equation that estimates the water supply in the internal reservoirs to obtain the water required to pre-wet the LWA. This equation can provide a good approximation of the amount of LWA dosage. Different levels of replacements values were used; these values were higher, lower, and equal to the value obtained from the equation. The results confirmed that higher percentages of LWA led to high internal relative humidity and reductions in cracking damage [Henkensiefken et al., 2009]. However, different factors can affect the correct dosage of LWA. For example, it was found that during the mixing process, hauling, and placement, there were partial losses of internal curing water; rate of loss of internal water depends on the grade of desorption; the water of internal curing was lost by excessive evaporation and drying; pozzolanic reactions between supplementary cementitious materials and calcium hydroxide were responsible for the autogenous contraction [Schlitter, Senter, Bentz, Nantung, and Weiss., 2010].

2.1.3 Drying Shrinkage

Concrete uses more water than just the water necessary to hydrate the paste. This is known as the water of convenience, which eventually evaporates, generating changes in the

volume of concrete. Drying shrinkage consequently involves the movement and loss of water within the pores in the hydrated paste and from within the structure of the gel hydration products, changing concrete volume [Kosmatka, Kerkhoff, and Panarese, 2003].

Drying shrinkage is similar to plastic shrinkage, but it happens after the concrete has hardened. At this time, the concrete skeletons are no longer allowed to collapse because the hydrated cement paste has already constructed a rigid structure. The result is not settlement of the concrete body, instead, predominant shrinkage in the longer direction will occur. The shrinking is most severe at an early age of concrete, especially in the first seven days. Drying shrinkage is recognized for high loss of free moisture that should have been used in the hydration activity. This problem is mainly caused by insufficient curing of concrete, so the best method to prevent this type of shrinkage is to have adequate curing. Internal curing concrete can assist to prevent drying shrinkage in concrete [Mehta & Monteiro, 2013].

Drying shrinkage is affected by internal curing, and prismatic mortar specimens were used to evaluate this property. The results show that there were reductions in drying shrinkage when high percentages of LWA replacement were used; meanwhile, low replacements did not have a large influence on the reduction of drying shrinkage. These results can be explained by the fact that water in LWA pores maintained saturation in the concrete thereby reducing plastic, autogenous, and/or drying shrinkage. Water is drawn from the LWA larger pores, causing less capillary stress, which also lessens both the measured strain and the propensity for early-age cracking [Bentz & Weiss, 2011].

2.1.4 Degree of Hydration and Isothermal Calorimetry

ASTM C1702, "Standard test method for measuring heat of hydration of hydraulic cementitious materials using isothermal conduction calorimetry" [ASTM International, 2014] uses isothermal calorimetry to evaluate the heat hydration of cementitious materials. For LWA,

this test is principally used to determine if water inside the internal curing reservoirs increases the degree of hydration of cement binder principally at later ages. Figure 2-1 shows a study conducted to evaluate the degree of hydration of three different samples using 0%, 50%, and 100% LWA replacements. This study also used ASTM C1702 to evaluate the mix design and obtained an increase in heat of hydration of the LWA mixes, as compared with the standard mix [Bentz & Weiss, 2011].

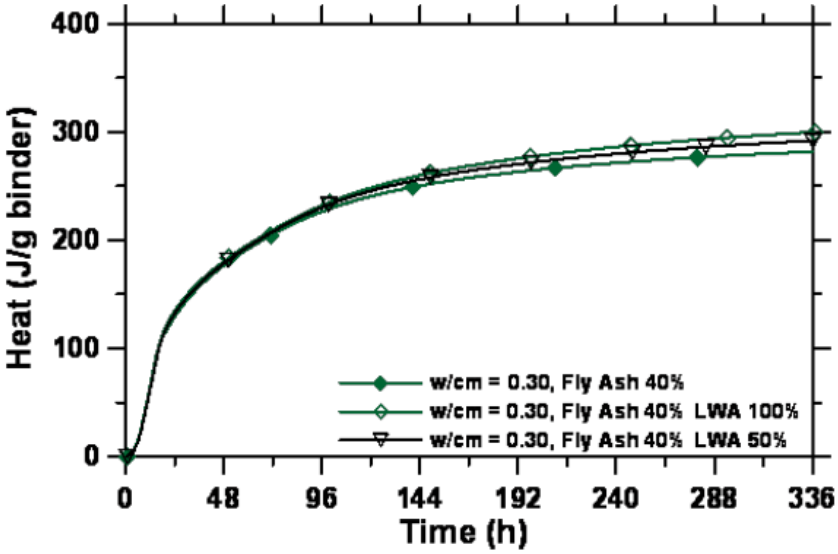

Figure 2-1. Effect of changing internal curing LWA replacement level on measured cumulative heat release for a blended cement/fly ash mortar [Bentz & Weiss, 2011]

Another test that can evaluate increases of heat of hydration is the loss-on-ignition (LOI) test. Figure 2-2 shows how the use of internal curing concrete has higher degrees of hydration than the control sample, even at early ages; the results were obtained using the calorimetry method. Likewise, the results from a test conducted using poor curing conditions validated the hypothesis that internal curing tends to increase the hydration. The concrete using LWA exhibited an increase in the degree of hydration as compared with concretes without LWA [Espinoza-Hijazin & Lopez, 2010].

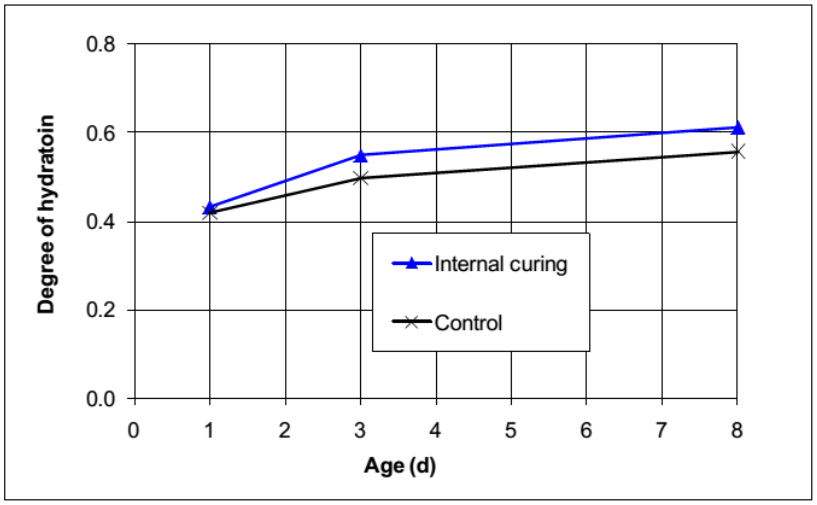

Figure 2-2. Measured degree of hydration for mortars with and without internal

2.1.5 Strength and Elastic Modulus

Internal curing could produce a better performance in strength and elastic modulus which is caused by an increase in the hydration degree of the cement paste. The interfacial bonds between cement gel and aggregates are strengthened by the increased hydration activities. This should help improve strength characteristics of the concrete, whether it is compressive, tensile, or flexural strength. However, the concrete's strength could be reduced because the curing agents of LWA are weaker when compared with the normal-weight aggregate that it is replacing. The internal curing is influenced by the mixture proportions, curing conditions, and testing age that generate an effect on compressive strength and modulus of elasticity. Internal curing could produce a decrease in a concrete's early strength and also an increase in its ultimate strength, and if supplementary cementitious materials are used, this ultimate strength will show even better performance [Bentz & Weiss, 2011].

Elastic modulus is an important property of concrete, usually overlooked by the concrete designer. Performance of concrete is mostly and traditionally imposed by the concrete strength. However, only analyzing the strength of the concrete cannot fully describe the quality of a

concrete. Weiss et al established that a reduced modulus of elasticity can reduce the potential cracking of the concrete. Having a lower modulus of elasticity, a concrete can be considered more flexible than one with a greater modulus. Therefore, less rigidity of the mixture can provide better performance, reducing early age cracking that is caused by thermal displacement, autogenous shrinkage, drying shrinkage, and restrained shrinkage. [Weiss et al, 1999].

Concrete's elastic modulus is affected by the elastic moduli of its constituents. Lightweight aggregates usually have lower elastic modulus than the typical aggregates. As a consequence, the LWA concrete has a lower elastic modulus as compared with a mixture made with conventional aggregates. The elastic modulus of concrete containing LWA at an early-age shows lower values than normal concrete, and the influence of LWA is smaller when compared to the influence on compressive strength. The lower values of elastic modulus are related to a reduction in potential cracking because the residual stresses are reduced [Bentz & Weiss, 2011]. Byard and Schindler characterized the modulus of elasticity of different mixtures and established that the reduced stiffness of lightweight aggregate can reduce the modulus of elasticity of the concrete when LWA were incorporated in the concrete [Byard & Schindler 2010].

2.1.6 Creep

The loss of adsorbed water in hardened cement paste, due to sustained load, is the primary cause of creep strain. A longer duration and a greater magnitude of the load would cause a higher creep strain. In a restrained structure, creep strain of concrete can relieve stresses that arise. This stress relaxation phenomenon helps in the reduction of potential of cracking in concrete [Kosmatka, Kerkhoff & Panarese, 2003]. Mehta & Monteiro also said that there is a relationship between creep strain and interfacial bonds of hydrated cement gel and the aggregates, especially at stress levels greater than 30 to 40 percent of the ultimate stress. This

implies that ICC would produce creep magnitude differently from the traditional concrete [Mehta & Monteiro, 2013].

Creep has not been studied thoroughly in LWA concrete, but some research shows that a pre-wetted LWA concrete shows less creep than normal concrete, and dry LWA concrete exhibits higher creep than the control mix [Bentz & Weiss, 2011]. Other recent studies have conflicting findings about the creep behavior of internally cured concrete. Lopez et al reported that the mixture with LWA exhibited less creep than the control [Lopez et al., 2008]. On the other hand, Cusson and Hoogeveen measured an increase in tensile creep coefficient of ICC as compared to a control concrete [Cusson & Hoogeveen, 2005].

2.1.7 Curling and Warping

Curling and warping occur as a result of differences in temperature throughout the thickness of a concrete slab. Concrete slabs with higher temperature gradient has a higher probability of being damaged from the effects of curling and warping. By maintaining higher and more uniform relative humidity across the concrete slab, a reduction of warping and curling can occur [Mehta & Monteiro, 2013].

LWA can reduce curling and warping of concrete, as the water is drawn from the LWA pores providing better hydration and high relative humidity. Consequently, the surface of the concrete which is moist can decrease curling and warping due to drying shrinkage. Some studies indicate that a reduction of 70% in warping can be perceived when the concrete has a high percentage of relative humidity [Wei & Hansen, 2008].

2.1.8 Microstructure

The microstructure is the fine structure of a material, which is evaluated with the aid of a microscope. The microstructure can show the type, quantity, size, shape, and distribution of the phases present in a solid [Mehta & Monteiro, 2013]. LWA concretes are expected to have a

denser microstructure that enhances the durability of the concrete. The transition zone is characterized as the weakest zone in concrete. As a consequence, the reservoirs in the LWA can provide a constant water supply for hydration reactions and generate a denser transition zone between the lightweight aggregates and the cement paste [Sun, Zhang, Dai, & Yu, 2015].

Cements blended with silica fume, slag, and fly ash were evaluated to establish the behavior of samples of each of these three types; all three contained either a LWA or did not contain LWA. For this purpose, the microstructure of the samples was obtained using scanning electron microscopy. The top row of Figure 2-3 shows the images of samples without LWA; for all cementitious materials, these samples exhibit more desiccated cement particles and larger spaces, as compared with the LWA mixes. The bottom row of Figure 2-3 shows LWA images whose transition zones are more homogeneous and denser [Bentz & Stutzman, 2008].

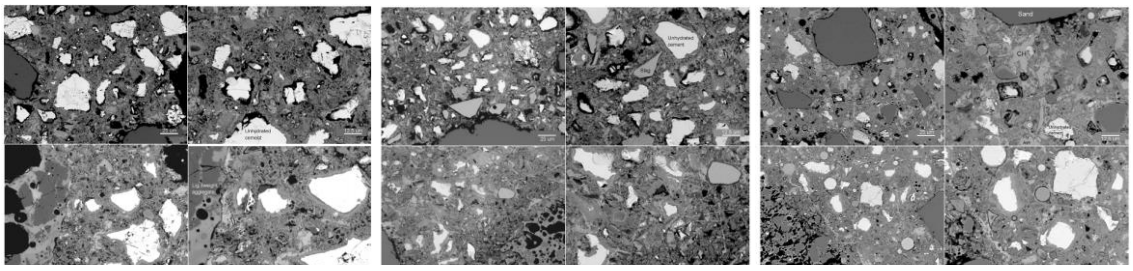

Figure 2-3. BSE/SEM images of mortar microstructures blended cement with silica fume (left), slag (middle), and fly ash (right). Without (top) and with (bottom) internal curing [Bentz & Stutzman, 2008].

An investigation conducted by Sun, Zhang, Dai, and Yu compared the behavior of the microstructure of concretes using internal curing and concretes without internal curing. For the analysis, scanning electron microscope (SEM) imaging, transport simulation, and hydration modeling techniques were used. Figure 2-4 (a) shows the SEM image of a cement mortar using LWA. The cement paste can be seen to be more hydrated and have more pores, and it is difficult to differentiate between the area of aggregates and the cement paste. Figure 2-4 (b) shows the

SEM image of a cement paste using normal aggregate. It can be seen that there are more pores in the interfacial transition zone (ITZ), aggregates limits are clearly distinguished, and more unhydrated cement particles are present [Sun, Zhang, Dai, & Yu, 2015].

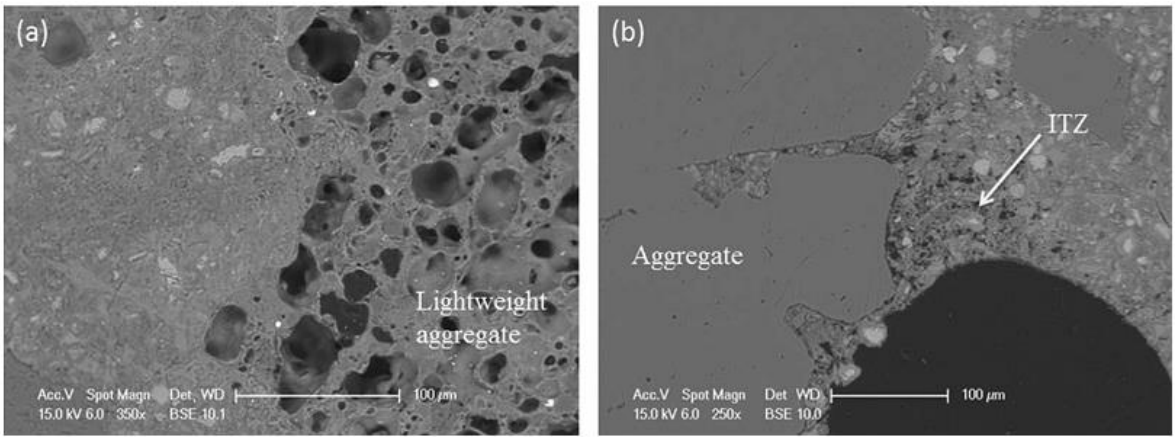

Figure 2-4. (a) SEM image of cement mortar with internal curing, (b) SEM image of cement mortar without internal curing [Sun, Zhang, Dai, & Yu, 2015].

2.1.9 Restrained Shrinkage and Thermal Cracking

The behavior of the concrete temperature in a structure is characterized by an initial increase during the first days, due to the liberation of heat generated by hydration, and then by a non-uniform decrease in temperature until ambient temperature is reached. This drop in temperature can generate thermal cracking due to the fact that thermal stresses can exceed the tensile strength of the material, generating microcracks or even macroscopic cracking. By reducing the tension that is developed by autogenous shrinkage, internally cured concrete will have enough water in its reservoirs to withstand the stresses generated by the thermal and / or applied loading [Bentz, Bognacki, Riding, & Villarreal, 2011].

Zou &Weiss in a recent study, compared the behavior of mortar using LWA and without when they were under restraint. Degree of restrained (DOR) was not constant, due to the rapid development of the elastic modulus of mortar; DOR had a significant decline in the first 2 days and then tended to be stable even if normal mortars had a higher elastic modulus than the

internally cured ones. When residual stress was compared for the first 2 days, both showed a lower development, but after that, normal mortars presented a higher development. The specimens were evaluated for 14 days. All normal mortars cracked at different stresses during this period of time, but the internally cured mortars did not exhibit cracking in the same period of time. This suggests that internally cured mortars tend to have a better cracking-resistance performance [Zou &Weiss, 2014].

2.1.10 Transport Coefficients and Service Life

The better hydration provided by internal curing creates a denser and homogeneous transition zone in the concrete structure that can reduce the transport coefficients, and increasing the service life [Halamickova, Detwiler, Bentz, & Garboczi, 1995]. Figure 2-5 shows on the left mortar using a normal aggregate and on the right mortar using a LWA; both include the transition zone paste, which is shown in grey. Percolation can be reduced by the incorporation of the LWA [Bentz, 2009]. Mixtures with a high w/cm exhibits percolated pathways and can easily link up with those in the LWA to provide increased transport. Mixtures with a lower w/cm has capillary porosity and will de-percolate [Powers, Copeland, & Mann, 1959]

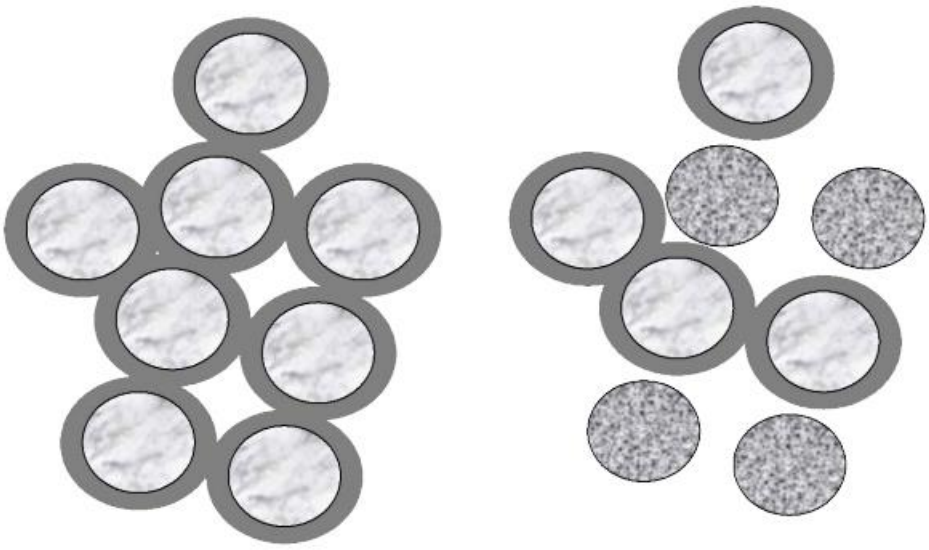

Figure 2-5. Comparison of model mortars with normal weight sand particles only [left] and LWA [right] [Bentz, 2009].

2.1.11 Freeze/Thaw Degradation

Recent studies analyzing the effect of LWA to freeze/thaw durability found that after 300 cycles of freeze/thawing, no evidence of damage was observed when LWA was used. LWA pores can supply extra volume to the air entrainment volume, which improves the durability of the concrete [Schlitter, Henkensiefken, Castro, Raoufi, Weiss, and Nantung, 2010]. However, the air contributed by LWA is not enough to eliminate the air entrainment because it does not provide the total air required. The air volume provided by LWA can be used as a complementary way to reduce damage due to freezing and thawing. Another concern is that LWA can increase humidity of these samples and provide more places to store additional water. Also, the use of LWA may be a problem if LWA fails to desorb quickly in oncoming winter weather [Bentz & Weiss, 2011].

2.1.12 Alkali-Silica Reaction

Alkali-silica reaction (ASR) could be affected by the use of internal curing using LWA, because the aggregates play a major role in this reaction. LWA could mitigate or exacerbate this

reaction. ASR is a chemical reaction between alkalis (sodium, hydroxyl, and potassium) in cement paste, and the reactive silica in the aggregates. ASR happens if the gel absorbs water and swells when the concrete is exposed to a moist environment. LWA can mitigate ASR for several reasons. First, if the porous aggregate can provide spaces to be filled by the resulting gel, it could reduce abnormal expansions in the concrete. Second, improvement in the cement hydration produces a stronger concrete matrix, reduced porosity of concrete and accessibility of fluids, and decreased rate of ASR reaction. Third, the use of LWA means that the reactive aggregate is partially replaced, reducing the amount of aggregates that potentially could develop ASR alleviating this phenomenon. But LWA can also promote ASR because more water which is present in the concrete tends to stimulate this reaction [Bentz & Weiss, 2011].

A study conducted to assess the alkali-silica reaction compared the behavior of a control mixture (100% reactive aggregate) with mixes where reactive aggregate is replaced by non-reactive aggregate or LWA. The percentage of replacement used was 15% and 28% for both non-reactive aggregate and LWA. For all samples, low expansion was evidenced before the 11 days. After 11 days, all samples showed greater expansion. The control samples showed greater expansions and mixtures with LWA showed a slower expansions. A probable cause of the relatively slow reaction of the samples is that the partial replacement of the reactive sand with LWA create a dilution effect on the reactive sand [Shin et al., 2010].

2.2 Tests to Evaluate Internally Cured Concrete

2.2.1 Mercury Intrusion Porosimetry (MIP)

Mercury intrusion Porosimetry (MIP) has been widely used to determine pore size distribution of a material either organic or inorganic. Examples of the use of MIP are in quantifying of pore size distribution of cortical bones [Cardoso et al, 2007], archaeological

pottery [Volzone et al., 2014], and lumber in paper and pulp industry [Moura et al., 2005]. The MIP technique is based on the idea that non-wetting liquid will only intrude the capillaries or pores of the material under pressure. So, under increasing pressure and higher volume of the liquid intruded, the pore size distribution of the material can be determined by relating the pressure and the intruded volume to material's pore diameters and amount. The relationship between the pressure and capillary diameter is as follows [Abell et al., 1998]:

$$P = \frac{-4\,\gamma \cos\theta}{d}$$

where P = pressure

γ = surface tension of the liquid

θ = contact angle of the liquid

d = diameter of the capillary

The pore quantity is determined from the volume of liquid intruded at each pressure increment. In general, the higher the pressure needed to force the intruding liquid, the smaller the pores size would be; and the higher the liquid volume intruded, the larger the amount of the pores would be. The pore size distribution is characterized by the pore diameters and pore quantity.

This same technique can be used to characterize pore size distribution of cement-based materials. Various research studies have shown good pore size distribution results from MIP test on cement paste and mortar [Abell et al, 1998; Cook et al., 1999], but little has been done on actual concrete. Figure 2-6 shows an example of cement-based mortar intruded by mercury in a MIP test. Figure 2-7 shows an example of pore size distribution of a cement-based mortar.

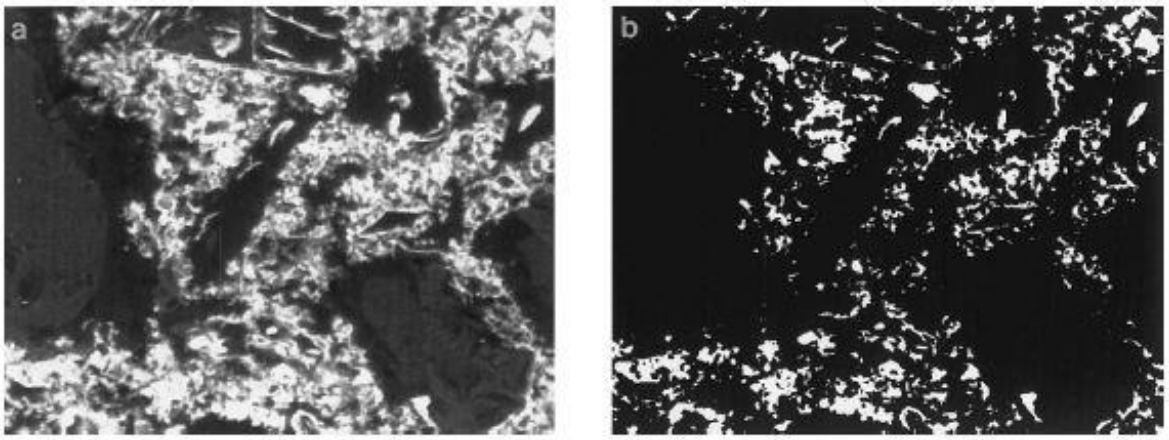

Figure 2-6. Microscopic picture of intruded mortar in a MIP test [Abell et al., 1998].

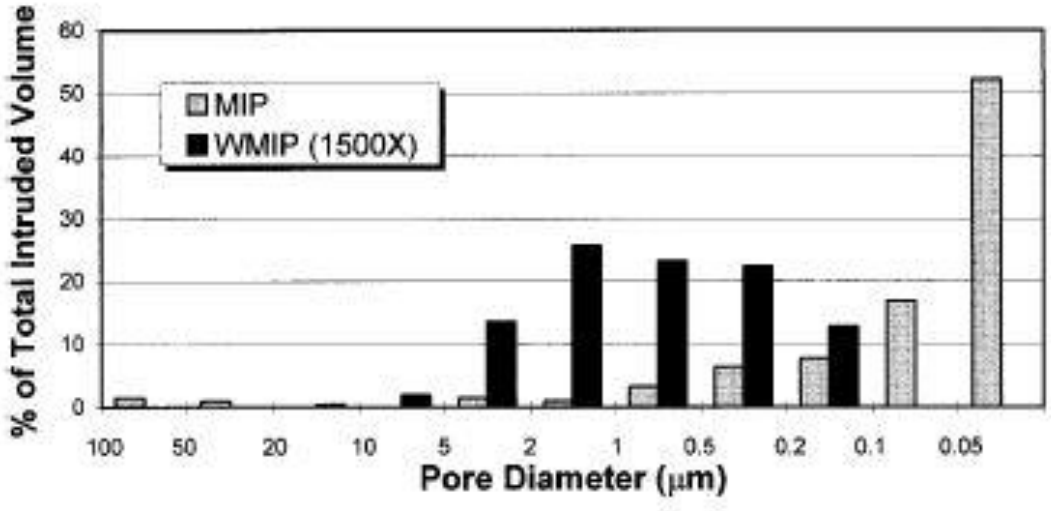

Figure 2-7. Diagram of pore size distribution of cement-based mortar [Abell et al., 1998].

The pore size distribution from MIP test can be used to evaluate a cement-based material in many ways. One example is that it can be used to compare interior microstructure development of the cement-based material i.e. how the pore size distribution changes over time [Ma, 2014]. Another example is to compare the cement-based material's interior microstructure in term of pore size distribution of different w/c ratios [Cook et al., 1999]. Whereas the pore size distribution is relatively useful information by itself, it can be more utilitarian if it can be related

to durability of the material. Katz-Thompson theory for predicting the permeability of sedimentary rock from pore size distribution was evaluated by researchers to see whether it is applicable to cement-based materials.

The prediction of permeability from Katz-Thompson theory was made by applying the percolation theory which defines a critical pore diameter and a characteristic length for a porous material. One research study concluded that the Katz-Thompson model is not applicable to cement-based materials [El-Dieb et al., 1994], but other researcher urged that the reliability of the permeability result from Katz-Thompson theory depends on the accuracy of the critical pore diameter obtained from MIP test [Ma, 2014]. Although, the validity of the model is still inconclusive, it is still be very interesting to see the pore size distribution of a concrete, not just a cement paste or mortar. The pore size distribution of a concrete could provide more information about concrete's microstructure and permeability.

2.2.2 Restrained Shrinkage Test

Figure 2-8 shows the stress and shrinkage development, and conceptual combination of shrinkage, creep, and stress relaxation in concrete at early age. Cracking will occur when the induced stress exceeds the tensile strength of the concrete. Restrained shrinkage test, which can incorporate the different effects of shrinkage, creep, and relaxation, have been used to evaluate the resistance of concrete to cracking at early age.

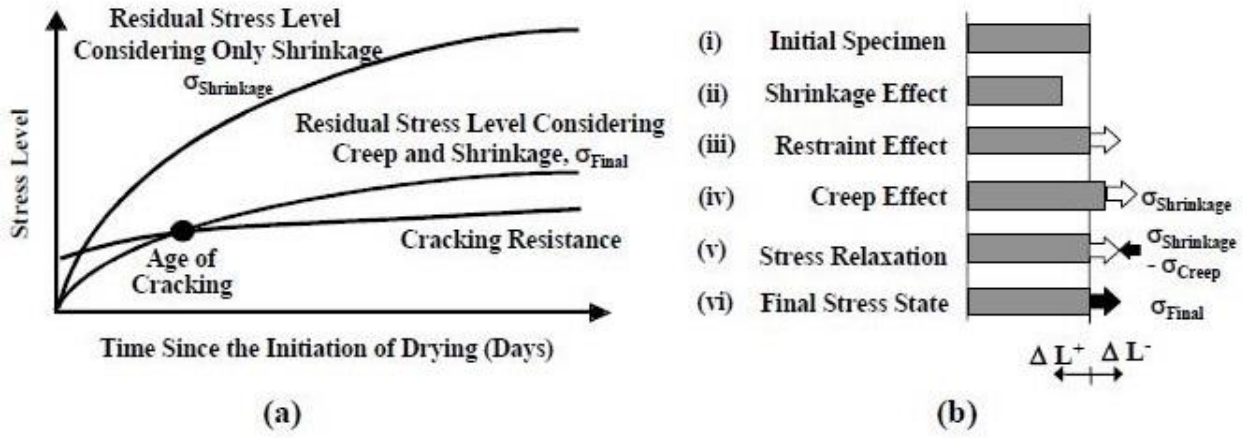

Figure 2-8. a) Stress and shrinkage development of concrete. b) Conceptual combination of shrinkage, creep, and relaxation effects in concrete. [TRB 2006]

The constrained shrinkage test selected for use in this research study is the ASTM C1581 Standard Test Method for Determining Age at Cracking and Induced Tensile Stress Characteristics of Mortar and Concrete under Restrained Shrinkage. This test is commonly called the Restrained Ring test. The test uses a circular steel ring to create the constraint for the concrete, which is placed on the outside of this ring. Multiple strain gauges are attached on the inner side of the steel ring, and connected to a data acquisition system. The readings from these strain gauges are monitored and recorded until the first sudden jump in the strain is observed. That time is determined as cracking moment of the concrete specimen. The width of the crack can also be measured.

The restrained ring test has been used with success by many researchers. Suksawang et al used the restrained ring test to evaluate Florida concrete in a research project done for the FDOT [Suksawang et al, 2014]. The project utilized this test to assess the effectiveness of different kinds and lengths of fiber to alleviate cracking problem in high-early-strength slab replacement concrete. Figure 2-9 shows a restrained ring test specimen and a typical strain history from the project.

a)

b)

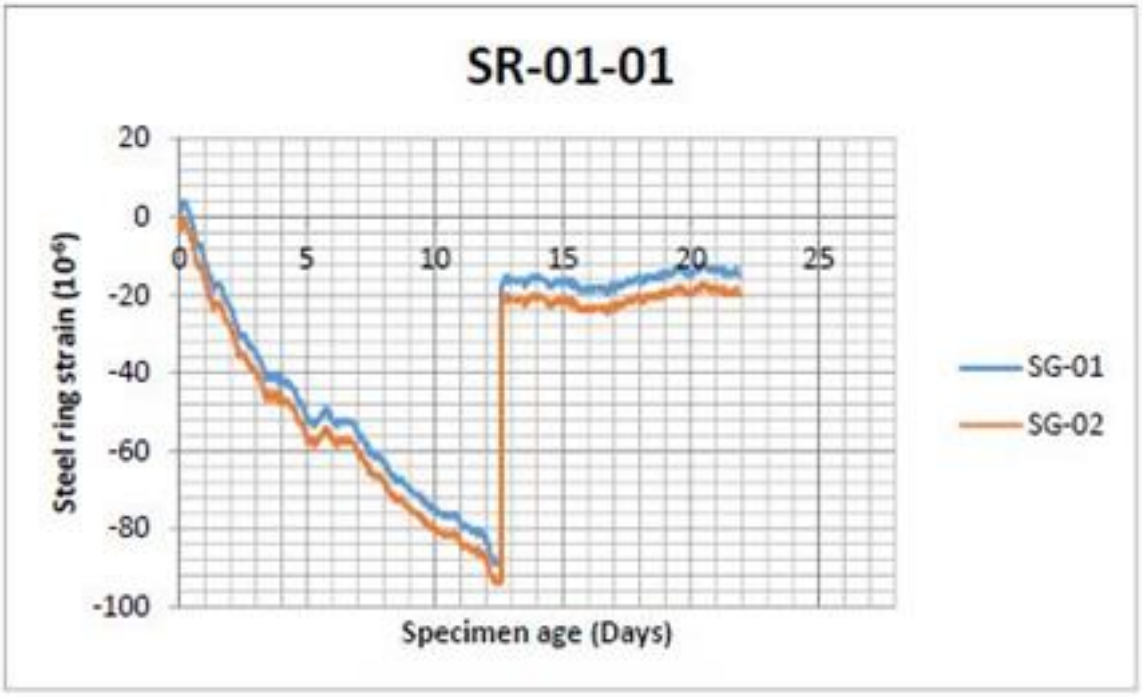

Figure 2-9. (a) Restrained ring specimen; (b) Typical strain history of restrained ring test. [Suksawang et al, 2014]

Li et al studied the effects of various supplementary binders on the crack growth of concrete using the restrained ring test [Li et al, 1999]. The research team successfully

demonstrated crack growth trends for each type of mixture tested, and had come to a conclusion that supplementary binders had adverse effects on the cracking age and crack growth (width) of the concrete. Figure 2-10 shows the crack width growth of concretes with and without supplementary binder.

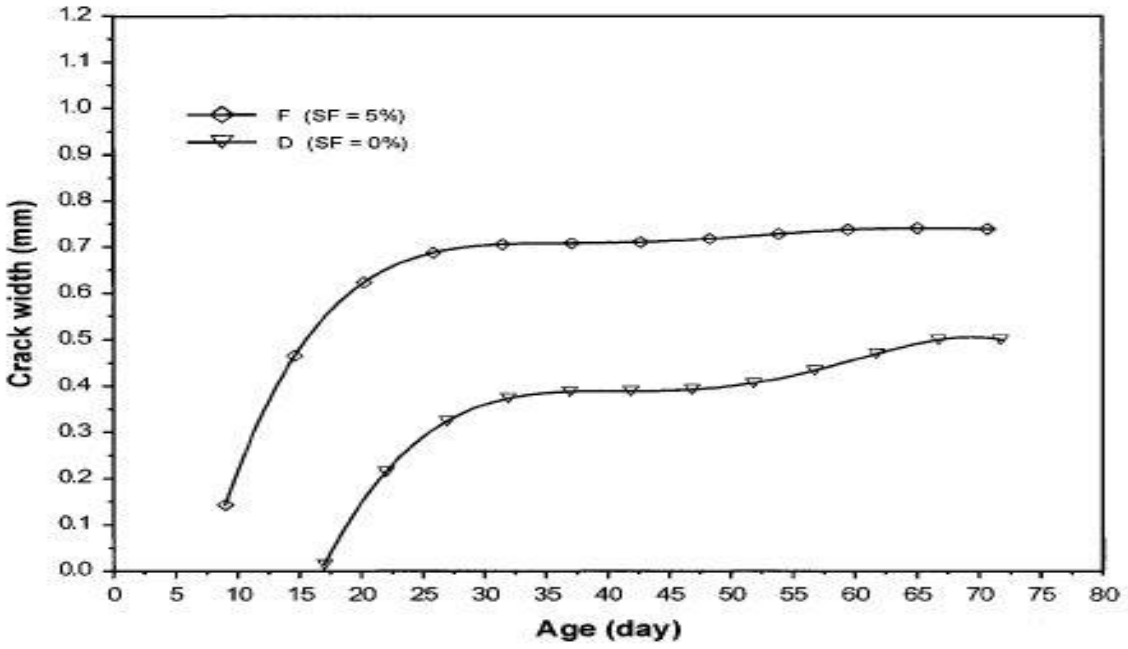

Figure 2-10. Crack width growth of concretes with and without silica fume [Li et al, 1999].

Ghezal et al. used the restrained ring test to evaluate self-consolidating concrete's cracking age and induced stress with different types of chemical admixtures [Ghezal et al., 2014]. From the results of the restrained ring test, the researchers were able to calculate the induced tensile stress of the specimens and were able to show the impact of different chemical admixtures used. Plots of the induced tensile stresses of the concrete specimens over time are shown in Figure 2-11.

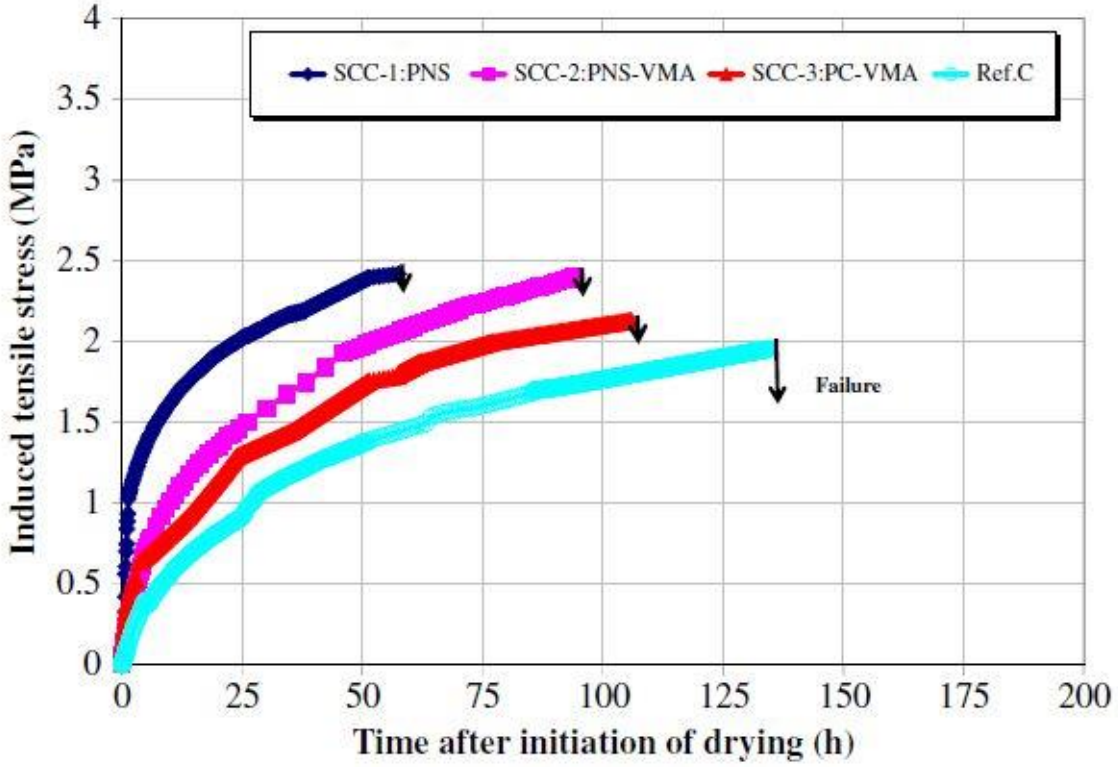

Figure 2-11. Induced tensile stresses of concrete over time [Ghezal et al, 2014].

A research group in Ohio used the restrained ring test to evaluate crack-resistive property of ICC mixtures using fine lightweight aggregate (LWA) and other concrete types. The results showed that the ICC mixtures had higher average time to crack as compared with concrete without internal curing. The researchers also suggested that the out-of-spec coarse aggregate (with absorption less than 1%) can be used when incorporating it with internal curing technique using fine LWA [Delatte et al, 2007].

Shuhui et al used the restrained ring test to evaluate the efficiency of internal curing using LWA with different moisture content in concrete with low w/c ratio [Shuhui et al, 2009]. They found that the shrinkage-induced tensile stresses were further reduced with higher LWA degree of saturation, which in turn postponed the corresponding cracking ages. Figure 2-12 shows the effect of varying degree of saturation of LWA in the restrained ring test.

a)

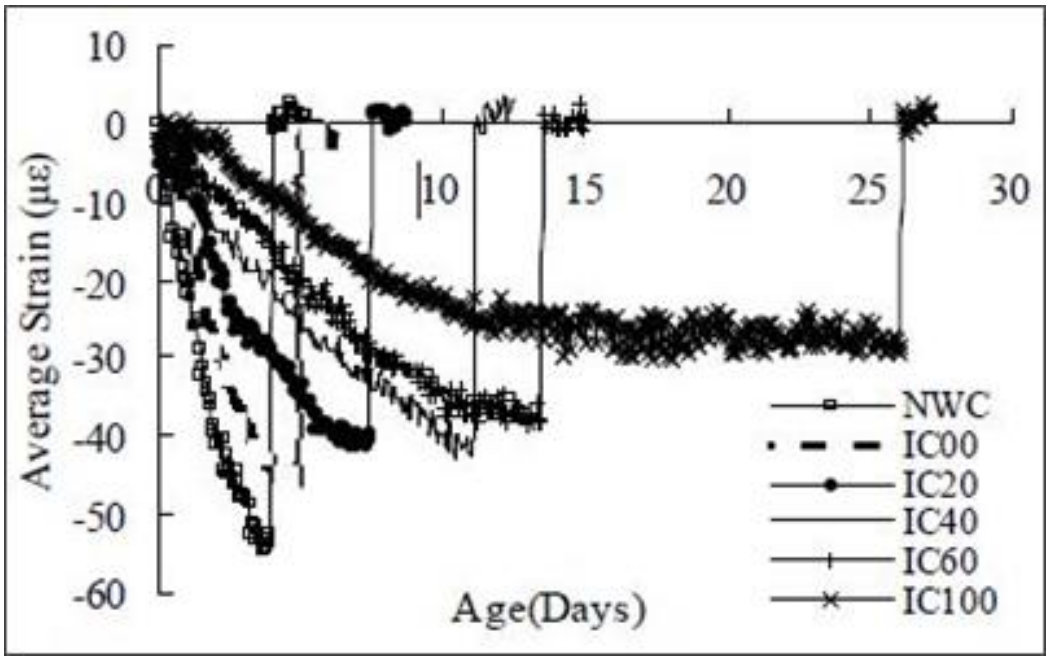

b)

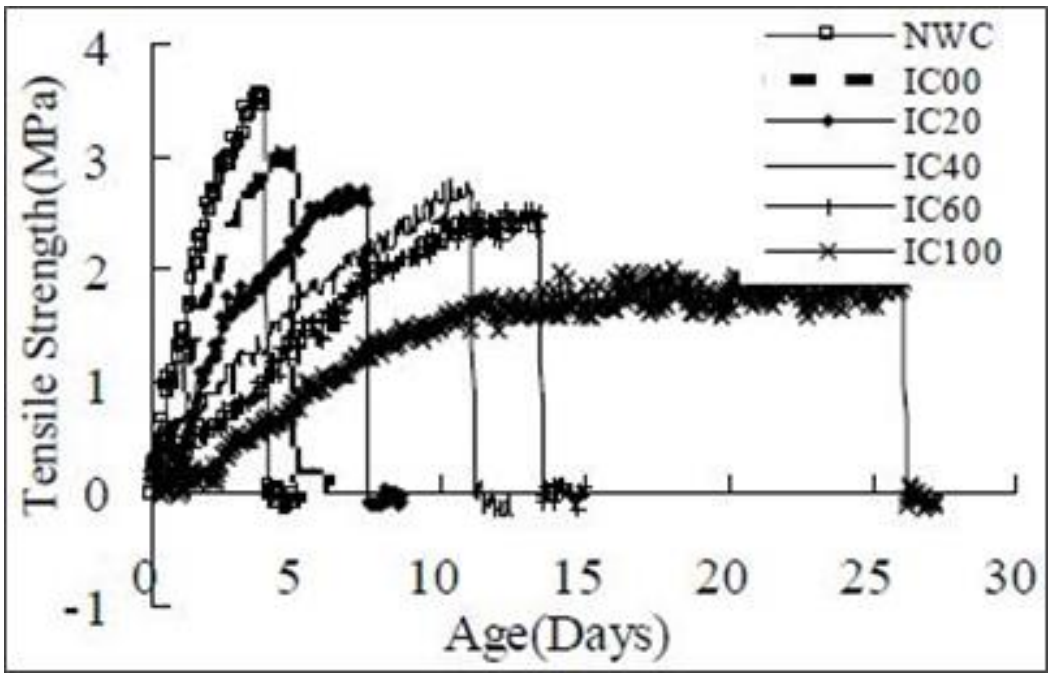

Figure 2-12. Effect of varying degrees of saturation of LWA in restrained ring test (a) Average strain; (b) Tensile stress [Shuhui et al, 2009]

CHAPTER 3
EXPERIMENTAL PLANNING AND DESIGN

3.1 Mix Designs Used

Six mix designs were evaluated in this laboratory testing program. Three typical mix designs for Florida Class II (Bridge Deck), Class IV, and Class V concretes were used. Another three mixes are internally cured concretes (ICC) based on these three typical mixes but with the use of lightweight fine aggregates. All six mixtures were duplicated for a total of 12 mixes.

The Class II (Bridge Deck), Class IV, and Class V concretes had total cementitious materials contents of 687 lb/yd^3 , 780 lb/yd^3, and 860 lb/yd^3 and w/c ratios of 0.40, 0.36, and 0.32, respectively. Mix proportions of these mixtures are shown in Table 3-1. Also, the ICC and its corresponding conventional reference mixes had the same cementitious materials contents and w/c ratios. However, a part of fine aggregates was replaced with pre-wetted lightweight aggregates. The quantity of LWAs to be used is an amount that will supply 7 lb of absorbed water per 100 lb of cement used. The requirements for the various FDOT concrete classes are presented in Table 3-2.

Table 3-1. Mix Proportions for Control and ICC Mixtures

Mix #	Concrete Classification	w/c ratio	Cement	Fly Ash	Water	Coarse Aggregate	Fine Aggregate		Target Air Content	Target Slump
							Sand	LWAs		
		(lb/lb)	(lb/yd^3)	(lb/yd^3)	(lb/yd^3)	(lb/yd^3)	(lb/yd^3)	(lb/yd^3)	(%)	(in)
1	II (Bridge Deck)	0.40	549.6	137.4	274.7	1618.5	1188.5	-	2 to 4	2 to 4
2	II (Bridge Deck) IC	0.40	549.6	137.4	274.7	1618.5	*	**	2 to 4	2 to 4
3	IV	0.36	624.0	156.0	280.7	1616.5	1092.1	-	2 to 4	2 to 4
4	IV IC	0.36	624.0	156.0	280.7	1616.5	*	**	2 to 4	2 to 4
5	V	0.32	688.0	172.0	275.1	1685.5	953.7	-	2 to 4	2 to 4
6	V IC	0.32	688.0	172.0	275.1	1686.5	*	**	2 to 4	2 to 4

* Sand content of ICC mixtures equals to original amount minus LWAs on volume basis

** LWAs content equals to an amount that will supply 7 lb of absorbed water per 100 lb of cement used

Table 3-2. Requirements for FDOT Concrete Classes

Class of Concrete	Minimum Strength	Over-designed Strength	Minimum Total Cementitious Materials Content	Maximum w/c ratio	Target Slump	Air Content Range
	(28 day) (psi)	(28 day) (psi)	(lb/yd^3)	(lb/lb)	(in)	(%)
II (Bridge Deck)	4,500	5,700	611	0.44	3	1 to 6
IV	5,500	6,900	658	0.41	3	1 to 6
V	6,500	7,900	752	0.37	3	1 to 5

3.2 Mix Constituents

The mix constituents that were used in producing the concrete mixtures are described in this section.

3.2.1 Cement and fly ash

Type I/II Portland cement was used to produce the concrete mixes to be used in this laboratory study. The cement met the requirements of the standard specification AASHTO M85.

Class F fly ash, which is derived from the combustion of ground or powered coal was used in the concrete mixes. The fly ash met the requirements of the standard ASTM C618 specifications.

3.2.2 Normal-weight aggregates

Typical local silica sand was used in this testing program as fine aggregate. The sand met the requirements of the standard specifications AASHTO M6. Typical local Florida limestone will be used in this program as coarse aggregate. Coarse aggregate size number 57 was used. The coarse aggregates met the requirements of the standard specifications AASHTO M80.

3.2.3 Lightweight aggregates

A porous fine lightweight aggregate which has desirable properties as internal curing agent was selected. Those desirable properties include high porosity, high absorption and desorption rate, and comparable strength to the sand it replaces. In this laboratory testing program, an expanded clay from Louisiana was used. The LWA was tested for its physical properties including gradation, density, specific gravity, and water absorption and desorption to ensure that it met the requirements of the standard ASTM C1761 specifications.

3.2.4 Water

Normal tap water supplied by local city water system was used.

3.2.5 Admixtures

Air-entraining admixture was used to help increase the air content of the concretes. Also, retarding, water-reducing, and high-range water-reducing admixtures were used as needed to achieve the FDOT concrete requirements. All admixtures met requirements of the standards ASTM C260 and ASTM C494 specifications.

3.3 Trial Mixes

Trial batches of the six mix designs as listed in Table 3-1 were produced and tested to determine the actual mix proportioning to be used in the laboratory testing program. Fresh concrete properties including slump, air content, unit weight, temperature, time of set, and bleeding were measured on the trial batches. Compressive strength test at 28 days was performed on the hardened 4" x 8" cylindrical concrete specimens to ensure that the required compressive strengths as listed on Table 3-2 were met for the various concrete classes.

3.4 Concrete Mixtures Preparation

Each standard concrete and its corresponding ICC were produced on the same day. Concrete preparation procedures as described in the ASTM C192 standard were followed. The order of the mixtures produced and tested is as follows:

Production 1 – Standard concrete Class IV and ICC Class IV

Production 2 – Standard concrete Class II (Bridge Deck) and ICC Class II (Bridge Deck)

Production 3 – Standard concrete Class V and ICC Class V

Production 4 – Standard concrete Class IV and ICC Class IV

Production 5 – Standard concrete Class II (Bridge Deck) and ICC Class II (Bridge Deck)

Production 6 – Standard concrete Class V and ICC Class V

3.5 Tests on Fresh Concrete

Tests were performed on freshly mixed concrete to measure the plastic properties of the studied concretes. The purpose of the fresh concrete tests was to evaluate the compliance of the mixtures to the FDOT specifications. Moreover, it was to compare performance and behavior of the ICCs to their corresponding reference concretes. Fresh concrete tests performed per batch of concrete include the following:

1) Slump (ASTM C143) one measurement

2) Air content (ASTM C231) one measurement

3) Unit weight (ASTM C138) one measurement

4) Temperature (ASTM C1064) one measurement

5) Time of set (ASTM C403) one measurement (trial mix only)

6) Bleeding (ASTM C232) one measurement (trial mix only)

3.6 Tests on Hardened Concrete

Tests performed on the hardened concrete per batch of concrete are shown in Table 3-3.

Table 3-3. Hardened Concrete Properties Tests

Tests	Samples	Days of Testing
Compressive Strength (ASTM C39)	4" x 8" cylinder (18 replicates)	At 1, 3, 7, 28, 91, and 182 days
Modulus of Elasticity (ASTM C469)	4" x 8" cylinder (12 replicates)	At 7, 28, 91, and 182 days
Splitting Tensile Strength (ASTM C496)	Use the same specimens from MOE test	At 7, 28, 91, and 182 days
Flexural Strength (ASTM C78)	4" x 4" x 14" beam (12 replicates)	At 7, 28, 91, and 182 days
Free Drying Shrinkage (ASTM C157)	3" x 3" x 11.25" prism (6 replicates)	At 1, 7, 28, 91, and 182 days
Restrained Shrinkage Ring (ASTM C1581)	13" – 16" Ø x 6" ring (2 replicates)	Monitor from 1 hr until 28 days or cracking occurs
Mercury Intrusion Porosimetry (MIP) (adapted from ASTM D4404)	0.3" Ø x 2" core (2 replicates)	At 28 days
Thermal Imaging	Picture files	Record image after each specimen is unmolded and after it is broken in strength tests

3.7 Fabrication and Curing of Concrete Specimens

Various types of test specimens including 4” x 8” cylinders, 4” x 4” x 14” beams, 3” x 3” x 11.25” prisms, 13” – 16” Ø x 6” rings, 0.3” Ø x 2” cores were fabricated to be evaluated in the tests described in the aforementioned sections. Preparations of those specimens followed their accompanying ASTM or AASHTO standards. The MIP core specimen was taken out of a broken beam from the flexural strength test by drilling.

For curing, 4” x 8” cylinders and 4” x 4” x 14” beams were kept inside their molds for 7 days before unmolding. Then, they were air-cured in a controlled storage room at room temperature in the range from 68 to 86°F and approximately 50% relative humidity. Prisms of size 3” x 3” x 11.25” were cured under similar condition as the 4” x 4” x 14” beams but were unmolded at 24 hours age. Ring of size 13” – 16” Ø x 6” were cured as per ASTM C1581 standard. Lastly, 0.3” Ø x 2” concrete cores for MIP testing were dried, after removal from the broken beam specimen. They were dried in an oven at a temperature of 75° F for at least two days.

CHAPTER 4
PERFORMANCE OF LABORATORY TESTING PROGRAM AND ANALYSIS OF RESULTS

4.1 Materials

4.1.1 Overview

This section describes the mix proportions and the mix ingredients of the standard control concretes and internally cured concrete (ICC) mixtures evaluated in this study. As the purpose of this study was to evaluate applicability of ICC mixtures to Florida conditions, all materials used in this research were approved materials from Florida except for the lightweight fine aggregate. Mix designs of these concretes were selected from the database of approved mix designs from actual Florida Department of Transportation (FDOT) projects in order to best represent the concrete mixes used in road, bridge, and other structures in the State of Florida.

4.1.2 Mix Constituents

The materials used were selected mostly from locally available sources in order to maintain similarity to the typical Florida concretes. This also limited the cost of transportation to a minimum. Moreover, the mix constituents used in this study were all from approved sources by FDOT except the LWA source, which is new to the FDOT. The mix constituents that were used in producing the concrete mixtures are described in this section.

4.1.2.1 Cement

Portland cement Type I/II from manufacturer Florida Rock Industries was used in this laboratory testing program. The cement was analyzed for its physical and chemical properties by FDOT's State Materials Office (SMO) and found to meet the requirements of the standard specification AASHTO M85. All cement lots acquired were evaluated by this method. All the cement was acquired in 94-lb bags and was kept in a temperature and humidity-controlled room

to maintain the quality of the cement as much as possible. The physical and chemical properties of the cement tested are shown in Table 4-1 and Table 4-2, respectively.

Table 4-1. Physical Properties of the Cement Type I/II

Tests	Standard Test Method	Unit	Cement[1]		Specification Limits
			Lot 1	Lot 2	
Autoclave Expansion	ASTM C151	%	0.03%	0.03%	<= 0.80%
Fineness	ASTM C204	m^2/kg	418	401	>= 260
Time of Set (Initial)	ASTM C191	min	140	145	>= 45
Time of Set (Final)	ASTM C191	min	315	225	<= 375
3-day Compressive Strength	ASTM C109	psi	3960	3810	>= 1740
7-day Compressive Strength	ASTM C109	psi	5370	4940	>= 2470

[1] Tested at FDOT SMO

Table 4-2. Chemical Properties of the Cement Type I/II

Tests	Standard Test Method	Unit	Cement[1]		Specification Limits
			Lot 1	Lot 2	
Loss on Ignition	ASTM C114	%	2.0%	2.1%	<= 3%
Insoluble Residue	ASTM C114	%	0.05%	0.10%	<= 0.75%
Aluminum Oxide	ASTM C114	%	4.7%	5.1%	<= 6%
Ferric Oxide	ASTM C114	%	4.0%	4.4%	<= 6%
Magnesium Oxide	ASTM C114	%	0.8%	0.9%	<= 6%
Sulfur Trioxide	ASTM C114	%	3.1%	3.1%	<= 3.6%
Tricalcium Aluminate	ASTM C114	%	6.0%	6.0%	<= 8%
Tricalcium Silicate	ASTM C114	%	70.0%	68.0%	none specified
Total Alkali as Na_2O	ASTM C114	%	0.31%	0.34%	<= 0.6%
$C_3S + 4.75C_3A$	ASTM C114	%	99.0%	97.0%	<= 100%

[1] Tested at FDOT SMO

4.1.2.2 Fly Ash

In Florida, fly ash usually is used to improve the durability of concrete, hence fly ash Class F from Crystal River power plant was used in this laboratory testing program. The fly ash was tested at the FDOT SMO and also by a third party laboratory. The fly ash met the requirements of the standard specification ASTM C618. Barrels of fly ash were acquired and kept in a temperature and humidity-controlled room. The physical and chemical properties of the fly ash used are shown in Table 4-3 and Table 4-4, respectively.

Table 4-3. Physical Properties of the Class F Fly Ash

Tests	Standard Test Method	Unit	Fly Ash		Specification Limits
			SMO	Third Party	
Fineness (Retained on 45 µm sieve)	ASTM C430	%	16.0%	16.6%	<= 34%
Strength Activity Index with Portland Cement					
- 7-day Compressive Strength	ASTM C109	%	-	85%	>= 75%
- 28-day Compressive Strength	ASTM C109	%	81%	83%	>= 75%
Water requirement	ASTM C311	%	95%	97%	<= 105%
Autoclave Expansion or Contraction	ASTM C151	%	-	-0.01%	<= ±0.8%
Specific Gravity	ASTM C188	NA	-	2.40	not specified

Table 4-4. Chemical Properties of the Class F Fly Ash

Tests	Standard Test Method	Unit	Fly Ash		Specification Limits
			SMO	Third Party	
Sum of Silicon Dioxide, Iron Oxide, & Aluminum Oxide	ASTM C114	%	90.8%	84.7%	<= 70%
Sulfur Trioxide	ASTM C144	%	1.90%	1.96%	<= 5%
Moisture Content	ASTM C311	%	0.20%	0.19%	<= 3%
Loss on Ignition	ASTM C114	%	-	1.34%	<=6%

4.1.2.3 Coarse Aggregate

A Florida limestone was selected for use as coarse aggregate in this study because it is typically used in FDOT projects and is easy to obtain from an approved source. The coarse aggregate used was from mine number 87-090 Miami Oolite formation. The physical properties of the limestone were determined by the FDOT SMO and met the requirements of the standard specification AASHTO M80. Before every mix production, the coarse aggregate was bagged from the covered stock pile. Then it was soaked in a water tank for 12 hours to reach a saturated condition. The physical properties of the coarse aggregate used are shown in Table 4-5 and its gradation is shown in Figure 4-1.

Table 4-5. Physical Properties of the Coarse Aggregate

Tests	Standard Test Method	Unit	Coarse Aggregate[1]	Specification Limits
Materials Finer Than 75 µm	AASHTO T11	%	1.39%	<= 1.75%
SSD Specific Gravity	AASHTO T85	NA	2.394	not specified
Apparent Specific Gravity	AASHTO T85	NA	2.532	not specified
Bulk Specific Gravity	AASHTO T85	NA	2.305	not specified
Absorption	AASHTO T85	%	3.90%	not specified

[1] Tested at FDOT SMO

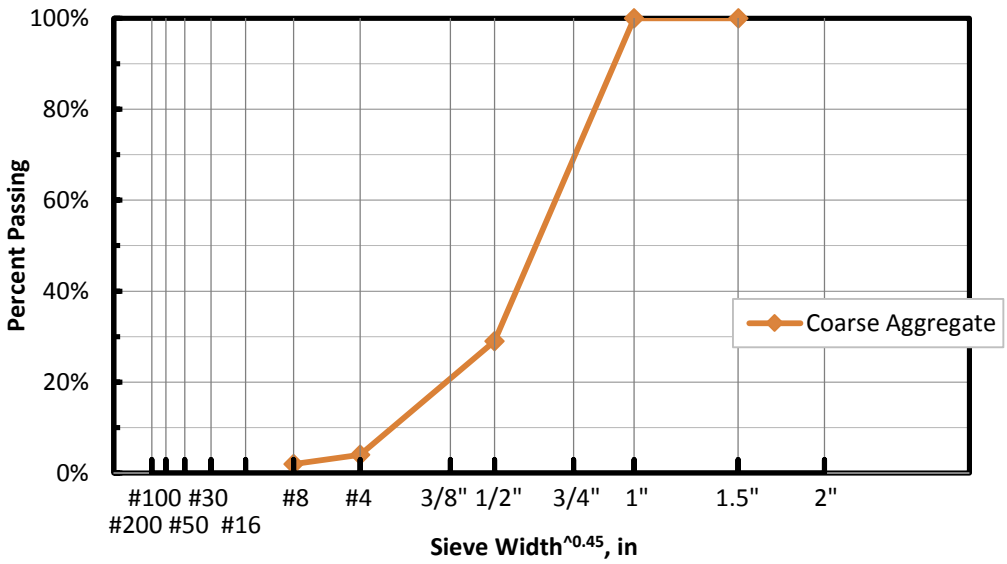

Figure 4-1. Gradation of the coarse aggregate (Limestone mine #87-090).

4.1.2.4 Fine Aggregate

Normal weight fine aggregates

The normal-weight fine aggregate used was a silica sand from Ludowicie, Georgia mine number GA-397. The physical properties of the sand were determined by the FDOT SMO and met the requirements of the standard specification AASHTO M6. Before every mix production, the fine aggregate was bagged from the covered stock pile and oven-dried for 12 hours. This was done to eliminate all moisture inside the aggregates. The physical properties of the silica sand used are shown in Table 4-6 and its gradation is shown in Figure 4-2.

Table 4-6. Physical Properties of the Fine Aggregate

Tests	Standard Test Method	Unit	Fine Aggregate[1]	Specification Limits
Materials Finer Than 75 µm	AASHTO T11	%	0.23%	<= 4%
Fineness Modulus	AASHTO T27	NA	2.26	not specified
Organic Impurities	AASHTO T21	NA	1	<= 3
SSD Specific Gravity	AASHTO T84	NA	2.639	not specified
Apparent Specific Gravity	AASHTO T84	NA	2.653	not specified
Bulk Specific Gravity	AASHTO T84	NA	2.631	not specified
Absorption	AASHTO T84	%	0.30%	not specified

[1] Tested at FDOT SMO

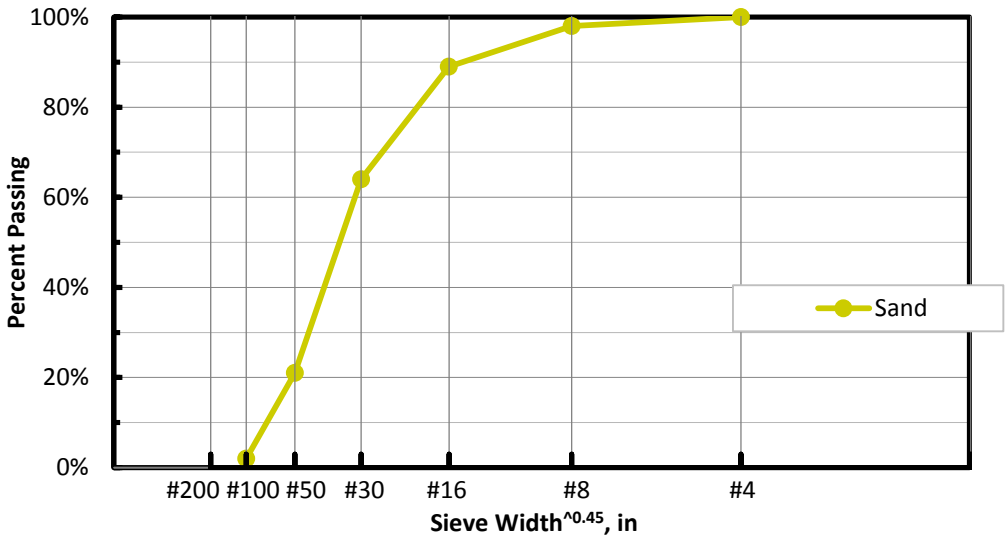

Figure 4-2. Gradation of the fine aggregate (Silica sand mine #GA-397).

Lightweight aggregates

The lightweight fine aggregate used was a manufactured expanded clay from Big River Industries Inc. Various sizes and sources of LWAs from this manufacturer were evaluated for their performances as IC agents. It was decided that LWA [3/16] from the Louisiana plant with 4.75 mm nominal maximum aggregate size was chosen for the production mixes. From many trial mixes, this particular aggregate demonstrated good workability and good plastic properties

in the fresh concrete. Also, from the high absorption characteristic of this LWA, it was judged to be a good IC agent and should give best benefits to the concrete. In order to use the LWA as an IC agent, multiple procedures had to be performed to assess its IC potential. By following the procedures in ASTM C1761, the physical properties of the LWA [3/16] were determined, including unit weight, specific gravity, absorption and desorption rates, minus 200 material, gradation, and abrasion resistance. The test results are shown in Table 4-7 and its gradation is shown in Figure 4-3.

Table 4-7. Physical Properties of the Lightweight Aggregate

Tests	Standard Test Method	Unit	Lightweight Fine Aggregate[1]	Specification Limits
Materials Finer Than 75 µm	AASHTO T11	%	0.63%	not specified
Fineness Modulus	AASHTO T27	NA	4.29	not specified
SSD Specific Gravity	AASHTO T84	NA	1.538	not specified
Apparent Specific Gravity	AASHTO T84	NA	1.780	not specified
Bulk Specific Gravity	AASHTO T84	NA	1.228	not specified
Absorption 72-hours	ASTM C1761	%	25.20%	>= 5%
Desorption	ASTM C1761	%	96.15%	>= 85%
Abrasion	FM1-T096	%	20.97%	not specified

[1] Tested at FDOT SMO

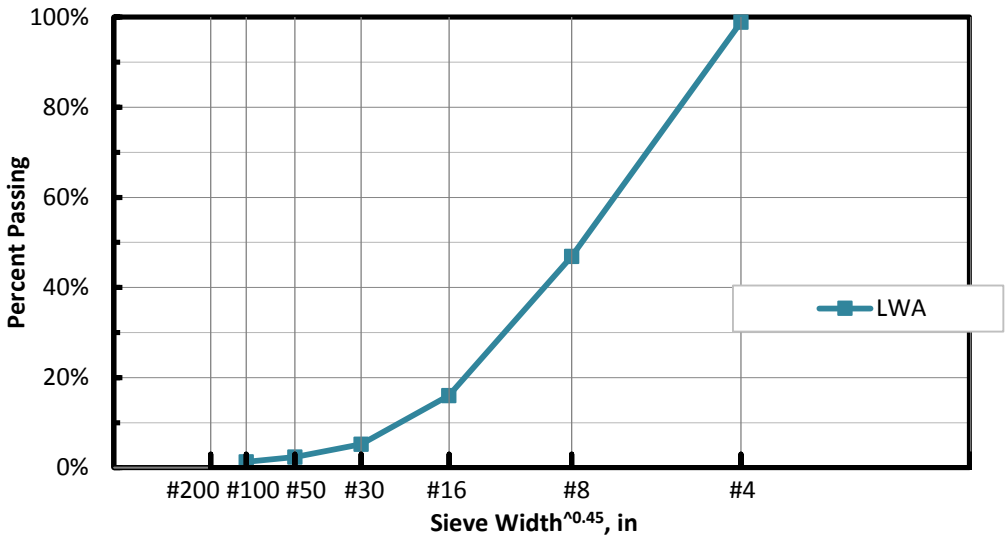

Figure 4-3. Gradation of the lightweight fine aggregate.

4.1.2.5 Water

Normal tap water supplied by local city water system was used as mixing water for all concrete mixes.

4.1.2.6 Admixtures

All the admixtures used were from approved admixture manufacturers, and the admixtures' physical and chemical properties are periodically determined by the FDOT SMO in accordance with standard test method ASTM C260.

Air-entraining admixture

An air-entraining admixture was used to help increase the air content of the concretes. The air-entraining admixture used was Darex AEA from W.R. Grace & Company. The admixture was mixed with the mixing water before adding the water into the concrete mixer.

Water-reducing and retarding admixture

The water-reducing and retarding admixture used was WRDA 60 from W.R. Grace & Company. It is a polymer-based liquid solution, and meets the requirements of the standard specification ASTM C494 Type A and Type D. The admixture was primarily used to help

produce good workability and good plastic properties. During concrete mixing, the admixture was added after all other mix ingredients were blended in the concrete mixer, to adjust the concrete to the desired workability.

High range water-reducing admixture

The high range water-reducing admixture used was AVDA CAST 600 from W.R. Grace & Company. It is a high efficiency polycarboxylate-based liquid superplasticizer solution, and meets the requirements of the standard specification ASTM C494 Type A and Type F. The admixture was primarily used to help achieve good workability and good plastic properties with no segregation in a low w/c ratio concrete. During concrete mixing, the admixture was used in the event that the addition of water reducer admixture Type D still was unable to get the mixture to achieve the desirable slump.

4.1.3 Mix Designs

In order to evaluate the performance of the new internal curing (IC) technique, FDOT approved mix designs were chosen from an approved mixtures database – one from Class II (Bridge Beck), one from Class IV, and one from Class V concrete classification. Three typical mix designs for each of the classes were selected as standard control mixes. Another three mixes were developed based on these three typical mixes with modification with IC technique using the lightweight aggregate. In total, six mix designs were used in this laboratory testing program, and all six mix designs were duplicated for a total of 12 mixes. They are called production mixes in this report.

The Class II (Bridge Deck), Class IV, and Class V concretes have total cementitious material contents of 687 lb/yd^3 , 780 lb/yd^3 , and 860 lb/yd^3, and w/c ratios of 0.40, 0.36, and 0.32, respectively. Mix proportions of concretes Class II (Bridge Deck), Class IV, and Class V are shown in Table 4-8, Table 4-9, and Table 4-10, respectively. In addition, the ICC mixture

correspondences also have the same cementitious material contents and w/c ratios. However, a portion of the fine aggregates was replaced with pre-wetted lightweight aggregate (LWA). The quantity of the LWA to be used was an amount that would supply 7 lb of absorbed water per 100 lb of cementitious materials used in the mix.

Table 4-8. Mix Proportions of Control and ICC Mixtures Class II (Bridge Deck) (0.40 w/c)

Material	Mix Number			
	#1	#2	#3	#4
Classification	II (Bridge Deck)	II (Bridge Deck)	II (Bridge Deck) IC	II (Bridge Deck) IC
Cement (lb/yd^3)	549.6	549.6	549.6	549.6
Fly ash (lb/yd^3)	137.4	137.4	137.4	137.4
Coarse aggregate (lb/yd^3)	1618.5	1618.5	1618.5	1618.5
Sand (lb/yd^3)	1188.5	1188.5	762.4	762.4
Lightweight aggregate (lb/yd^3)	-	-	248.5	248.5
Air entraining admixture (oz/yd^3)	-	-	1.3	1.3
Water reducer admixture (oz/yd^3)	27.5	27.5	27.5	27.5
High-range water reducer admixture (oz/yd^3)	7.7	7.7	4.4	4.4
Water (lb/yd^3)	274.7	274.7	274.7	274.7
w/c	0.40	0.40	0.40	0.40

Table 4-9. Mix Proportions of Control and ICC Mixtures Class IV (0.36 w/c)

Material	Mix Number			
	#5	#6	#7	#8
Classification	IV	IV	IV IC	IV IC
Cement (lb/yd^3)	624.0	624.0	624.0	624.0
Fly ash (lb/yd^3)	156.0	156.0	156.0	156.0
Coarse aggregate (lb/yd^3)	1616.5	1616.5	1616.5	1616.5
Sand (lb/yd^3)	1092.1	1092.1	608.2	608.2
Lightweight aggregate (lb/yd^3)	-	-	282.1	282.1
Air entraining admixture (oz/yd^3)	2.0	2.0	3.9	3.9
Water reducer admixture (oz/yd^3)	31.2	31.2	31.2	31.2
High-range water reducer admixture (oz/yd^3)	4.5	8.2	0.0	0.0
Water (lb/yd^3)	280.7	280.7	280.7	280.7
w/c	0.36	0.36	0.36	0.36

Table 4-10. Mix Proportions of Control and ICC Mixtures Class V (0.32 w/c)

Material	Mix Number			
	#9	#10	#11	#12
Classification	V	V	V IC	V IC
Cement (lb/yd^3)	688.0	688.0	688.0	688.0
Fly ash (lb/yd^3)	172.0	172.0	172.0	172.0
Coarse aggregate (lb/yd^3)	1685.5	1685.5	1685.5	1685.5
Sand (lb/yd^3)	953.7	953.7	420.2	420.5
Lightweight aggregate (lb/yd^3)	-	-	311.1	311.1
Air entraining admixture (oz/yd^3)	4.7	4.7	5.2	5.2
Water reducer admixture (oz/yd^3)	43.0	43.0	43.0	43.0
High-range water reducer admixture (oz/yd^3)	26.0	26.0	28.7	0.0
Water (lb/yd^3)	275.1	275.1	275.1	275.1
w/c	0.32	0.32	0.32	0.32

In addition, FDOT has a practice to ensure the high quality of concretes and to factor in the variability that will occur when the batch is produced in a ready-mix batch plant. It is called

the over-designed method. The over-designed method is done by increasing the required strength of concrete during the approval process over the minimum required strength. It requires the producer to design the mix with a higher strength to ensure the strength is met during production. In short, in order to get approved, a mix design has to achieve a minimum required strength plus an over-designed strength. Each class of concrete has its own over-designed requirement. Those requirements for FDOT concrete classes are presented in Table 4-11 (references from FDOT Standard Specification for Road and Bridge Construction 2014, Section 346, Table 2, Table 3, and FDOT Materials Manual Section 9.2.7)

As a mean to guarantee a legitimate comparison between the standard control and ICC mixtures, the over-designed method was used in this study.

Table 4-11. Requirements for FDOT Concrete Classification

Class of Concrete	Minimum Strength	Over-designed Strength	Minimum Total Cementitious Materials Content	Maximum w/c ratio	Target Slump	Air Content Range
	(28 day) (psi)	(28 day) (psi)	(lb/yd^3)	(lb/lb)	(in)	(%)
II (Bridge Deck) (0.40 w/c ratio)	4,500	5,700	611	0.44	2 to 4	1 to 6
IV (0.36 w/c ratio)	5,500	6,900	658	0.41	2 to 4	1 to 6
V (0.32 w/c ratio)	6,500	7,900	752	0.37	2 to 4	1 to 6

4.2 Laboratory Testing Program

4.2.1 Overview

This section describes the laboratory testing procedures utilized to evaluate the performance and usability of Internally Cured Concrete (ICC) using lightweight aggregate (LWA) for bridge decks and pavements applications. All mixing and testing were carried out at FDOT's State Materials Office (SMO) in Gainesville, FL, except for the tests that this office cannot accommodate. This section also explains the standard method of preparation of the

concrete mixtures, and fabrication and curing of the concrete specimens in the laboratory. Standard ASTM, AASHTO, and other related testing methods performed on the mixtures and specimens are described here as well.

Concrete mixtures were prepared in the laboratory and tested for their properties in both fresh and hardened forms. ICC and standard concrete mixtures were tested to evaluate (1) the differences between ICC using LWA and the standard mixtures and (2) the effectiveness of ICC mixtures for use by FDOT.

4.2.2 Trial Mixes

Trial mixes were carried out for each mix design for this laboratory testing program in order to ensure that the evaluated concretes had proper fresh and hardened concrete properties. Hence, a trial mix had to meet its design plastic properties, which included slump, air content, concrete temperature, time of set, and bleeding. After three base mix designs from the database were chosen, the first step was to substitute the mix constituents from the original mix designs which were not readily available or difficult to procure. Those materials were substituted with materials that were available. It was important that the replacement materials had similar properties as the original materials. In the end, the previously described mix constituents were chosen. Once the mix materials were selected, each of the mixes, with w/c of 0.40, 0.36, and 0.32, was trial-batched in a 4.5-ft^3 mixer. The tests for plastic properties were performed on the trial-batched concretes. Afterward, 4" x 8" concrete cylinders were cast to test for the compressive strength. The strength results were then compared to the target over-designed strengths, shown in Table 4-9, for all the mixes evaluated.

Air entraining, water reducing, and high-range water-reducing admixtures were utilized, when necessary, in all mixtures to help adjust the properties of the fresh concrete. The results of the trial batches are described in the following sections.

4.2.2.1 Mixtures with 0.40 w/c Ratio

In the first trial mixes of both the standard control mixture (SM) and ICC mixture using LWA, the produced concretes exceeded the allowable air content and slump. They were 5% and 4% in air content and 4.5 inches and 7.75 inches in slump, respectively. Then, the quantities of air entraining and high range water-reducing admixture were reduced in the next two trial batches. As a result, all of the slump values from the SM and LWA concretes were within the target range for the trials except for the slump of the LWA mixture in the third trial. The slump was 2.25 inches and 3.5 inches in the second trial, and 2.75 inches and 8.0 inches in the third trial for the SM and LWA mixes, respectively. Nevertheless, the air contents still stayed above the desired range even without the addition of any air entraining admixture to the mixes. The air content was 4.50% and 4.75% in the second trial, and 5.25% and 9.75% in the third trial for the SM and LWA mixes, respectively.

Inevitably, the aggregate ratio had to be amended to solve the problem. The fine aggregate ratios (by volume) were then reduced from 46% to 40% for both SM and LWA concretes. This proved to be effective as two air contents for SM and LWA decreased to the target range in the fourth trial batch (2.5% and 2.2%, respectively), and the fifth trial batch (2.3% and 2.3%, respectively). As for the concrete temperatures, they were satisfactory at temperature range from 71 to 76°F since the first trial. The workability was also considered good for the last two trial mixes. The slumps of the SM and LWA were 2.5 and 2.25 inches for the fourth trial batch, and 3.25 and 3.25 inches for the fifth trial batch for the SM and LWA mixes, respectively. Lastly, time of set and bleeding tests were conducted on the last trial mixes. The initial and final setting times for SM and LWA were 335 and 465 minutes and 340 and 475 minutes, respectively. And the bleeding results for SM and LWA were 0.099 ml/in^2 and 0.105 ml/in^2,

respectively. All the setting times and bleeding quantities were found to be satisfactory according to FDOT specification.

After all the plastic properties of the mixtures were satisfied, the compressive strengths of the concretes were evaluated. In the last trial batch, concrete cylinders were cast and tested at the ages of 3, 7, and 28 days. The SM mixture's cylinder compressive strengths were 5,300, 6,150, and 7,260 psi at 3, 7, and 28 days, respectively. The 28-day compressive strength was higher than the 5,700 psi target over-designed strength, and met the standard specification. Likewise, the LWA mixture's cylinder compressive strengths were 5,060, 5,640, and 7,490 psi at 3, 7, and 28 days, respectively. The 28-day compressive strength was higher than the 5,700 psi target over-designed strength, and also met the standard specification. From the results of the trial batches, the mix designs for the mixtures with 0.40 w/c ratios were decided as previously shown in the Table 4-8 were adopted for use in the production mixes.

4.2.2.2 Mixtures with 0.36 w/c Ratio

The first trial batches of SM and LWA showed good results with plastic properties being close to the target range with slumps at 3.0 inches and 3.75 inches for the SM and the LWA mixes. But the air contents were low as compared with the target range. The air contents were 3.25% and 1.75% for SM and LWA, respectively. The second trial batches were adjusted by increasing air entraining admixture quantities. In the second trial batches, the slumps and air contents were within the target ranges with slumps of 2.75 inches and 3.0 inches, and air contents of 3.25% and 2.25% for the SM and the LWA mixtures, respectively. The concrete temperatures ranged from 71 to 78 degrees Fahrenheit for both SM and LWA, which were satisfactory according to the FDOT specification. The workability and air content of both mixtures were satisfactory. In the third trials, the concretes were additionally tested for their time of set and bleeding properties. Both test results met the FDOT standard. The initial and

final setting times for the SM and the LWA mixes were 345 and 450 minutes, and 350 and 450 minutes, respectively. The SM and LWA showed bleed water of 0.331 ml/in^2 and 0.328 ml/in^2, which were acceptable. Additionally, the slump and air content of the mixes showed consistent numbers and were within the desired limits.

After all the plastic properties of the mixtures were satisfied, the compressive strength of the concretes were evaluated. Concrete cylinders of size 4" x 8" were cast and tested at 1, 7, and 28 days. The SM mixture's cylinder compressive strengths were 3,490, 6,680, and 7,660 psi at 1, 7, and 28 days, respectively. The 28-day compressive strength was higher than the 6,900 psi target over-designed strength, and met the standard specification. The LWA concrete strengths were 3,490, 6,680, and 7,660 psi at 1, 7, and 28 days, respectively. The 28-day compressive strength was higher than the 6,900 psi target over-designed strength, and also met the standard specification. From the results of all the trial batches, the mix designs for the mixtures with 0.36 w/c ratios as previously shown in the Table 4-9 were adopted for use in the production mixes.

4.2.2.3 Mixtures with 0.32 w/c Ratio

All plastic properties of SM and LWA mixes were well within the target ranges in the first trial mixes, which included slumps (3.25 inches and 2.5 inches), air contents (2.3% and 2.9%), and concrete temperatures (73° and 73° F) for the SM and LWA mixtures, respectively. Time of set and bleeding tests were then performed on the second trial batch. Plastic properties of the second trial batch did equally well as the first trial. In addition, the time of set and bleeding results also met the FDOT standard. The initial setting times for the SM and the LWA were 415 and 360 minutes, and the projected final setting times for the SM and LWA were 520 and 470 minutes, respectively. The bleeding test results were 0.006 ml/in^2 and 0.002 ml/in^2 for SM and LWA, respectively. The setting times and bleeding test results met the FDOT standard.

Similar to the concretes with 0.40 and 0.36 w/c ratios, the mixes with 0.32 w/c ratios were tested for their compressive strengths at ages of 3, 7, and 28 days. The SM mixture's cylinder compressive strengths were 6,760, 7,790, and 9,610 psi at 3, 7, and 28 days in the second trial batch, respectively. The 28-day compressive strength was higher than the 7,900 psi target over-designed strength, and met the standard specification. The LWA concrete strengths at various ages were 6,590, 7,580, and 9,170 at 3, 7, and 28 days in the second trial batch, respectively. The 28-day compressive strength was higher than the 7,900 psi target over-designed strength, and also met the standard specification. From the results of all the trial batches, the mix designs for the concretes with 0.32 w/c ratio as previously shown in the Table 4-10 were adopted for use in the production mixes.

4.2.3 Testing

Testing was carried out to evaluate the mixture's characteristics and performance. The tests performed are described in this section.

4.2.3.1 Tests on Fresh Concrete

These tests were performed when the concrete was still in plastic state. Plastic properties were performed in a temperature controlled room with temperature ranging from 68° to 76° F. These plastic property tests included slump, air content, unit weight, concrete temperature, workability, time of set, and bleeding tests.

Slump test

The slump test was performed in accordance with the standard test method ASTM C143. Slump test was measured from the fresh concrete. Figure 4-4 shows a picture of the performing of the slump test.

Figure 4-4. Performing of slump test.

Air content test

The air content test by pressure method was performed in accordance with the standard test method ASTM C231. Once the slump test had been performed and the result satisfied the target range, the mixture was transferred from the mixer into a wheel barrow and the air content was then measured. The test apparatus used for this test is shown in Figure 4-5.

a)  **b)** 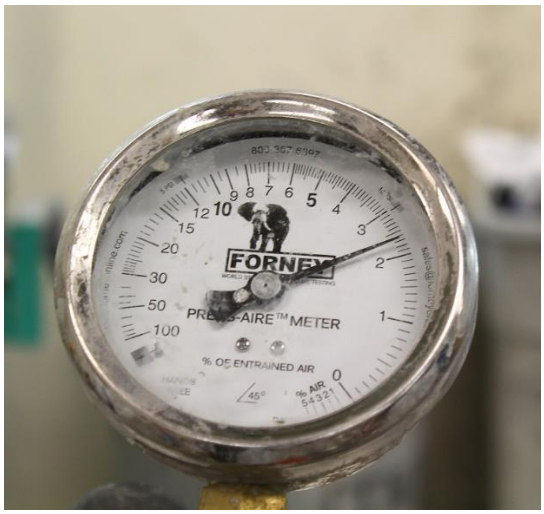

Figure 4-5. a) Air content test apparatus. b) Reading of air content.

Unit weight test

The unit weight test method was performed in accordance with the standard test method ASTM C138. The test was performed on the fresh concrete, and was done with the same material and same apparatus used for the air content test. The test apparatus for the unit weight test is shown in Figure 4-6.

Figure 4-6. Unit weight test apparatus.

Temperature test

The concrete temperature test was performed in accordance with the standard test method ASTM C1064 and measured from the fresh concrete. The thermometer used is shown in Figure 4-7.

Figure 4-7. Thermometer used in the temperature test.

Time of set test

The time of set test by penetration resistance method was run in accordance with the standard test method ASTM C403. This test was conducted on the trial mixes. The initial and final setting times were not expected to be different between the trial mix and the production mix for the same mix design. Hence, it was omitted from the production mixes.

During the trial mix operation, a portion of the fresh concrete was wet-sieved through a 4.75-mm standard sieve. The mortar passing the sieve was placed into a standard cubic container until reaching the depth of at least 5.5 inches. The container was tapped on the sides with a rubber hammer to consolidate the fresh mortar, then the top surface was made smooth by a trowel. Upon completion of the specimen preparation, a plastic sheet was used to cover the specimen until the time for the penetration test. The initial penetration test was made after an elapsed time of 3 to 4 hours after initial contact between the cement and water. The force required to produce 1-in depth was recorded along with the elapsed time at the application. Subsequent tests were made at half to 1 hour intervals. The test apparatuses for this test are shown in Figure 4-8.

a)  b) 

Figure 4-8. a) Penetration test apparatus. b) Time of set test specimen.

Bleeding test

The bleeding test was run according to the standard test method ASTM C232. Similar to the time of set test, this test was conducted only in trial batches because bleeding of the concrete was not expected to be different between the trial mix and the production mix for the same mix design. Hence, it was omitted from the production mixes.

During the trial mix operation, a portion of the mixed material from the concrete mixer was transferred to a standard steel bucket, and was consolidated by a standard tamping rod. After the bucket was filled to a height of about 10 in, the mixture's surface was leveled by a trowel. A plastic sheet was used to cover the top of the container to prevent loss of moisture. A plastic pipet was used to draw accumulated water off the surface at 30-minute time intervals until cessation of bleeding. The withdrawn water was transferred to a graduated cylinder. Then, the accumulated quantity of water was recorded after each transfer. The apparatus for this test is shown in Figure 4-9.

Figure 4-9. Bleeding test specimen.

4.2.3.2 Tests on Hardened Concrete

Concrete specimens were cast in different sizes and shapes as per test methods. The concrete samples were air cured in a temperature-controlled room with temperature ranging from 65° to 75° F and relative humidity at about 50% until the time of testing. These tests included compressive strength, flexural strength, splitting tensile strength, modulus of elasticity, restrained shrinkage ring, and drying shrinkage tests.

Compressive strength test

The compressive strength test specimens were made by following the standard test method, ASTM C192. Concrete specimens were cast in 4" x 8" single-use cylindrical plastic molds using a vibrating table to consolidate the specimens. The consolidated specimens, in molds, were covered with plastic sheets to prevent loss of moisture, then placed in the control room for one night. Within the next 12 hours, the concrete samples were removed from the molds. The samples were then stored on a shelf in the same control room until the time of testing. A group of concrete cylinders is shown in Figure 4-10.

Figure 4-10. Concrete cylinder specimens just after removing from molds.

The preparation of the concrete cylinders for compressive strength testing was done in accordance with the standard test method ASTM C39. Prior to compressive strength testing, each sample was ground on both ends of the specimens to make the cylinders ends plane to the horizontal axis. All specimens were ground on top and bottom ends using an automatic grinding machine. Furthermore, the side of the cylinder was checked for its verticality as well. Two perpendicular diameters and one length dimensions of the sample were measured to calculate the loading area. Lastly, the weight of the specimen was measured to calculate unit weight of each sample.

The compressive strength testing was done in accordance with the standard test method ASTM C39. A Forney automatic computer-controlled loading machine was used to perform the test. The machine has a capability of controlling rate of loading within 3 psi/sec of the specified rate. The machine eliminated operator error that is associated with manual testing machines. Maximum load at failure and breaking type were recorded after testing the sample. The

compressive testing machine is shown in Figure 4-11. A specimen after the test is shown in Figure 4-12.

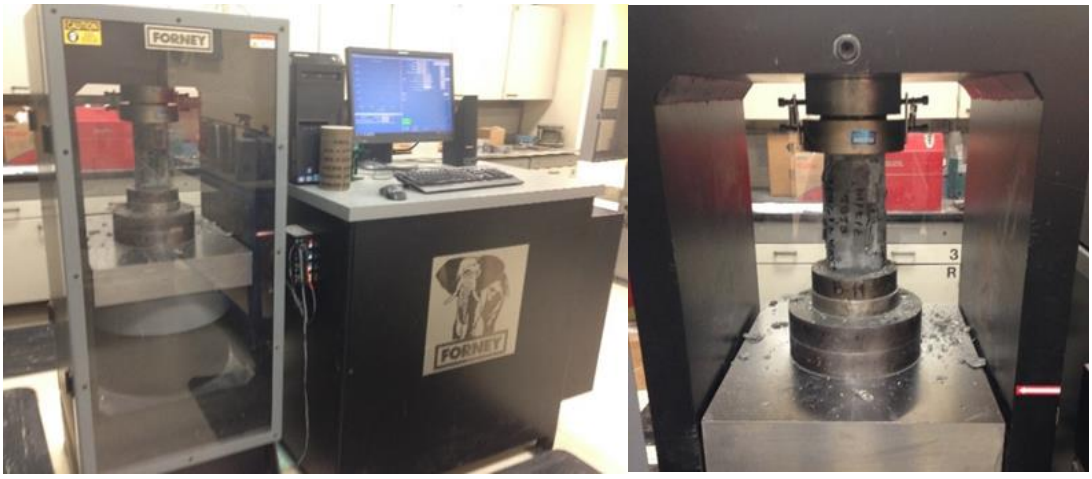

Figure 4-11. Compressive testing machine.

Figure 4-12. Concrete cylinders after compressive strength test.

Flexural strength test

The flexural strength test specimens were made in accordance with standard test method ASTM C192. Concrete specimens were cast in 4" x 4" x 14" steel molds using a vibrating table to consolidate the materials. Similar to the 4" x 8" samples, the beam samples were covered with plastic sheets to prevent loss of moisture, then placed in the temperature-controlled room for one night. Within the next 12 hours, the concrete beam samples were removed from the molds. The samples were then stored on a shelf in the same control room until the time of testing. A set of concrete beams is shown in Figure 4-13.

The preparation of the concrete beams for testing was done in accordance with standard test method, ASTM C78. Additionally, procedure for moisture conditioning as per standard test method ASTM C42 Appendix X1 was followed. Essentially, the air-cured beams were submerged in lime-saturated water for 40 hours before testing. As stated in the Appendix X1 of ASTM C42, relatively small amount of drying could induce tensile stress in the extreme fibers that would markedly reduce its flexural strength. Promptly after removal from water, irregularities were scrubbed off the specimens' side faces. Line markings were made on the side face and the top face of the specimen, at 1, 5, 9, and 13 inches away from the beam edge. They were used to align the specimen to the loading head. The specimens were then ready for testing.

Figure 4-13. Concrete beams for flexural test.

The flexural strength testing method was done in accordance with the ASTM C78. A 90K Tinius Olsen automatic-computer-controlled loading machine was used to perform the test. After starting the test, the machine was run at a slow rate of loading in the first part of the test, then increased to a specified rate afterward. Upon breaking of a test specimen, the location of the breaking point was recorded. On the shorter piece of the broken sample, three depths and three widths of the breaking cross-section were measured to calculate the breaking area. The testing machine used is shown in Figure 4-14. A specimen after the testing is shown in Figure 4-15.

a)  b) 

Figure 4-14. a) Testing machine for flexural strength test. b) Flexural strength testing on a concrete beam.

Figure 4-15. Concrete beams after flexural strength test.

Modulus of elasticity test

The modulus of elasticity (MOE) test specimens were made in accordance with standard test method, ASTM C192. Concrete specimens were cast in the same fashion as the samples for the compressive strength test. A group of concrete cylinders is shown in Figure 4-10. The preparation of the concrete cylinders and the testing procedure for the MOE test followed the

standard test method ASTM C469. Similar to the preparation for the compressive strength test, the specimen was ground, checked for planeness, and measured for their dimensions.

A Forney automatic computer-controlled loading machine was used to run the test. A special compressometer from Epsilon Company was employed. It was easier to use, took less time to affix, and gave more precise results than the old apparatus. However, this model did not have an extensometer to measure the transverse strain; therefore, the Poisson's ratio of the concrete could not be determined. The Epsilon and the old apparatuses are shown in Figure 4-16. After mounting the Epsilon compressometer, the sample was loaded in the testing machine as shown in Figure 4-17. The average MOE value from three MOE values calculated from three cycles of loading was used as the MOE for the test specimen

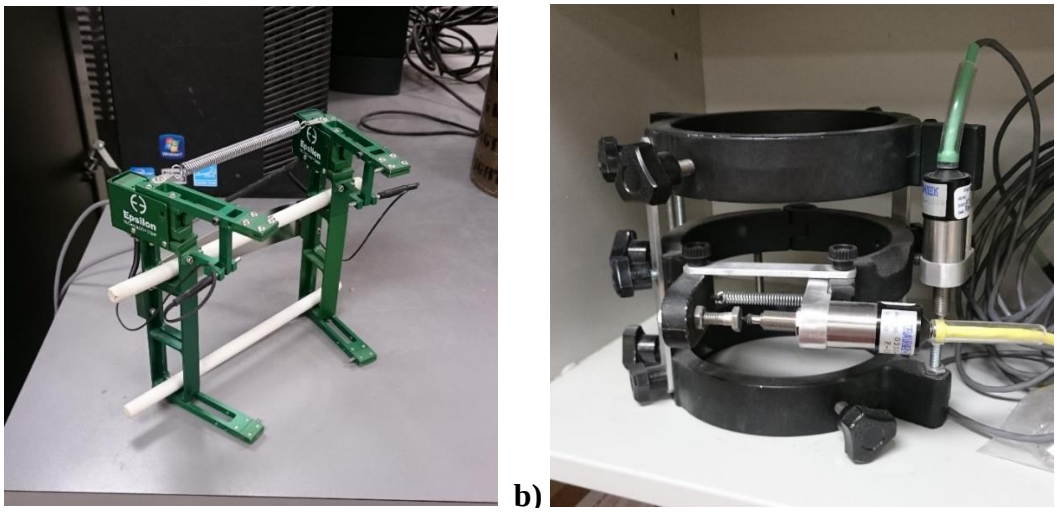

Figure 4-16. a) Compressometer by Epsilon. b) Compressometer with extensometer.

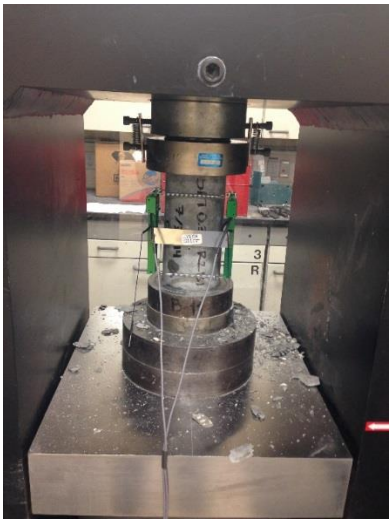

Figure 4-17. MOE test with Epsilon apparatus.

Splitting tensile strength test

The splitting tensile strength test specimens were made in accordance with the standard test method ASTM C192. The MOE specimens were re-used in the splitting tensile strength test. After the MOE test was finished, the concrete cylinder was measured for its diameter with three readings and length with two readings, all along the loading axis.

The splitting tensile strength testing method was done in accordance with ASTM C496. A Forney manual-loading machine was used to perform the test. A concrete cylinder was arranged in the horizontal axis with a specially-made apparatus as shown in Figure 4-18. Then the specimen was transferred to the loading machine. The apparatuses for the splitting tensile strength test are shown in Figure 4-18. Two specimens after the splitting tensile testing are shown in Figure 4-19.

a)  b) 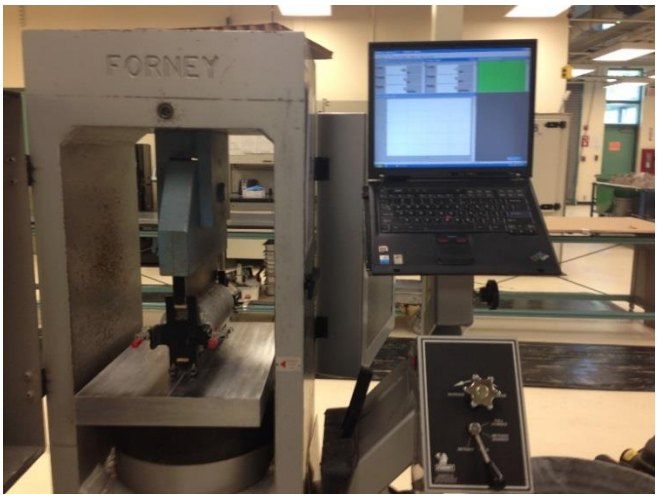

Figure 4-18. a) Concrete cylinder on a specially-made apparatus for splitting tensile strength test. b) Splitting tensile testing on a concrete cylinder.

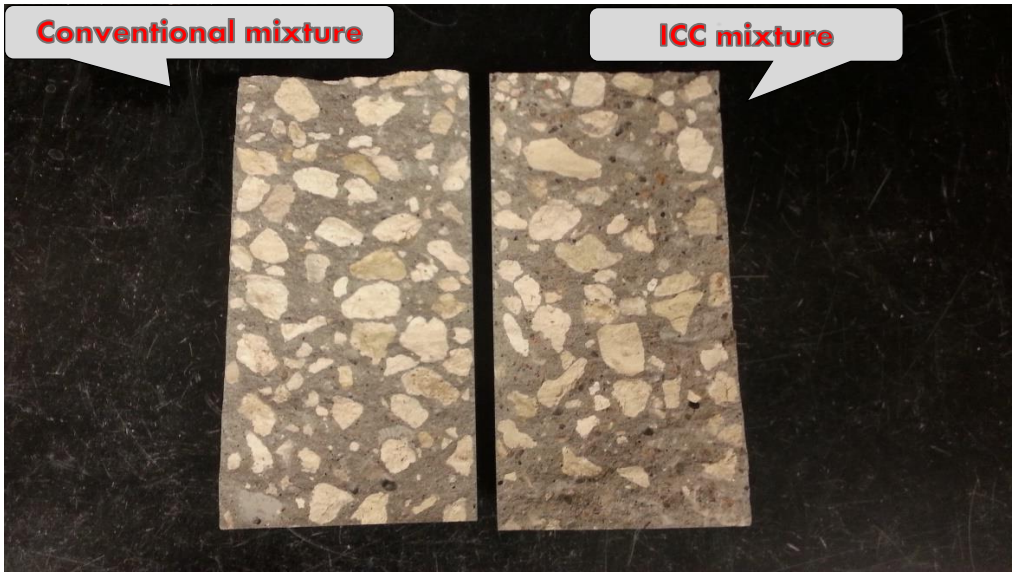

Figure 4-19. Concrete cylinder after splitting tensile test.

Restrained shrinkage ring test

Restrained shrinkage ring test was performed in accordance with ASTM C1581. It was used to determine and compare ages of cracking of different mixtures under restrained condition. The shrinkage was a combined result from drying shrinkage, autogenous shrinkage, and heat of hydration deformation.

The fresh concrete, with aggregates larger than 0.5 inch sieved out, was compacted and consolidated in an instrumented circular steel ring mold. The sieved concrete was compacted in two layers with each layer rodded 75 times by a steel bar and consolidated on a vibrating table for 5 seconds. The surface was struck off the access material, and smoothened. Then, the concrete specimen was transferred to a temperature-controlled testing room and covered with plastic sheets. Once the concrete was starting to set (in about 2 hours), the bolts and washers locking the steel mold were loosened, and the strain gauges on the mold were connected to a data acquisition (DAC) unit. In the same way, a thermocouple which was placed inside the concrete specimen was also connected to the DAC unit. Upon connecting the strain gauges and the thermocouple to the DAC unit, the LabVIEW application on a laptop which was linked to the DAC unit was started in order to record the strain and temperature information from the specimen. The test was started as early as 2 hours after the mixing had been done. This allowed the early-age shrinkage to be observed and recorded. The steel ring mold is shown in Figure 4-20 a). Figure 4-20 b) shows the concrete ring specimen connecting to DAC unit and under testing.

After curing for 24 hours, the outer ring was removed to expose the specimen to the air to let it dry. However, only the top part of the specimen was sealed by aluminum foil tape to prevent moisture evaporation. Monitoring and data recording were continued until physical cracking was visible on the side of the sample; at that point, the test was terminated. A crack on a concrete ring specimen is shown in Figure 4-21. The actual cracking age, nonetheless, was determined by the notable sudden change in strain from the recorded data. The plot of this data will be shown in the forthcoming test results section.

a)  b) 

Figure 4-20. a) Steel ring mold for restrained shrinkage ring test. b) Concrete ring specimen connecting to DAC unit under testing.

Figure 4-21. Crack on a concrete ring specimen.

Drying shrinkage test

Drying shrinkage test was performed in accordance with ASTM C157. It was used to determine the length change that is not produced by an external force and temperature change. The drying shrinkage test specimens were made by following the standard ASTM C192. Concrete prism specimens were cast in 3" x 3" x 11.25" steel molds using a vibrating table to consolidate the materials. Similar to the 4" x 4" x 14" beam samples, the consolidated molds

were covered with plastic sheets to prevent loss of moisture, then placed in a control room, as described previously, for one night. Within the next 12 hours, the concrete prism samples were removed from the molds. The samples were then stored on a shelf in the same control room until the time of testing. A LVDT length comparator was used to measure the change in length of the specimen. The concrete prism specimens used for the drying shrinkage test are shown in Figure 4-22a. Figure 4-22b shows how the length of the concrete prism was measured by a length comparator.

a)  b) 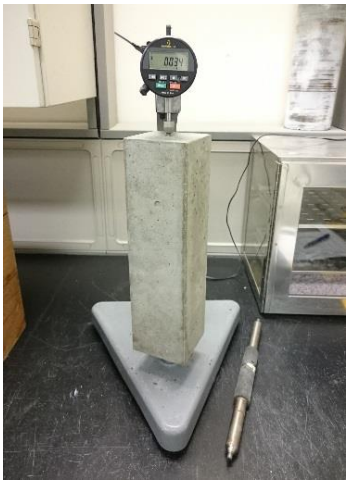

Figure 4-22. a) Concrete prism specimens. b) Drying shrinkage testing on a concrete prism specimen.

Coefficient of thermal expansion (CTE) test

The test was performed in accordance with the AASHTO T 336 Standard Method of Test for Coefficient of Thermal Expansion of Hydraulic Cement Concrete. Each of the 4" x 8" cylindrical concrete specimens was cut to the desired 7-inch height by a grinding machine, and then the specimen was submerged in a lime saturated water for at least 48 hours. After soaking, the specimen was placed into a LVDT-mounted frame in a temperature-controlled bath. The LVDT measured the height of the test specimen at various temperatures. The bath was connected to a computer, and controlled by the CTE test software. Once all the information

about the sample was entered into the software, a CTE test was then started. The CTE testing machine used two spans of temperature, from 10°C to 50°C and from 50°C to 10°C, to determine the CTE value of the specimen. The test performed at 28 days provides stable and reliable data. Figure 4-23 shows the CTE test setup.

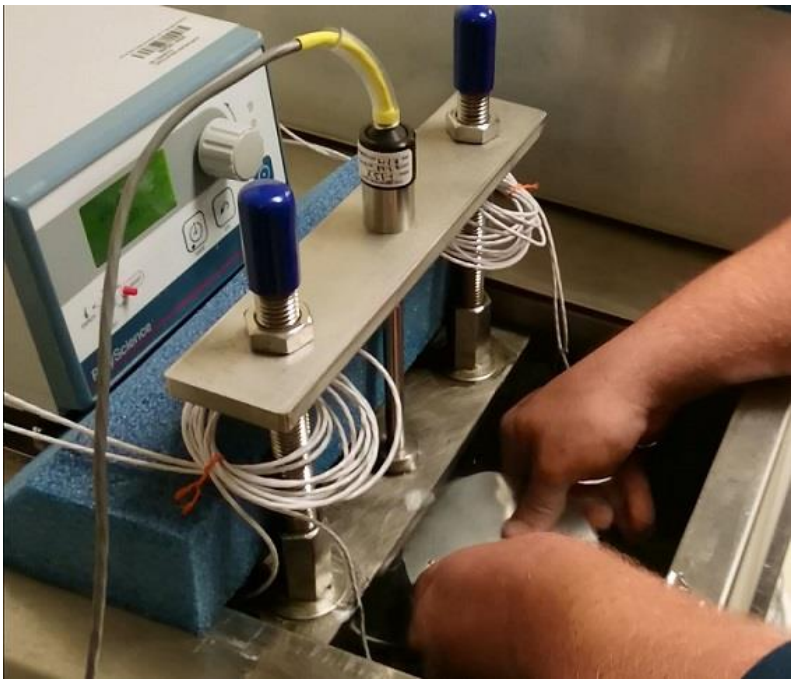

Figure 4-23. CTE test setup

4.3 Analysis of Results of Laboratory Testing Program

4.3.1 Overview

This section presents the results of the laboratory testing program on the standard control concretes and internally cured concrete (ICC). The test results include both fresh and hardened concrete properties. The hardened concrete properties include test results up to six months. Analysis of results and comparison of the standard and ICC mixtures are also made.

4.3.2 Results of Tests on Concrete

These test results from the laboratory testing program are grouped by their w/c ratios. Within a group, the control and ICC mixtures results are presented. The control and ICC

mixtures are named SM and LWA 7 accordingly, and they are followed by their w/c ratios. The number 7 refers to the optimal 7% mass of water to mass of cement for the internal curing system. For example, standard control mix with w/c ratio 0.40 is named SM 0.40 and ICC mix with w/c ratio 0.32 is called LWA 7 0.32.

4.3.2.1 Results of Tests on Fresh Concrete

The allowable ranges of some of the tests on fresh concrete properties, such as air content, temperature, and time of set, are governed by FDOT specifications. Consequently, the target ranges for these properties are specified to be within the FDOT specification ranges. Table 4-12 shows the FDOT specification and target ranges of the fresh concrete properties used. For each mixture, the fresh concrete test results are averaged from two measurements with one measurement being made in each production mix. The fresh concrete test results are presented in Table 4-13.

Table 4-12. FDOT Specification and Target Ranges of Fresh Concrete Properties

Tests	Slump	Air Content	Unit Weight	Temperature	Time of Set , Initial	Time of Set , Final	Bleeding
	(in)	(%)	(lb/ft3)	(F)	(min)	(min)	(ml/cm2)
FDOT Specification	1 to 6	1 to 6	NA	68 to 86	-60 to +90	-60 to +90	NA
Target	2 to 4	2 to 4	NA	68 to 86	NA	NA	NA

Table 4-13. Average Fresh Concrete Properties of the Mixtures Tested

w/c ratio	Mixture	Slump (in)	Air Content (%)	Unit Weight (lb/ft^3)	Temper-ature (°F)	Time of Set, Initial (min)	Time of Set, Final (min)	Bleeding (ml/cm^2)
0.40	SM	2.50	2.50%	142.25	75.0	335	465	0.099
	compliance	√√[2]	√√	-	√√	-	-	-
	LWA 7	5.25	2.00%	136.25	75.5	340	475	0.105
	compliance	√[1]	√√	-	√√	-	-	-
0.36	SM	2.75	2.75%	142.25	75.0	345	450	0.331
	compliance	√√	√√	-	√√	-	-	-
	LWA 7	3.75	2.00%	135.75	75.0	350	450	0.328
	compliance	√√	√√	-	√√	-	-	-
0.32	SM	6.00	3.75%	141.25	74.0	415	520 (proj)*	0.006
	compliance	√	√√	-	√√	-	-	-
	LWA 7	3.00	2.50%	134.25	75.0	360	470 (proj)	0.002
	compliance	√√	√√	-	√√	-	-	-

[1] √ the results comply with FDOT specs only * projected result

[2] √√ the results comply with both FDOT specs and the classification target

4.3.2.2 Results of Tests on Hardened Concrete

The hardened concrete properties measured include compressive strength, flexural strength, modulus of elasticity, splitting tensile strength, restrained shrinkage, and drying shrinkage. Similar to the fresh concrete properties, the compressive strength is regulated by FDOT specifications. The specification requires achievement of two strengths; one is minimum requirement and the other is over-designed requirement as described in the mix design section of the specification. The requirements for each concrete class are shown in Table 4-11.

Compressive strength

The average compressive strength for each mix is computed from the strengths of three 4" x 8" cylinders from one production mix and three 4" x 8" cylinders from another production

mix, with a total of six cylinders. The average strength results are shown in Table 4-14. Figure 4-24 presents the plots of the average compressive strengths by their w/c ratios

Table 4-14. Average Compressive Strength of the Concrete Mixtures Used

Curing Time	Compressive Strength (psi)					
	0.40 w/c ratio		0.36 w/c ratio		0.32 w/c ratio	
(days)	SM 0.40	LWA 7 0.40	SM 0.36	LWA 7 0.36	SM 0.32	LWA 7 0.32
1	3,005	2,620	4,135	3,675	4,480	3,880
3	5,195	4,545	5,985	5,480	6,535	5,890
7	6,170	5,430	6,710	6,305	7,660	6,905
28	7,785	6,945	8,230	7,635	8,860	7,870
91	8,090	6,940	8,525	7,835	9,150	8,075
182	7,860	6,800	7,920	7,100	8,775	8,070

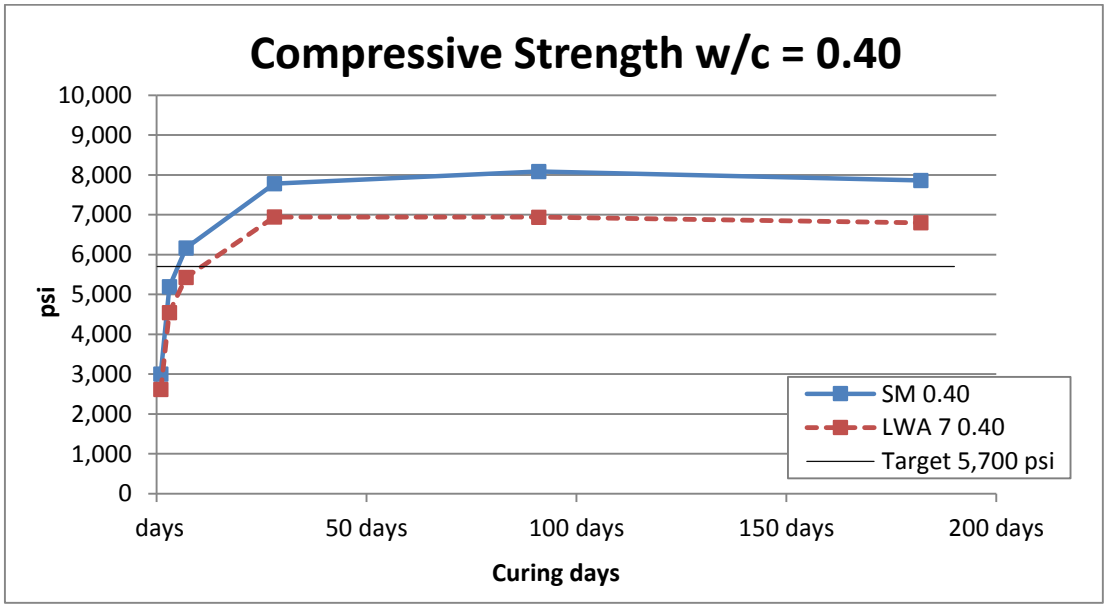

Figure 4-24a. Average compressive strengths of concrete with 0.40 w/c ratio at various curing times.

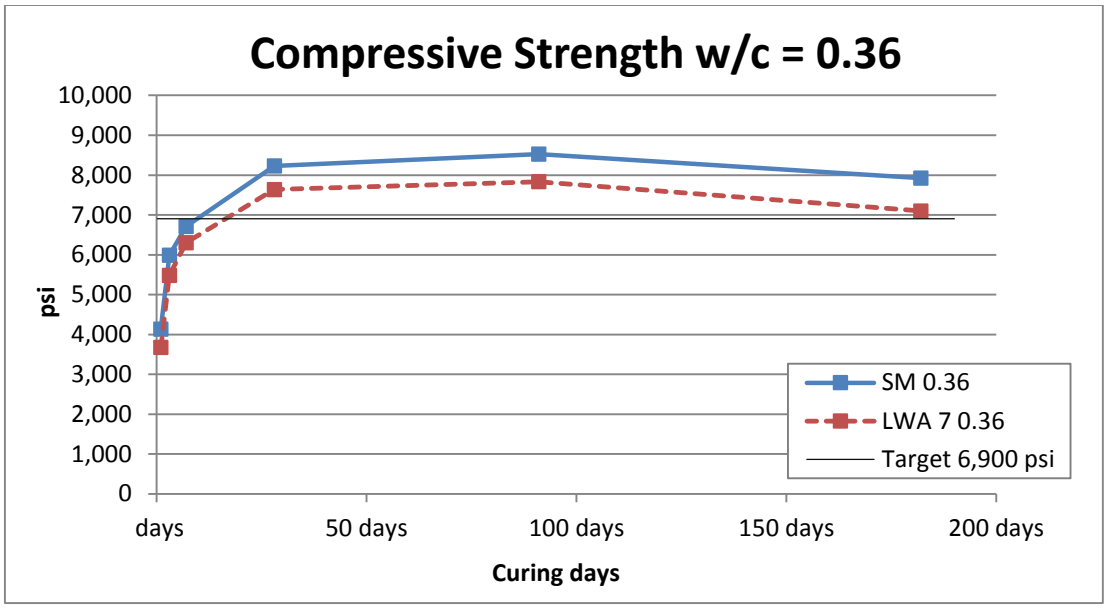

Figure 4-24b. Average compressive strengths of concrete with 0.36 w/c ratio at various curing times.

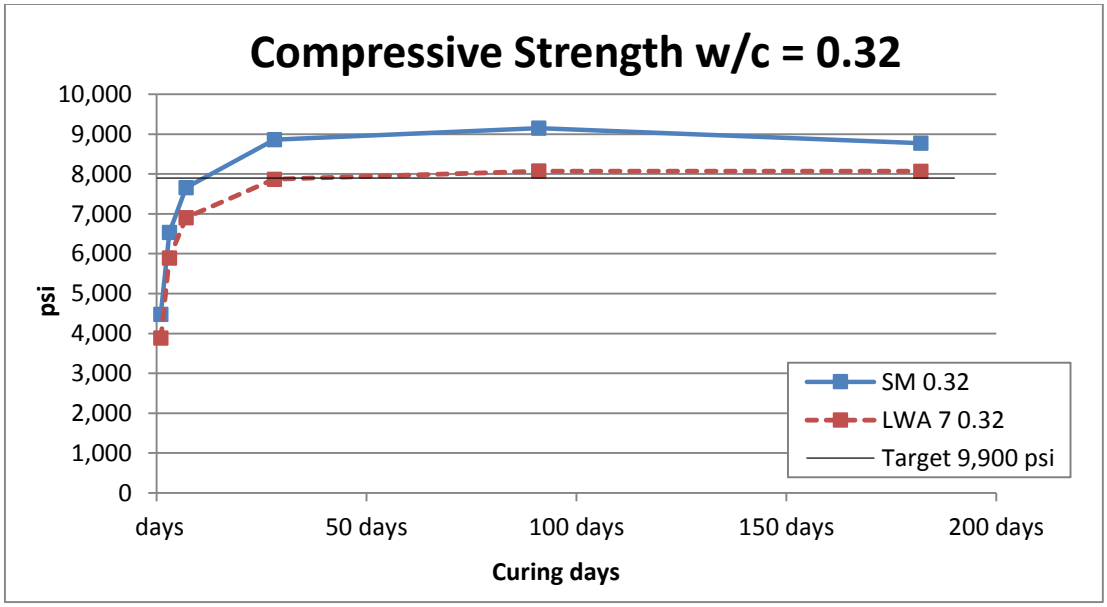

Figure 4-24c. Average compressive strengths of concrete with 0.32 w/c ratio at various curing times.

Flexural strength

The average flexural strength of each mix is computed from the strengths of three 4" x 4" x 14" beams from one production mix and three 4" x 4" x 14" beams from another production mix, with a total of six beams. The average strength results are shown in Table 4-15. Figure 4-25 presents the plots of the average flexural strengths by their w/c ratios.

Table 4-15. Average Flexural Strength of the Concrete Mixtures Used

Curing Time	Flexural Strength (psi)					
	0.40 w/c ratio		0.36 w/c ratio		0.32 w/c ratio	
(days)	SM 0.40	LWA 7 0.40	SM 0.36	LWA 7 0.36	SM 0.32	LWA 7 0.32
7	675	673	683	718	790	753
28	834	784	898	829	953	820
91	845	773	948	880	1,018	945
182	760	648	895	875	960	893

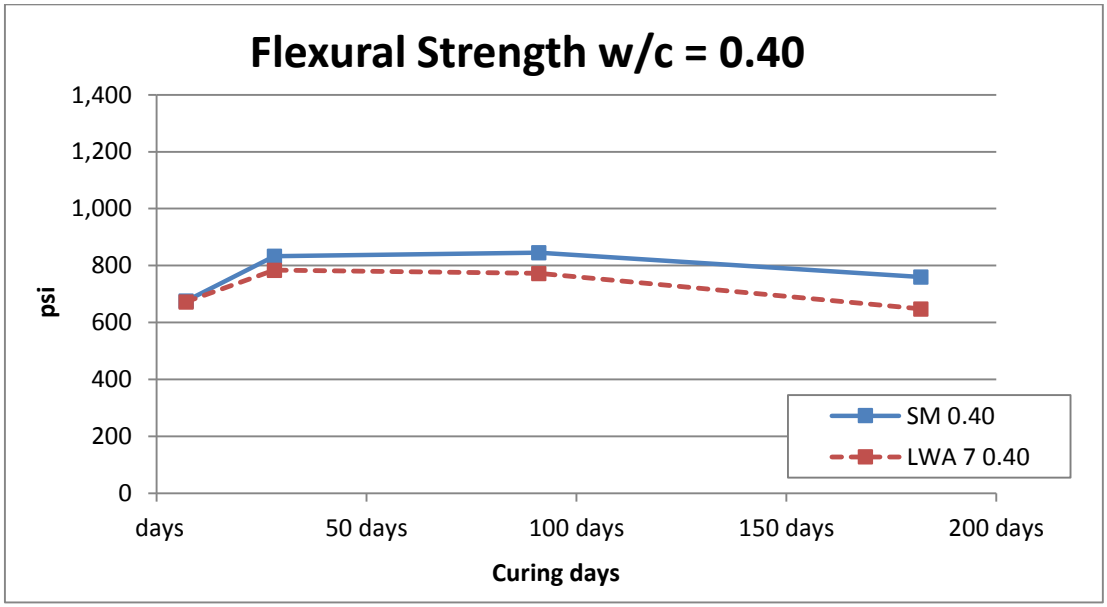

Figure 4-25a. Average flexural strengths of concrete with 0.40 w/c ratio at various curing times.

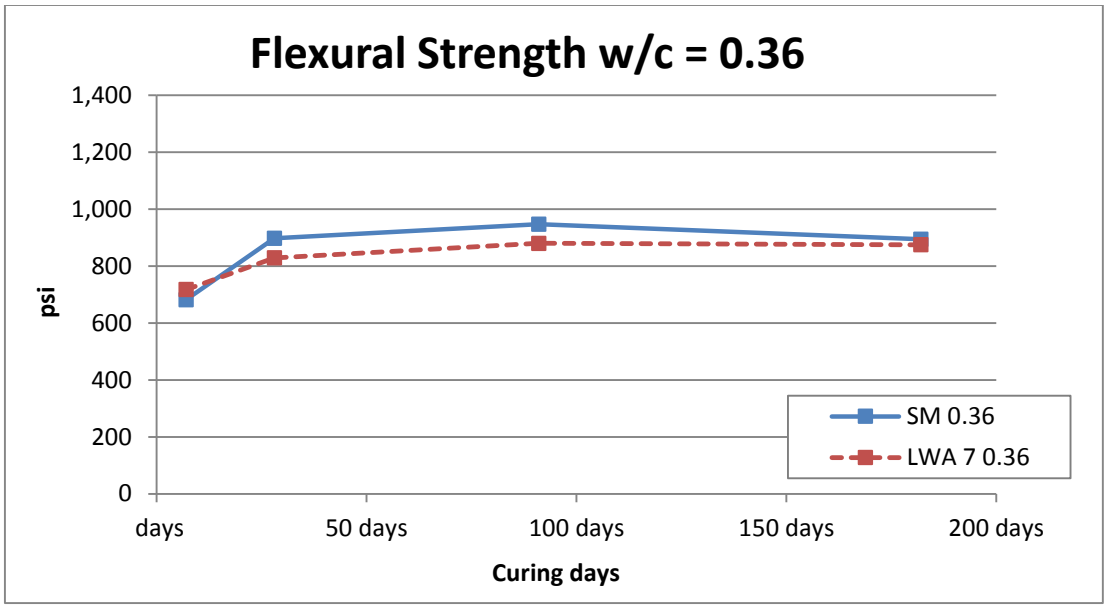

Figure 4-25b. Average flexural strengths of concrete with 0.36 w/c ratio at various curing times.

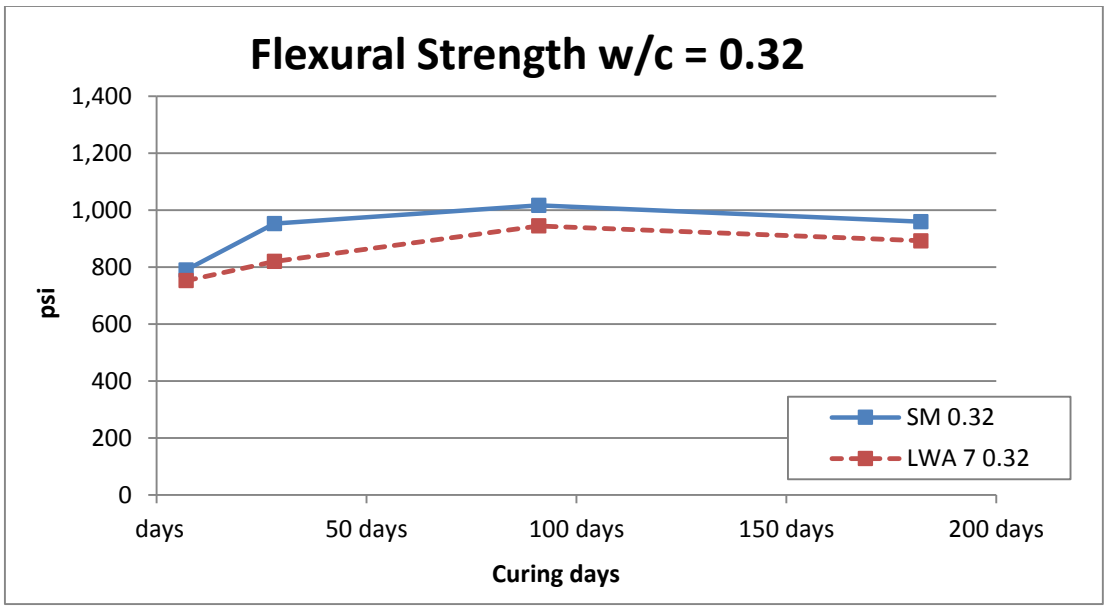

Figure 4-25c. Average flexural strengths of concrete with 0.32 w/c ratio at various curing times.

Modulus of elasticity

The average modulus of elasticity (MOE) of each mix is computed from the MOEs of three 4" x 8" cylinders from one production mix and three 4" x 8" cylinders from another production mix, with a total of six cylinders. The MOE results are shown in Table 4-16. Figure 4-26 presents the plots of the average MOE by their w/c ratios.

Table 4-16. Average Moduli of Elasticity of the Concrete Mixtures Used

Curing Time	MOE, (Mpsi)					
	0.40 w/c ratio		0.36 w/c ratio		0.32 w/c ratio	
(days)	SM 0.40	LWA 7 0.40	SM 0.36	LWA 7 0.36	SM 0.32	LWA 7 0.32
7	4.68	3.78	4.65	3.83	4.88	3.90
28	4.70	3.90	4.78	3.93	4.90	4.05
91	4.53	3.80	4.65	3.80	4.85	4.05
182	4.53	3.73	4.38	3.65	4.88	3.90

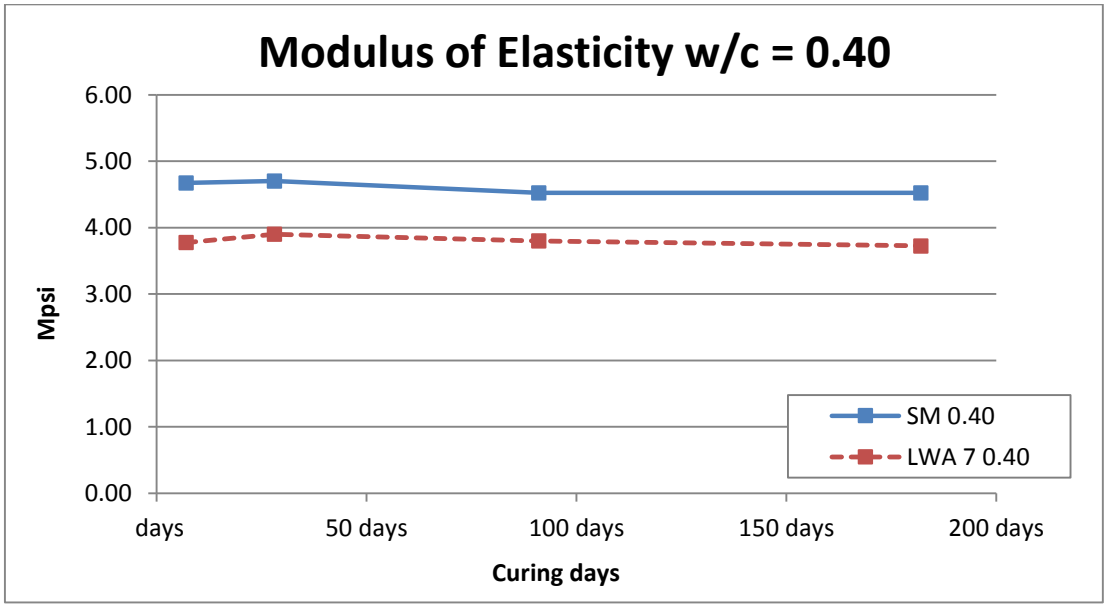

Figure 4-26a. Average moduli of elasticity of concrete with 0.40 w/c ratio at various curing times.

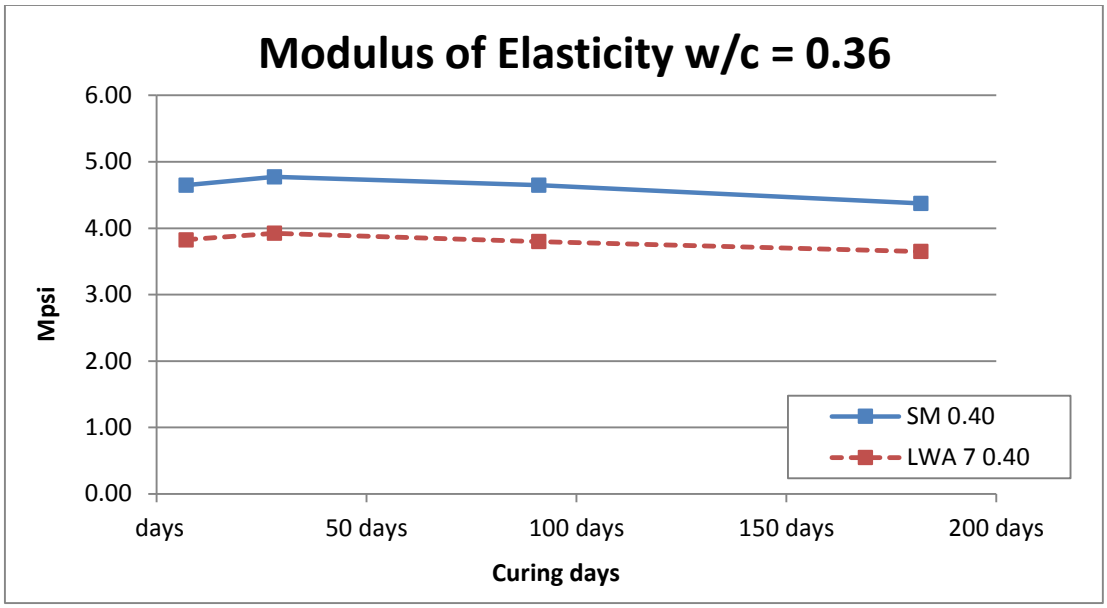

Figure 4-26b. Average moduli of elasticity of concrete with 0.36 w/c ratio at various curing times.

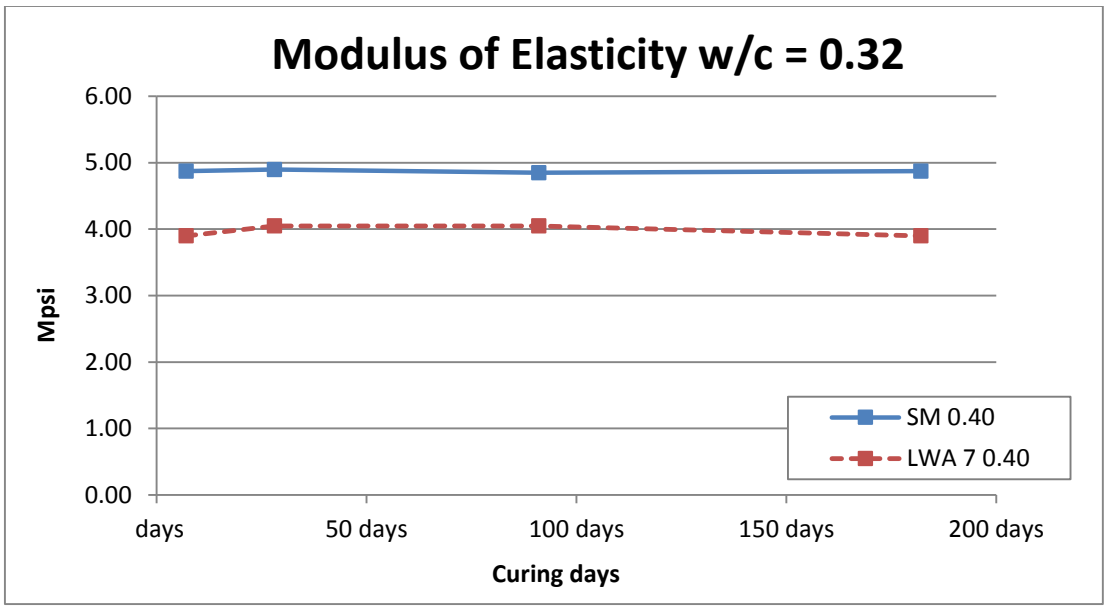

Figure 4-26c. Average moduli of elasticity of concrete with 0.32 w/c ratio at various curing times.

Splitting tensile strength

The average splitting tensile strength of each mix is computed from the strengths of three 4" x 8" cylinders from one production mix and three 4" x 8" cylinders from another production mix, with a total of six cylinders. The samples were the ones from the MOE test samples. The strength results are shown in Table 4-17. Figure 4-27 presents the plots of the average splitting tensile strengths by their w/c ratios

Table 4-17. Average Splitting Tensile Strength of the Concrete Mixtures Used

Curing Time	Splitting tensile strength (psi)					
	0.40 w/c ratio		0.36 w/c ratio		0.32 w/c ratio	
(days)	SM 0.40	LWA 7 0.40	SM 0.36	LWA 7 0.36	SM 0.32	LWA 7 0.32
7	578	423	570	463	673	605
28	603	580	653	605	668	630
91	600	560	615	523	573	588
182	545	525	558	478	583	538

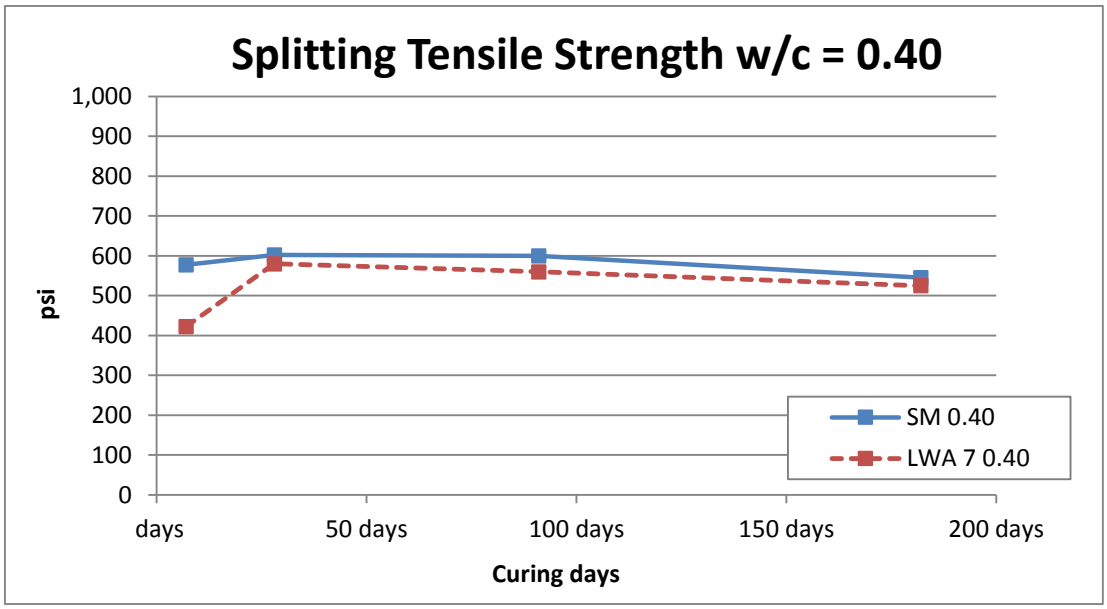

Figure 4-27a. Average splitting tensile strengths of concrete with 0.40 w/c ratio at various curing times.

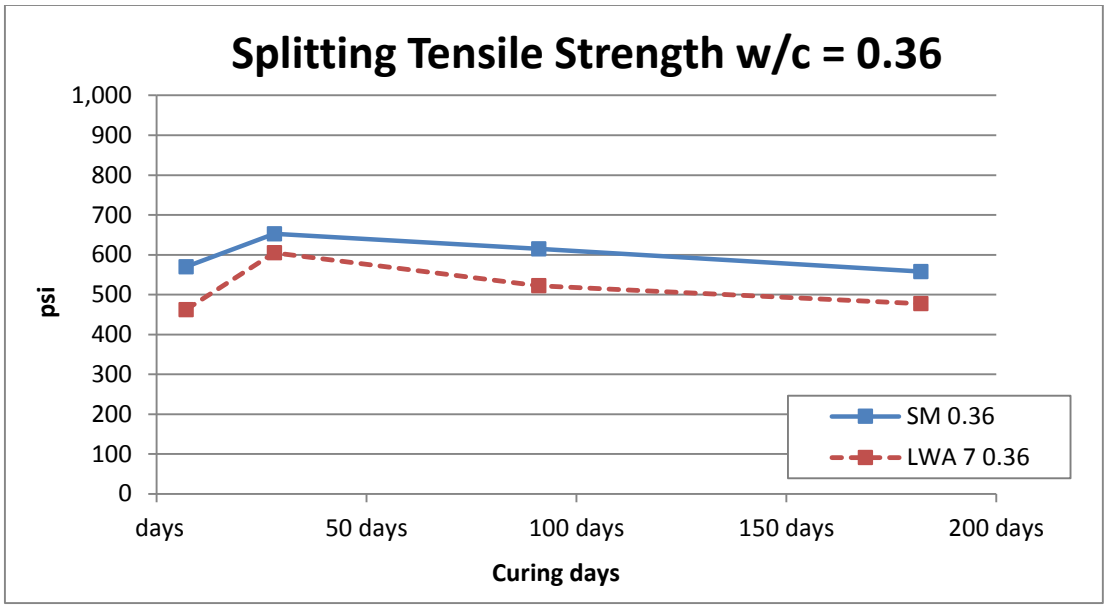

Figure 4-27b. Average splitting tensile strengths of concrete with 0.36 w/c ratio at various curing times.

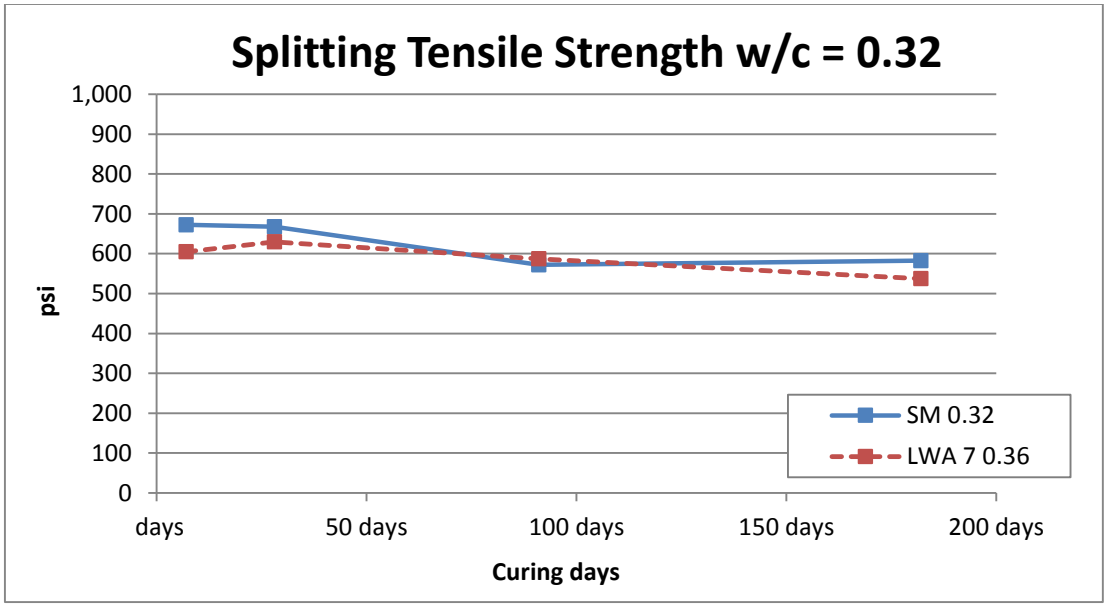

Figure 4-27c. Average splitting tensile strengths of concrete with 0.32 w/c ratio at various curing times.

Restrained shrinkage

The ages at which the restrained concrete rings cracked are shown in Table 4-18. Figure 4-28 shows the information of the strain history and cracking moments of the mixture at w/c ratio of 0.40; Figure 4-29 shows the information of the strain history and cracking moments of the mixture with w/c ratio of 0.36; Figure 4-30 shows the information of the strain history and cracking moments of the mixture with w/c ratio of 0.32

Table 4-18. Age of Cracking of Restrained Shrinkage Rings of the Concretes Tested

Rings	Age of cracking, (day)											
	0.40 w/c ratio				0.36 w/c ratio				0.32 w/c ratio			
	SM 0.40		LWA 7 0.40		SM 0.36		LWA 7 0.36		SM 0.32		LWA 7 0.32	
	Ring no.1	Ring no.2	Ring no.1	Ring no.2	Ring no.1	Ring no.2	Ring no.1	Ring no.2	Ring no.1	Ring no.2	Ring no.1	Ring no.2
Individual Rings	6	1	11	11	1	1	1	1	1	1	5	3
Average	3.5		11		1		1		1		4	

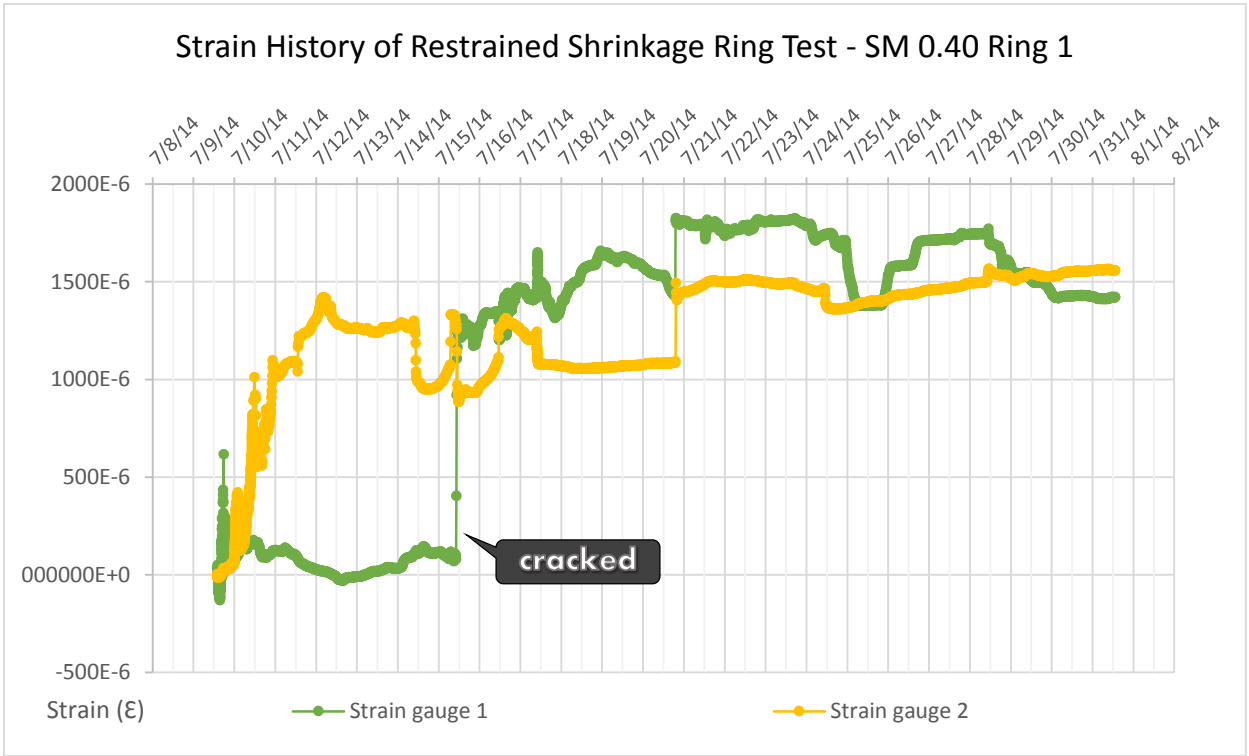

Figure 4-28a. Strain history of standard control mixture with 0.40 w/c ratio for ring 1.

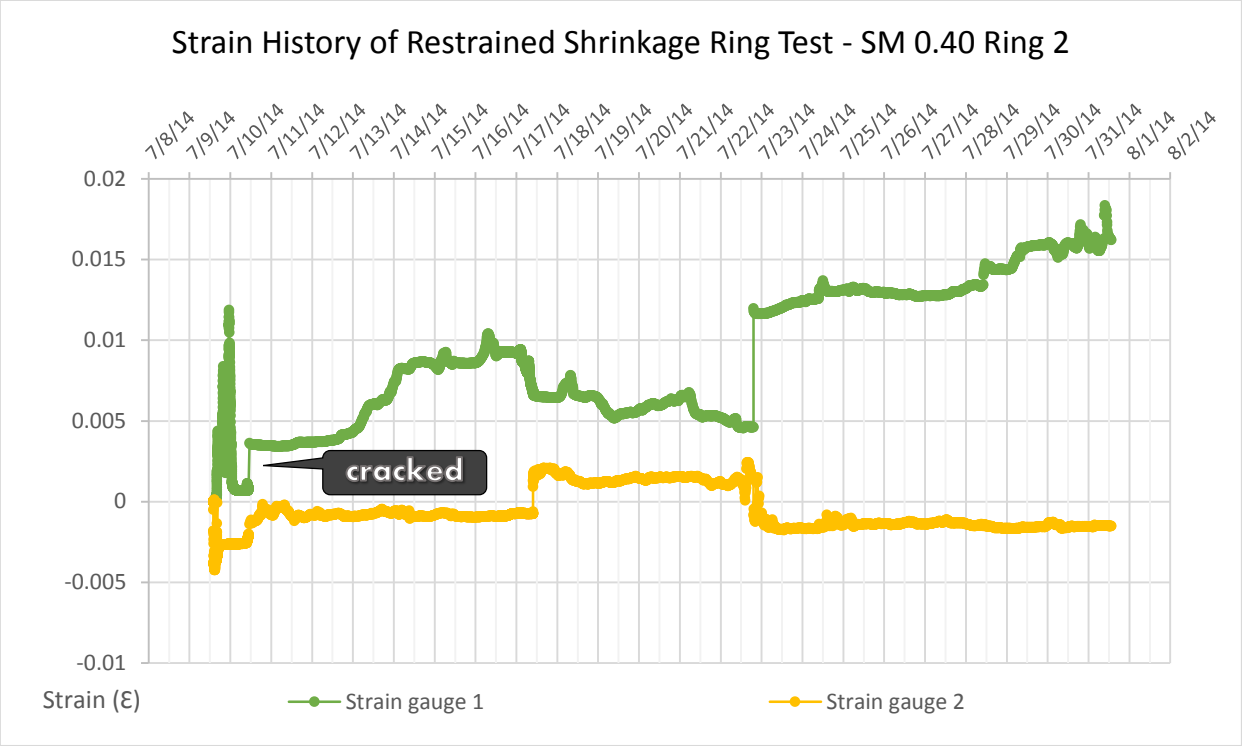

Figure 4-28b. Strain history of standard control mixture with 0.40 w/c ratio for ring 2.

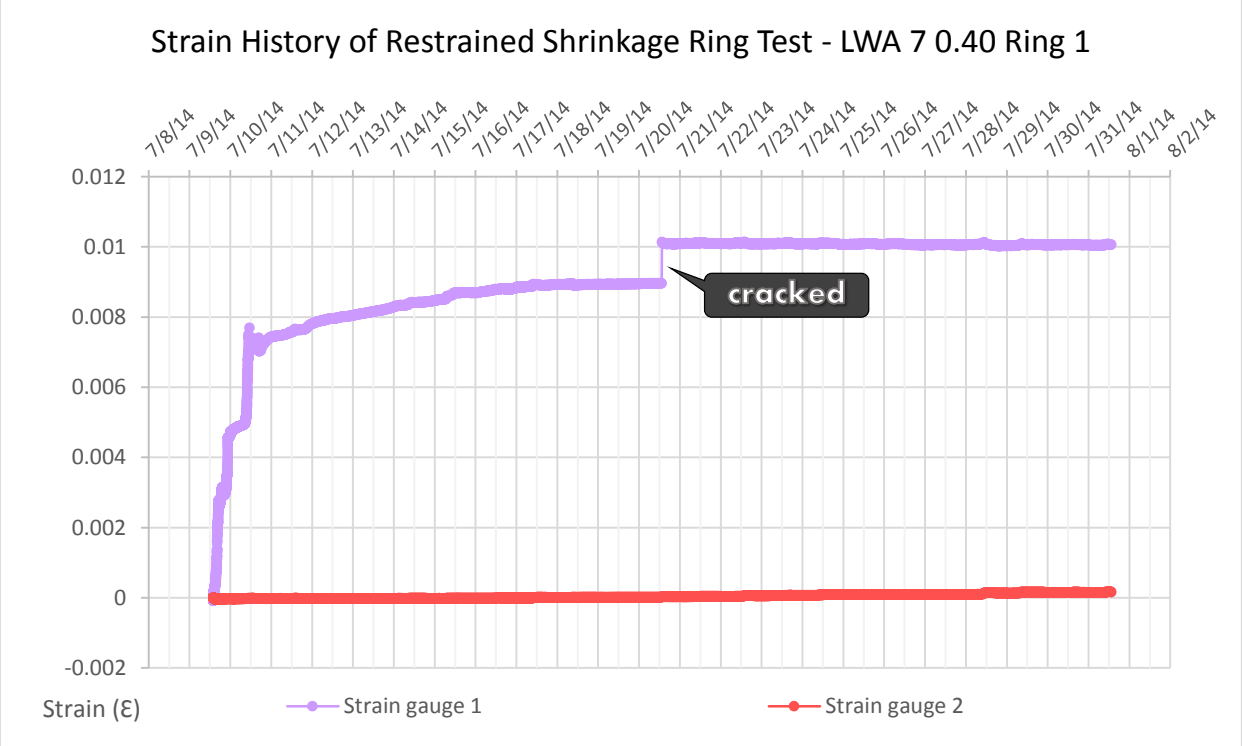

Figure 4-28c. Strain history of ICC mixture with 0.40 w/c ratio for ring 1.

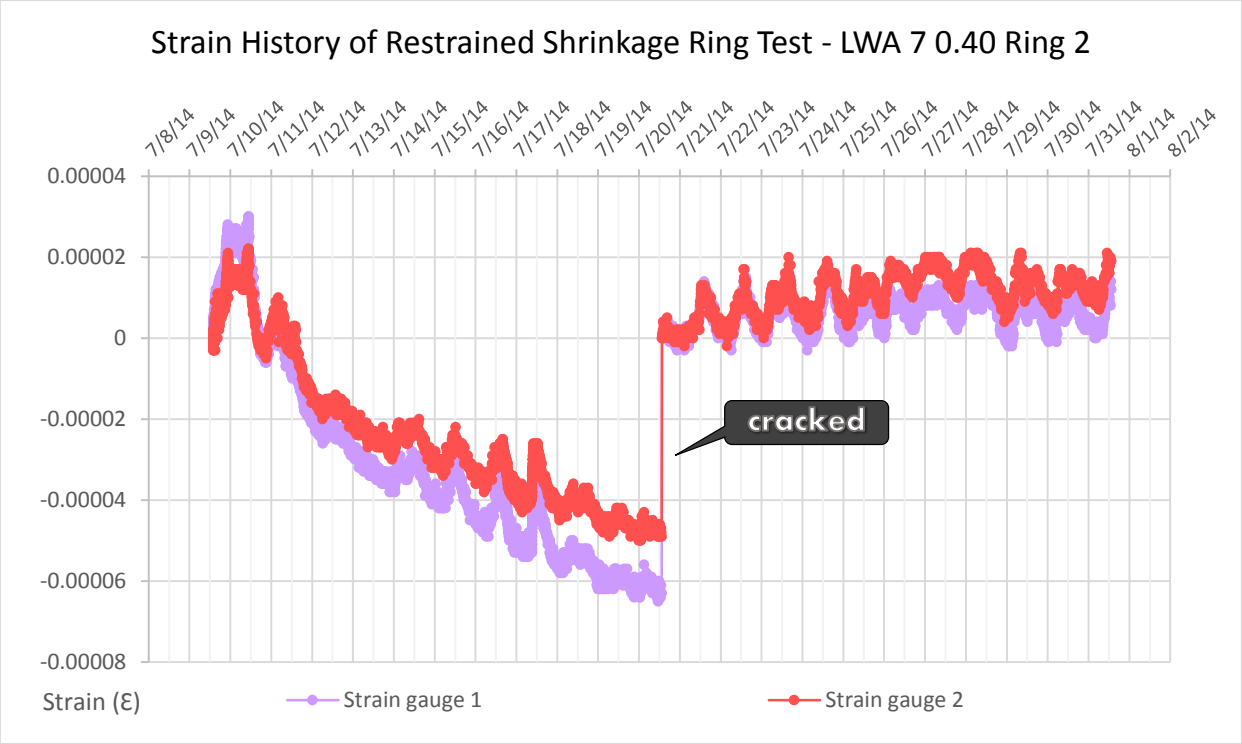

Figure 4-28d. Strain history of ICC mixture with 0.40 w/c ratio for ring 2.

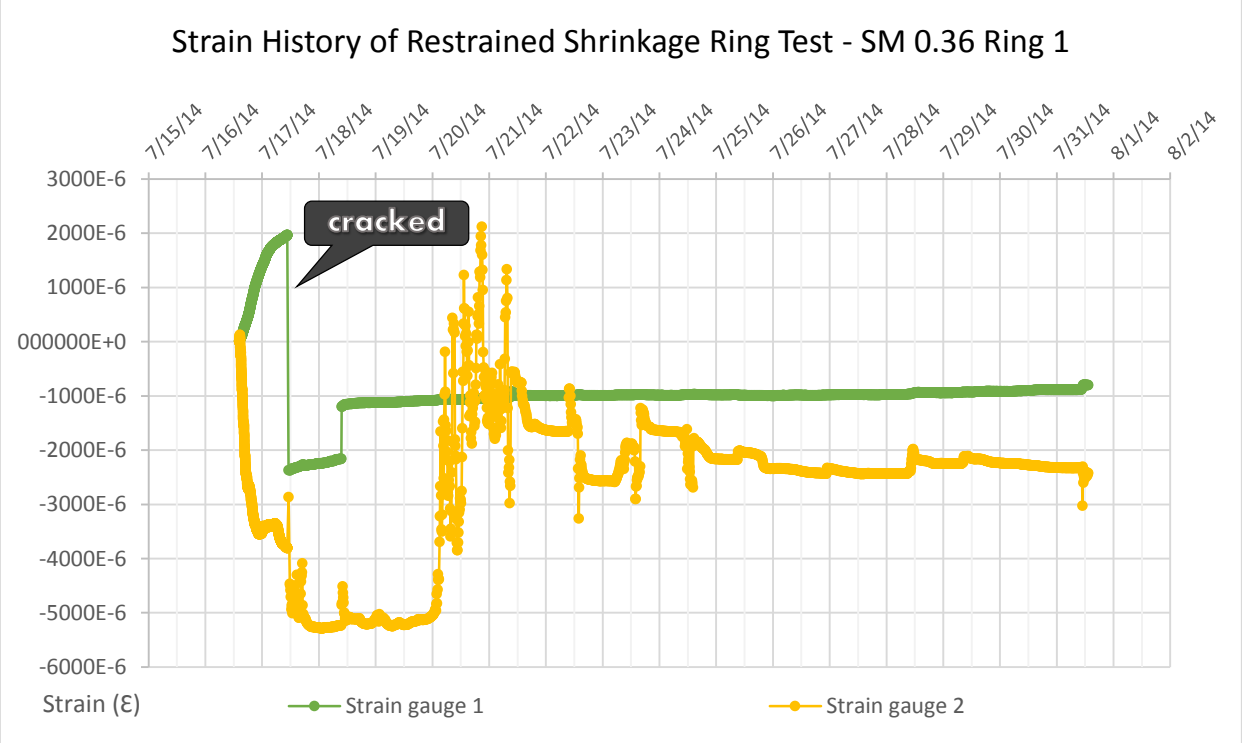

Figure 4-29a. Strain history of standard control mixture with 0.36 w/c ratio for ring 1.

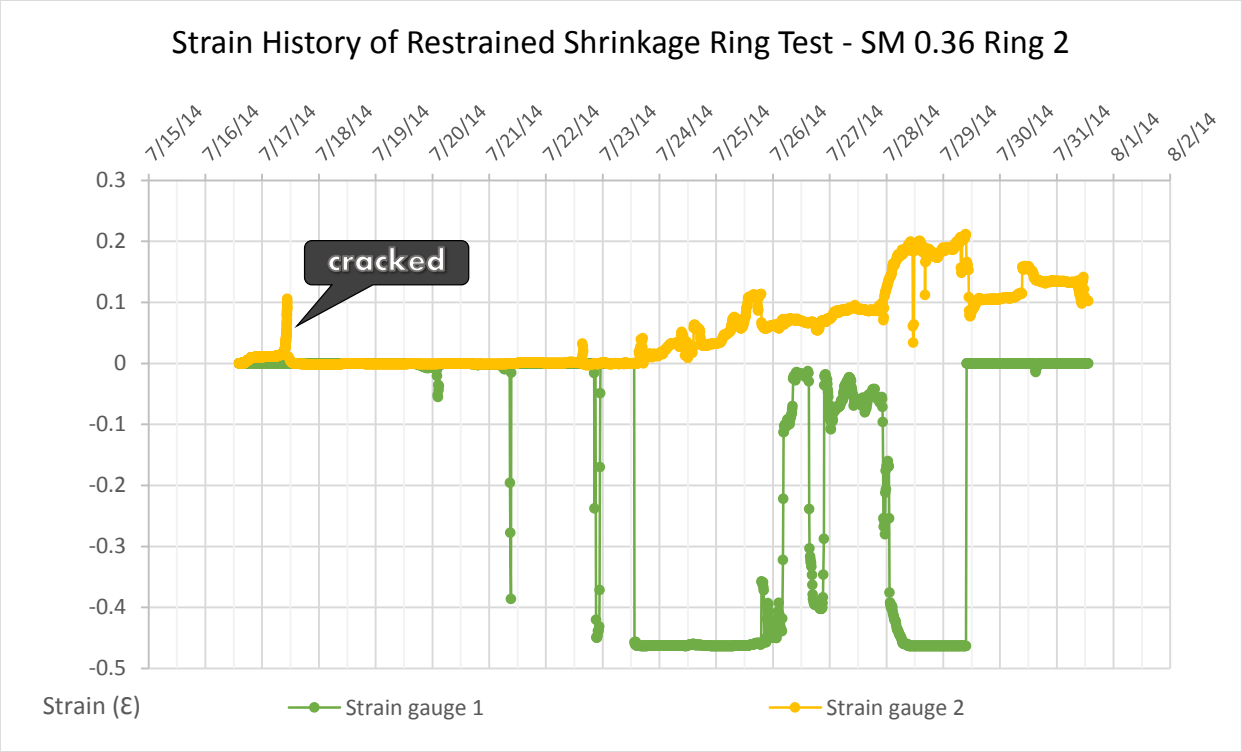

Figure 4-29b. Strain history of standard control mixture with 0.36 w/c ratio for ring 2.

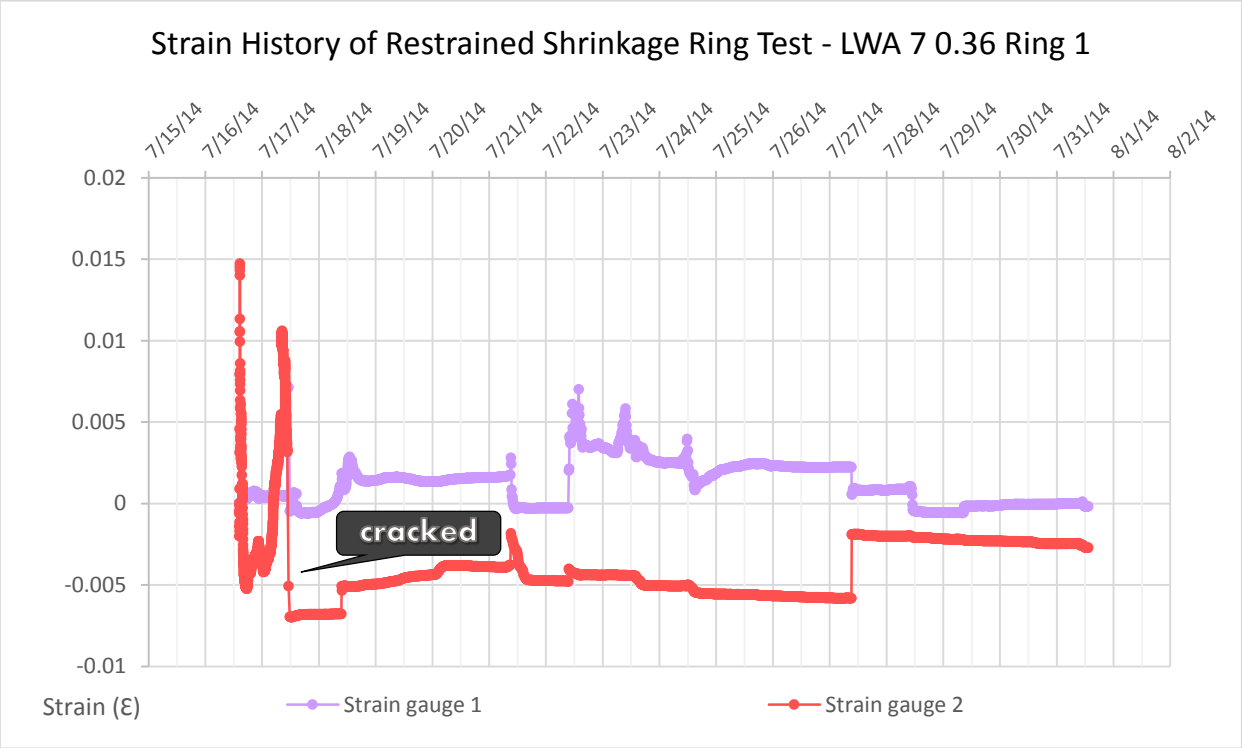

Figure 4-29c. Strain history of ICC mixture with 0.36 w/c ratio for ring 1.

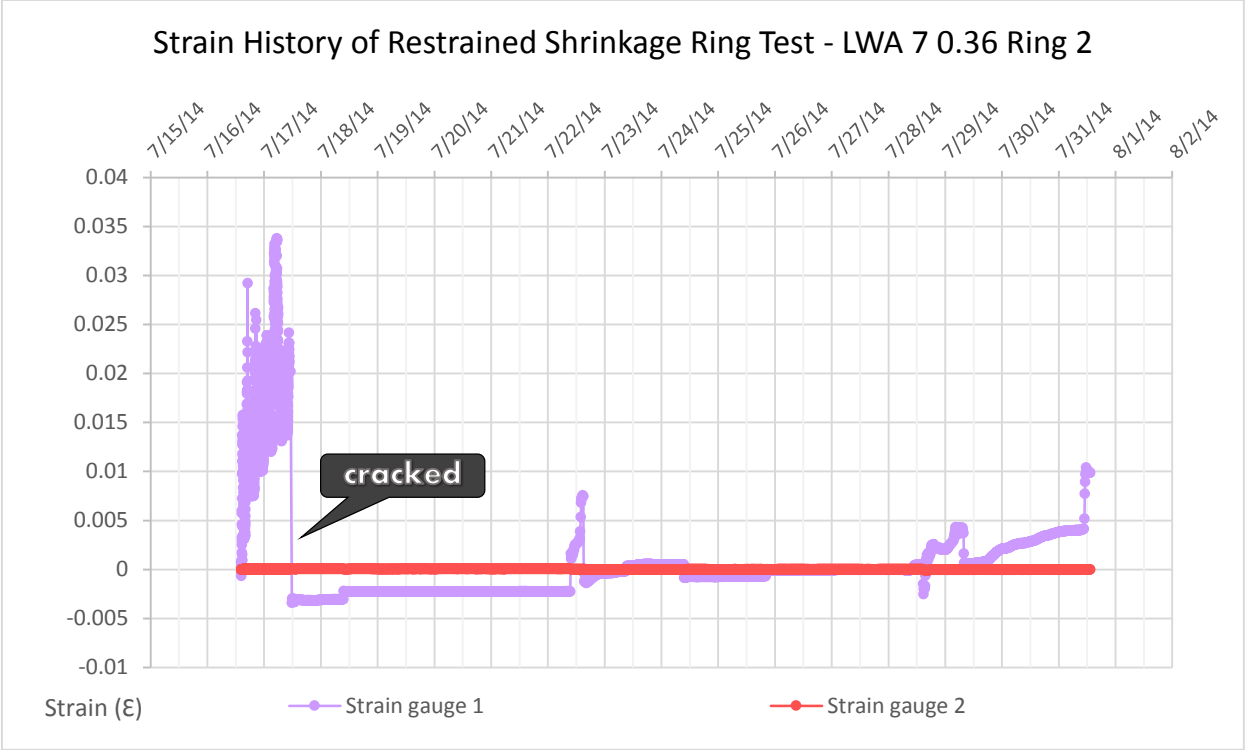

Figure 4-29d. Strain history of ICC mixture with 0.36 w/c ratio for ring 2.

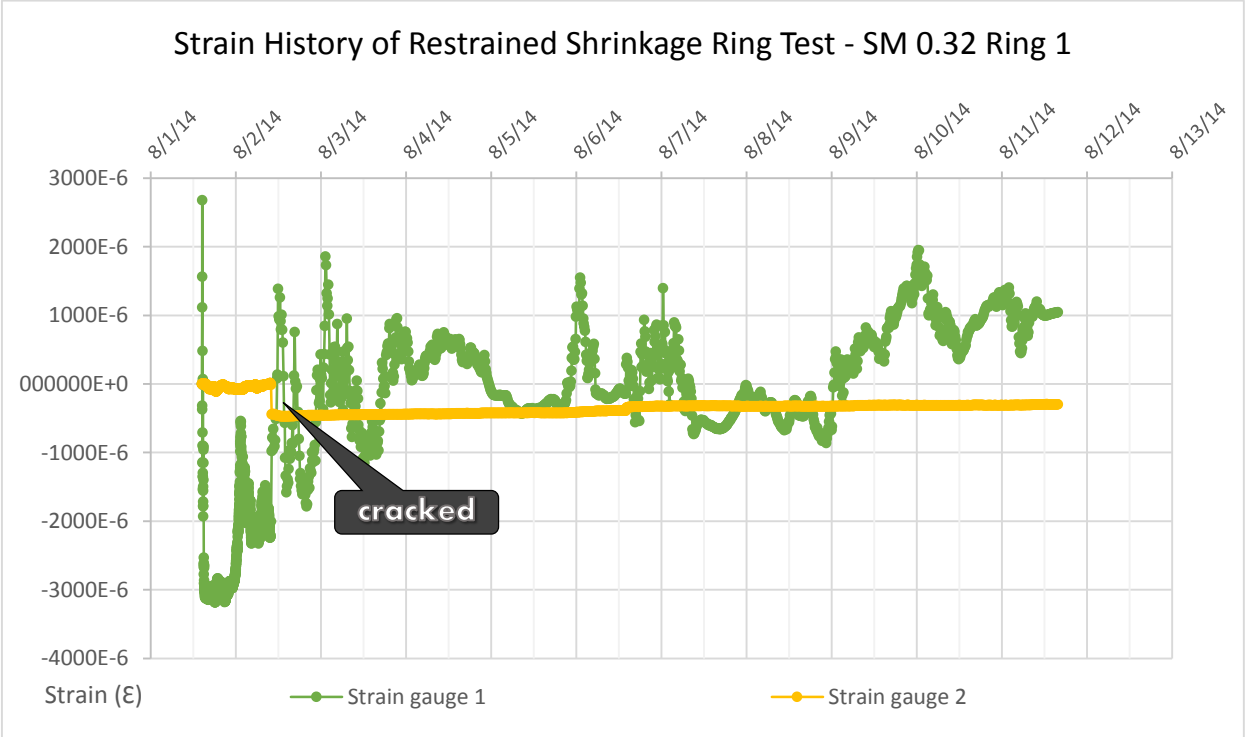

Figure 4-30a. Strain history of standard control mixture with 0.32 w/c ratio for ring 1.

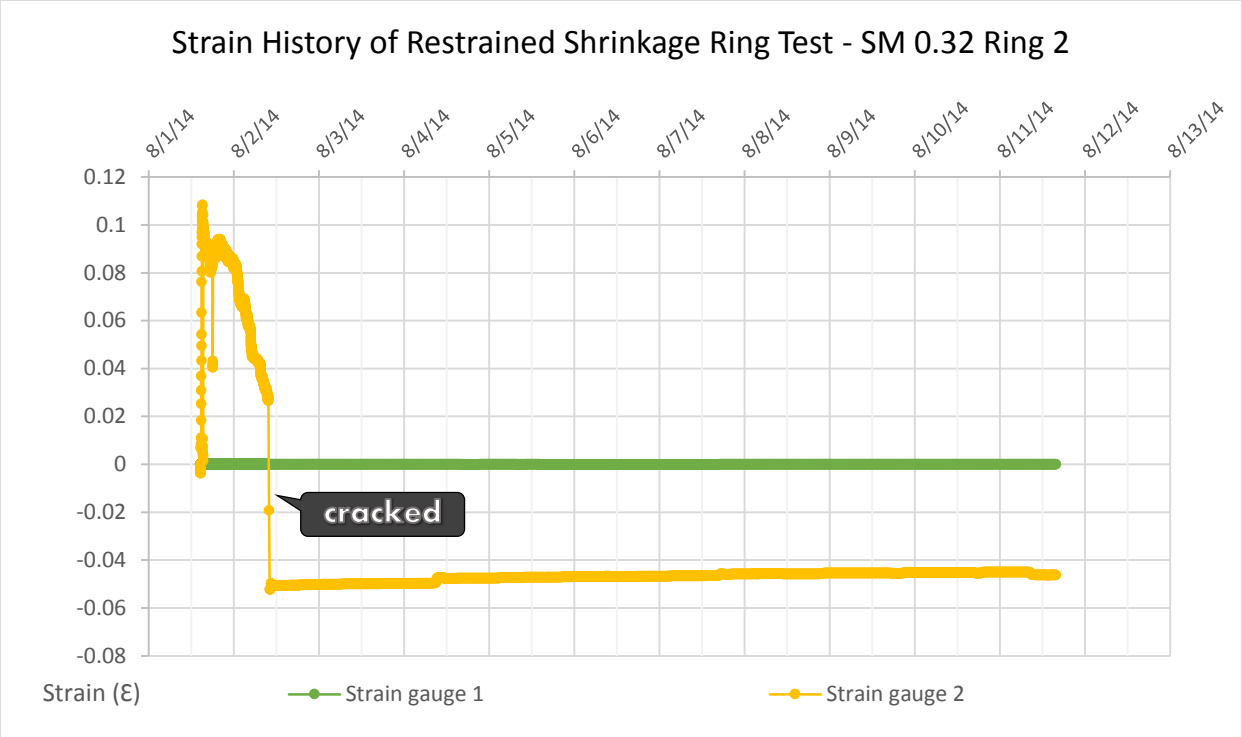

Figure 4-30b. Strain history of standard control mixture with 0.32 w/c ratio for ring 2.

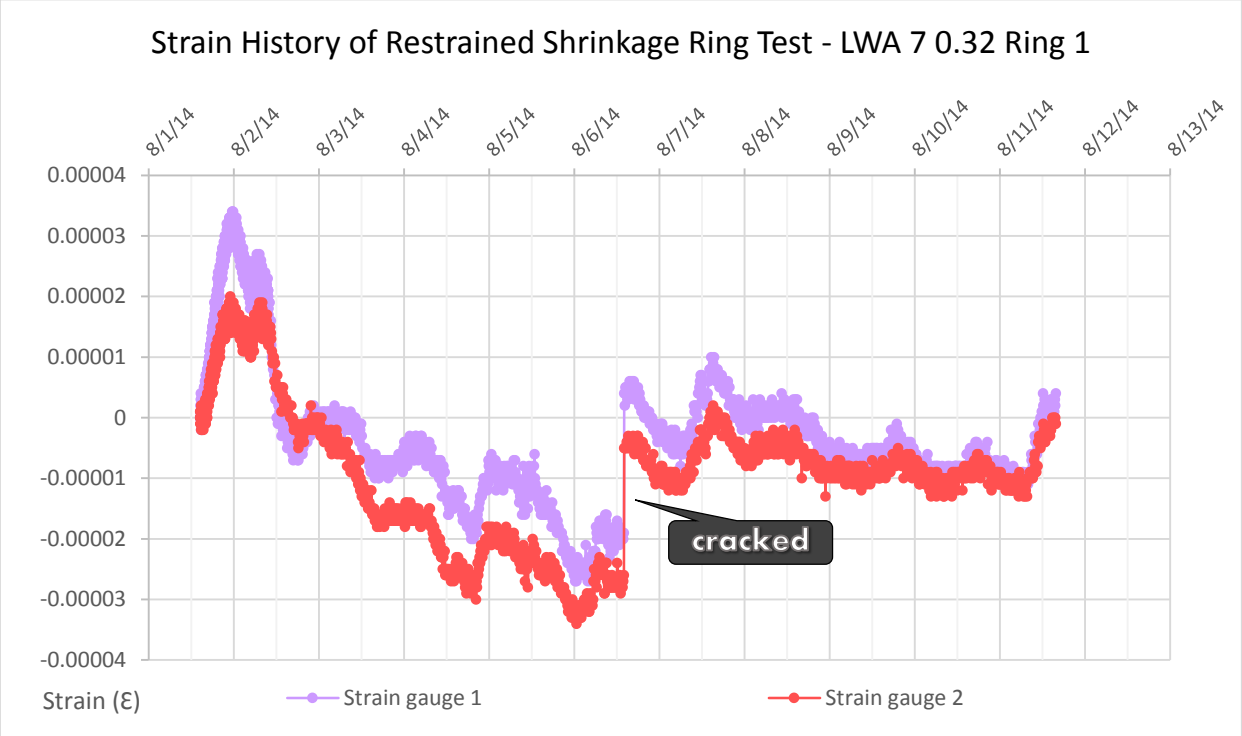

Figure 4-30c. Strain history of ICC mixture with 0.32 w/c ratio for ring 1.

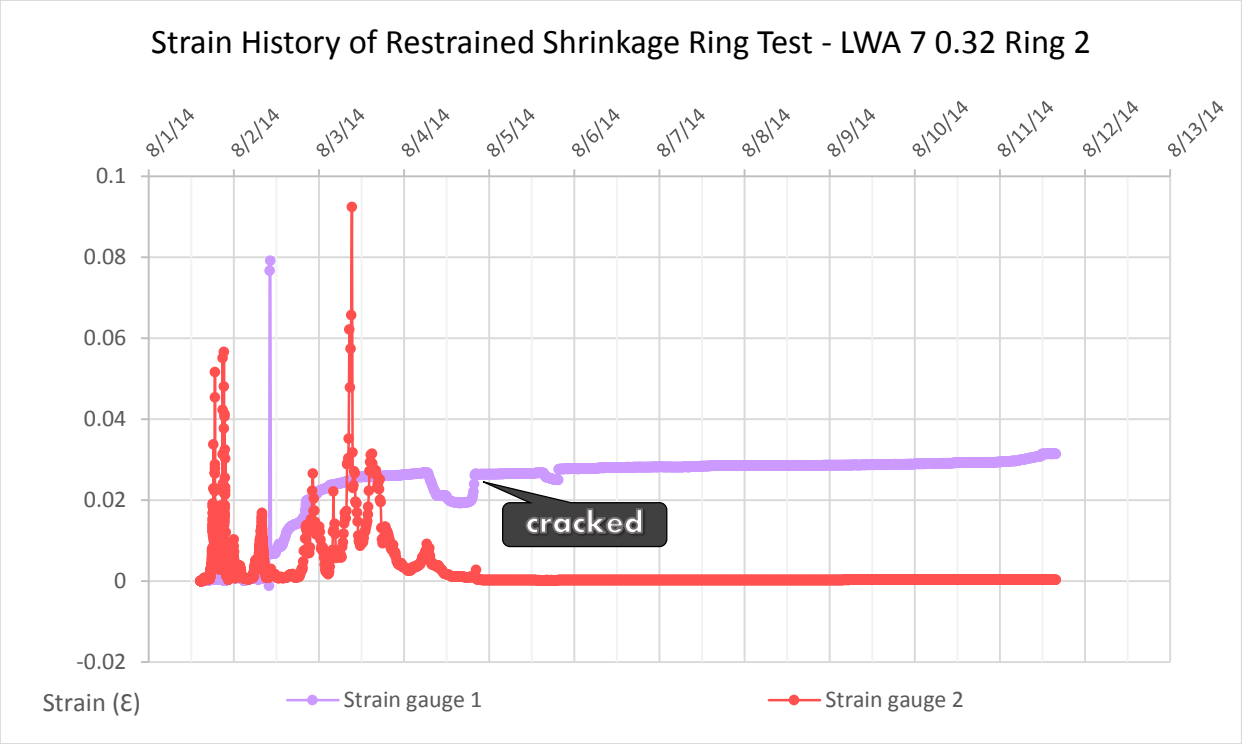

Figure 4-30d. Strain history of ICC mixture with 0.32 w/c ratio for ring 2.

Drying shrinkage

The average drying shrinkages for each mix are computed from the drying shrinkage values of six 3" x 3" x 11.25" prisms from one production mix and six 3" x 3" x 11.25" prisms from another production mix, with a total of 12 prisms. The shrinkage results are shown in Table 4-19. Figure 4-31 presents the plots of the average drying shrinkages by their w/c ratios.

Table 4-19. Average Drying Shrinkages of the Concrete Mixtures Tested

Curing Time	Drying shrinkage (Ɛ)					
	0.40 w/c ratio		0.36 w/c ratio		0.32 w/c ratio	
(days)	SM 0.40	LWA 7 0.40	SM 0.36	LWA 7 0.36	SM 0.32	LWA 7 0.32
7	180E-6	-235E-6	-5E-6	-45E-6	-45E-6	-60E-6
28	-250E-6	-300E-6	-310E-6	-365E-6	-290E-6	-355E-6
91	-355E-6	-410E-6	-360E-6	-410E-6	-315E-6	-415E-6
182	-300E-6	-385E-6	-350E-6	-470E-6	-350E-6	-415E-6
364	-275E-6	-360E-6	-290E-6	-375E-6	-335E-6	-395E-6

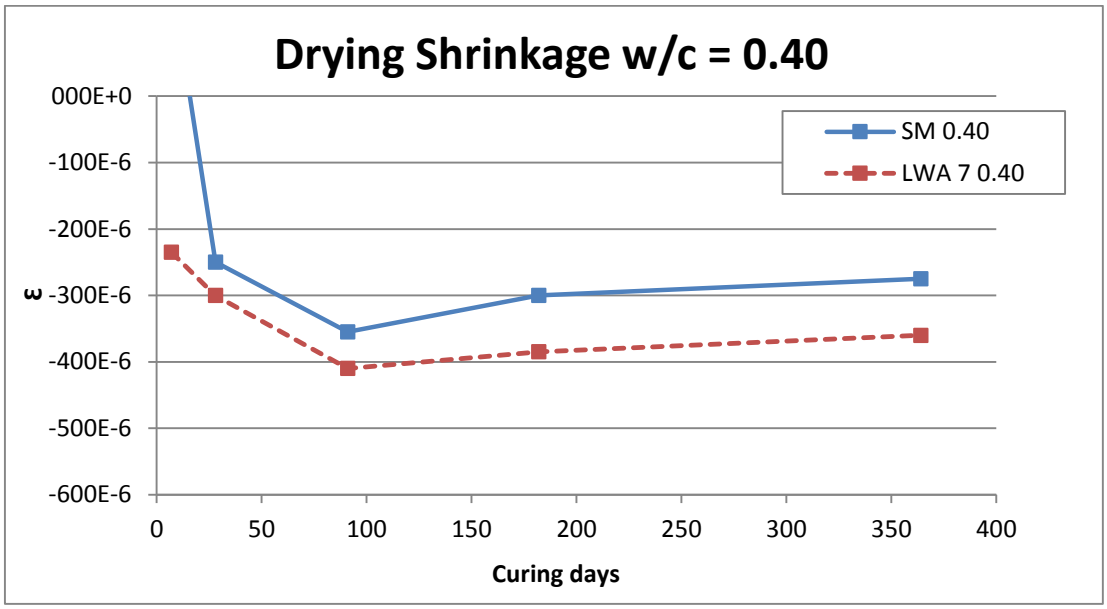

Figure 4-31a. Average drying shrinkages of concrete with 0.40 w/c ratio at various curing time

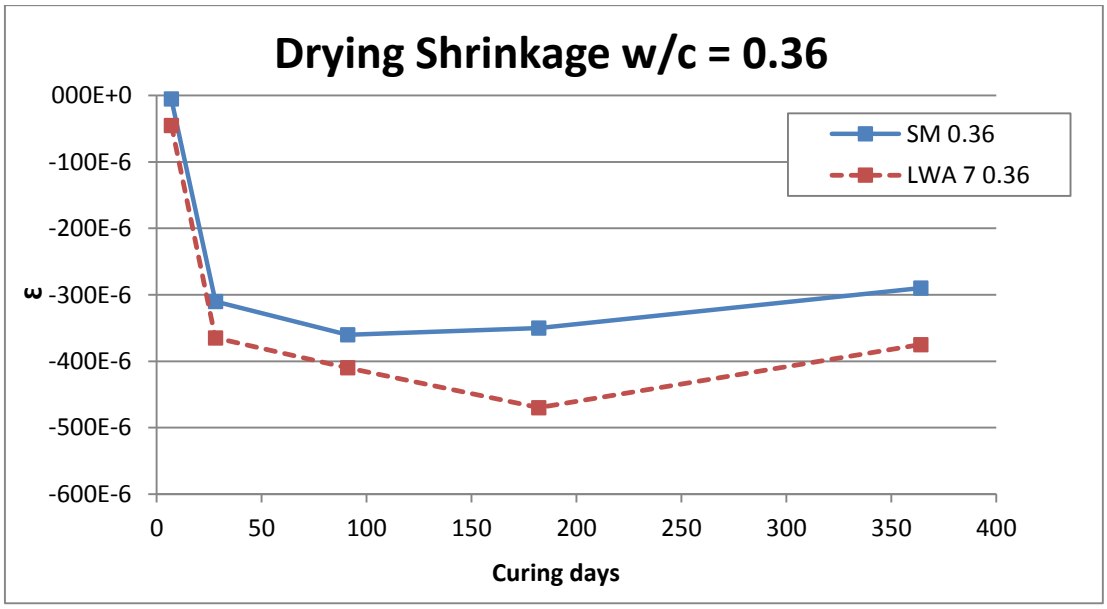

Figure 4-31b. Average drying shrinkages of concrete with 0.36 w/c ratio at various curing time

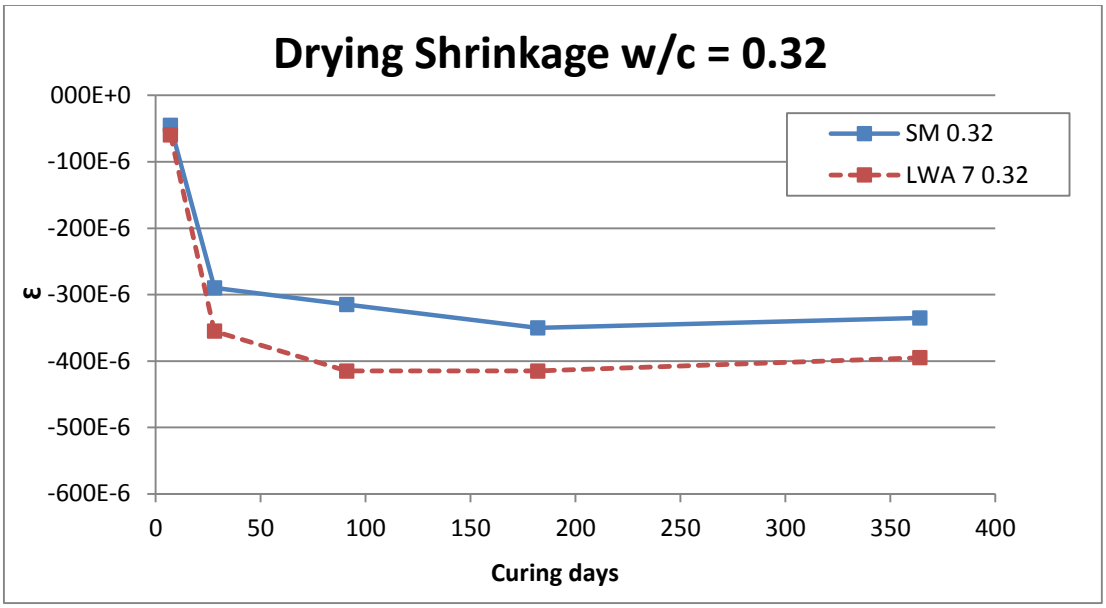

Figure 4-31c. Average drying shrinkages of concrete with 0.32 w/c ratio at various curing time

Coefficient of thermal expansion (CTE)

Concrete samples from MOE test were re-used in CTE test. Only the mixtures with 0.36 w/c ratio were tested. CTE values were measured at 127 days. The average CTE values from two replicate specimens per mix are shown in Table 4-20.

Table 4-20. Average CTE Values of the Concrete Mixtures Used

Mixture	Curing Time (days)	CTE (με/°C)
SM 0.36	127	8.1849
LWA 7 0.36	127	7.3404

4.3.3 Analysis of Test Results

This section presents the analysis of the test results to evaluate the advantages and disadvantages of ICC mixtures as compared with the conventional concrete. The properties of these concretes will also be evaluate by FDOT standard specifications.

4.3.3.1 Analysis of Fresh Concrete Properties

Mixtures with 0.40 w/c ratio

For mixtures with 0.40 w/c ratio, slumps for SM and ICC were 2.50 and 5.25 inches, respectively. Both complied with the FDOT specification of 1 to 6 inches, but only the SM's slump fell within the 2 to 4 inches required for that class of concrete. Air contents for SM and ICC were 2.50 % and 2.00 %, respectively. Both results are within the FDOT specification of 1 to 6 percent and the target of 2 to 4 percent. From the combination of the slump and air content results, visual observation, experience in performing the tests, and consolidation of the test specimens, the mixture's workability was very good. In terms of temperature, SM and ICC concrete temperature was 75.0° and 75.5° F, respectively. Both results are well within the 68° to 86° F range of the FDOT specification and target values. The FDOT specification and the target ranges of fresh concrete properties are shown in the Table 4-12 in the section 4.3.2.1.

Initial and final setting times of SM were 335 minutes and 465 minutes, respectively, and initial and final setting times of ICC were 340 minutes and 475 minutes, respectively. All time of set results were similar to concrete of the same classification and were in close agreement with each other. Bleeding test results for SM and ICC were 0.099 ml/cm^2 and 0.105 ml/cm^2, respectively. Not only are their results close to each other, but also they showed no excessive bleeding water on the surface.

To summarize, from all trial and production mix data, ICC mixtures with 0.40 w/c ratio performed similarly to SM concretes with the same w/c ratio in terms of workability.

Mixtures with 0.36 w/c ratio

For mixtures with 0.36 w/c ratio, slumps for SM and ICC were 2.75 and 3.75 inches, respectively. Both complied with the FDOT specification of 1 to 6 inches and the target range of

2 to 4 inches for this study. Air contents for SM and ICC were 2.75% and 2.00%, respectively. Both results are within the FDOT specification of 1 to 6 percent and target range of 2 to 4 percent. From the combination of the slump and air content results, visual observation, experience in performing the tests, and consolidation of the test specimens, the mixture's workability was good. In terms of temperature, SM and ICC concrete temperatures were same at 75° F. Both results are well within the 68° to 86° F range of the FDOT specification and target range.

Initial and final setting times of SM were 345 minutes and 450 minutes, respectively, and initial and final setting times of ICC were 350 minutes and 450 minutes, respectively. All time of set results are typical that could be seen from another concrete mix of the same classification, and the values are close to each other. Bleeding test results for SM and ICC were 0.331 ml/cm^2 and 0.328 ml/cm^2, respectively. Not only are their results close, but they showed no excessive bleed water on the surface.

To summarize, from all trial mixes and production mixes data, ICC mixtures with 0.36 w/c ratio performed similarly to SM concretes with the same w/c ratio in terms of workability.

Mixtures with 0.32 w/c ratio

For mixtures with 0.32 w/c ratio, slumps for SM and ICC were 6.00 and 3.00 inches, respectively. Both of them comply with the FDOT specification of 1 to 6 inches, but only the ICC's slump fell within the target range of 2 to 4 inches. Air content for SM and ICC were 3.75% and 2.50%, respectively. Both results are within the FDOT specification of 1 to 6 percent and the target range of 2 to 4 percent. The concretes workability was considered good. In terms of temperature, SM and ICC concrete temperatures were 74° and 75° F. Both results are well within the 68° to 86° F range of the FDOT specification and the target range.

Initial and final setting times of SM were 415 minutes and 520 minutes, respectively, and initial and final setting times of ICC were 360 minutes and 470 minutes, respectively. All the setting times were similar to those of concrete of the same classification, although the SM setting times were slight longer as compared with the ICC's times. Bleeding test results for SM and ICC were 0.006 ml/cm^2 and 0.002 ml/cm^2, respectively. The fresh concretes showed no excessive bleeding water on the surface. As compared with the concrete mixes with a higher w/c ratio, these mixes required higher amount of water reducing admixtures to obtain the desired slumps.

To summarize, from all trial and production mix data, ICC mixtures with 0.32 w/c ratio performed similarly to SM concretes with the same w/c ratio in terms of workability.

4.3.3.2 Analysis of Hardened Concrete Properties

Hardened concrete properties usually describe how concrete structures can withstand applied loads and environmental effect. The load withstanding ability are projected by its various strengths properties such as compressive strength, flexural strength, and tensile strength; while, properties like MOE, restrained shrinkage, and drying shrinkage affect the durability of the concrete. Each of these hardened concrete properties from a pair of SM and ICC mixtures with the same w/c ratio were analyzed and evaluated for its respective related-performances.

Analysis of compressive strength test results

Average compressive strengths of SM and ICC mixtures at w/c ratio 0.40, 0.36, and 0.32 at different curing times are shown in Table 4-14 in the section 4.3.2.2. Since FDOT specification considers only 28-day strengths, only 28-day strengths are discussed in this section. Compressive strengths of SM and ICC with 0.40 w/c ratio at 28 days were 7,785 and 6,945 psi, respectively. Both values are higher than the minimum and over-designed required strengths for FDOT Class II (Bridge Deck) concrete, which are 4,500 and 5,500 psi, respectively.

Compressive strengths of SM and ICC with 0.36 w/c ratio were 8,230 and 7,635 psi, respectively. Both values are higher than the minimum and over-designed required strengths for FDOT Class IV concrete, which are 5,500 and 6,700 psi, respectively. Compressive strengths of SM and ICC with 0.32 w/c ratio were 8,860 and 7,870 psi, respectively. The SM compressive strength is higher than the minimum and over-designed required strengths for FDOT Class V concrete, which are 6,500 and 7,900 psi, respectively. The ICC strength is over the minimum required strength, but it is 30 psi lower than the over-designed required strength.

Table 4-21 presents the comparison of the compressive strength of ICC mixture to the SM concrete counterparts in terms of percentages of the strength of the SM concrete. As shown in the table, at 0.40 w/c ratio, ICC mixture strengths average at 87% of the SM strength at the same ages with very small standard variation of 1.1% among the results from all of the different curing times. At 0.36 w/c ratio, ICC mixture strengths average at 91% of the SM strength at the same ages with very small standard variation of 1.7%. Similarly, at 0.32 w/c ratio, ICC mixture strengths average at 89% of the SM strength at the same ages with very small standard variation of 1.7%. In summary, the tested ICC mixtures showed 13% reduction in compressive strength for the 0.40 w/c mixtures, 9% reduction for the 0.36 w/c mixtures, and 11% reduction for the 0.32 w/c mixtures. With consideration of all test results, the overall average compressive strength reduction for all ICC mixtures is 11%.

Table 4-21. Compressive Strength by Percentage to Standard Control Mixtures

Curing Time	Percentage to standard control mixes (%)					
	0.40 w/c ratio		0.36 w/c ratio		0.32 w/c ratio	
(days)	SM 0.40	LWA 7 0.40	SM 0.36	LWA 7 0.36	SM 0.32	LWA 7 0.32
1	100%	87%	100%	89%	100%	87%
3	100%	87%	100%	92%	100%	90%
7	100%	88%	100%	94%	100%	90%
28	100%	89%	100%	93%	100%	89%
91	100%	86%	100%	92%	100%	88%
182	100%	87%	100%	90%	100%	92%
Average	100%	87%	100%	91%	100%	89%

Analysis of flexural strength test results

Average flexural strengths of SM and ICC mixtures at w/c ratio 0.40, 0.36, and 0.32 at different curing times are shown in Table 4-15 in the section 4.3.2.2. Table 4-22 presents the comparison of the flexural strengths of ICC mixture to the SM concrete counterparts in terms of percentages of the strength of the SM concrete. As shown in the table, at 0.40 w/c ratio, ICC mixtures strengths average at 93% of the SM strength at the same ages with small standard variation of 5.2% among the results from all of the different curing times. At 0.36 w/c ratio, ICC mixtures strengths average at 97% of the SM strength at the same ages with small standard variation of 5.1%. Similarly, at 0.32 w/c ratio, ICC mixtures strengths average at 92% of the SM at the same ages with small standard variation of 3.4%. In summary, the tested ICC mixtures show 7% reduction in flexural strength for the 0.40 w/c mixtures, only 3% reduction for the 0.36 w/c mixtures, and 8% reduction for the 0.32 w/c mixtures. With consideration of all test results, the overall average flexural strength reduction for all ICC mixtures is 6%.

Table 4-22. Flexural Strength by Percentage to Standard Control Mixtures

Curing Time	Percentage to standard control mixes (%)					
	0.40 w/c ratio		0.36 w/c ratio		0.32 w/c ratio	
(days)	SM 0.40	LWA 7 0.40	SM 0.36	LWA 7 0.36	SM 0.32	LWA 7 0.32
7	100%	100%	100%	105%	100%	95%
28	100%	94%	100%	92%	100%	86%
91	100%	91%	100%	93%	100%	93%
182	100%	85%	100%	98%	100%	93%
Average	100%	93%	100%	97%	100%	92%

Analysis of modulus of elasticity test results

Average MOE of SM and ICC mixtures at w/c ratio 0.40, 0.36, and 0.32 at different curing times are shown in Table 4-16 in the section 4.3.2.2. Table 4-23 presents the comparison of the MOE of ICC mixture to the SM concrete counterparts in terms of percentage of the MOE of the SM concrete. As shown in the table, at 0.40 w/c ratio, ICC mixtures moduli average at 83% of the SM moduli at the same ages with very small standard variation of 1.2% among the results from all of the different curing times. At 0.36 w/c ratio, ICC mixtures moduli average at 82% of the SM moduli at the same ages with very small standard variation of 0.6%. Similarly, at 0.32 w/c ratio ICC mixtures moduli average at 82% of the SM moduli at the same ages with very small standard variation of 1.6%. In summary, the tested ICC mixtures saw 17% reduction in modulus of elasticity for the 0.40 w/c mixtures, 18% reduction for the 0.36 w/c mixtures, and 18% reduction for the 0.32 w/c mixtures. With consideration of all test results, the overall average elastic modulus reduction for all ICC mixtures is 18%.

Table 4-23. Modulus of Elasticity by Percentage to Standard Control Mixtures

Curing Time	Percentage to standard control mixes (%)					
	0.40 w/c ratio		0.36 w/c ratio		0.32 w/c ratio	
(days)	SM 0.40	LWA 7 0.40	SM 0.36	LWA 7 0.36	SM 0.32	LWA 7 0.32
7	100%	81%	100%	82%	100%	80%
28	100%	83%	100%	82%	100%	83%
91	100%	84%	100%	82%	100%	84%
182	100%	82%	100%	83%	100%	80%
Average	100%	83%	100%	82%	100%	82%

Analysis of splitting tensile strength test results

Average splitting tensile strengths of SM and ICC mixtures with w/c ratio 0.40, 0.36, and 0.32 at different curing times are shown in Table 4-17 in the section 4.3.2.2. Table 4-24 presents the comparison of the splitting tensile strength of ICC mixture to the SM concrete counterparts in terms of percentage of the strength of the SM concrete. As shown in the table, at 0.40 w/c ratio, ICC mixtures strengths average at 90% of the SM strength at the same ages with standard variation of 9.7% among the results from all of the different curing times. At 0.36 w/c ratio, ICC mixtures strengths average at 86% of the SM strength at the same ages with small standard variation of 4.2%. Similarly, the 0.32 w/c ratio ICC mixtures strengths average at 95% of the SM strength at the same ages with small standard variation of 4.8%. In summary, the tested ICC mixtures showed 10% reduction in splitting tensile strength for the 0.40 w/c mixtures, 14% reduction for the 0.36 w/c mixtures, and 5% reduction for the 0.32 w/c mixtures. With consideration of all test results, the overall average splitting tensile strength reduction for all ICC mixtures is 10%.

Table 4-24. Splitting Tensile Strength by Percentage to Standard Control Mixtures

Curing Time	Percentage to standard control mixes (%)					
	0.40 w/c ratio		0.36 w/c ratio		0.32 w/c ratio	
(days)	SM 0.40	LWA 7 0.40	SM 0.36	LWA 7 0.36	SM 0.32	LWA 7 0.32
7	100%	73%	100%	81%	100%	90%
28	100%	96%	100%	93%	100%	94%
91	100%	93%	100%	85%	100%	103%
182	100%	96%	100%	86%	100%	92%
Average	100%	90%	100%	86%	100%	95%

Analysis of restrained shrinkage ring test results

Average ages of cracking of restrained shrinkage rings of SM and ICC mixtures with w/c ratio 0.40, 0.36, and 0.32 are shown in Table 4-18 in the section 4.3.2.2. Table 4-25 presents the comparison of the cracking age of ICC mixture to the SM concrete counterparts in terms of percentage of the cracking age of the SM concrete. As shown in the table, at 0.40 w/c ratio, ICC mixtures cracking ages averaged at 314% of the SM. At 0.36 w/c ratio, ICC mixtures cracking age averaged at 100% of the SM. At 0.32 w/c ratio, ICC mixtures cracking age averaged at 400% of the SM. With consideration of all test results, the overall average cracking age of all ICC mixtures was 2.7 times that of the SM concrete

Table 4-25. Age of Cracking of Restrained Shrinkage Rings by Percentage to Standard Control Mixtures

Rings	Percentage to standard control mixes (%)					
	0.40 w/c ratio		0.36 w/c ratio		0.32 w/c ratio	
	SM 0.40	LWA 7 0.40	SM 0.36	LWA 7 0.36	SM 0.32	LWA 7 0.32
Average	100%	314%	100%	100%	100%	400%

Analysis of drying shrinkage test results

Average drying shrinkages of SM and ICC mixtures with w/c ratio 0.40, 0.36, and 0.32 at different curing times are shown in Table 4-19 in the section 4.3.2.2. Table 4-26 presents the

comparison of the drying shrinkage of ICC mixture to the SM concrete counterparts in terms of percentage of the drying shrinkage of the SM concrete. As shown in the table, at 0.40 w/c ratio, ICC mixtures shrinkages average at 124% of the SM shrinkage at the same ages with standard variation of 6.2% among the results from all of the different curing times. At 0.36 w/c ratio, ICC mixtures shrinkages average at 124% of the SM shrinkage at the same ages with standard variation of 8.3%. Similarly, at 0.32 w/c ratio ICC, mixtures shrinkage average at 125% of the SM shrinkage at the same ages with small standard variation of 6.2. In summary, the tested ICC mixtures showed 24% increase in drying shrinkage for the 0.40 w/c mixtures, 24% increase for the 0.36 w/c mixtures, and 25% increase for the 0.32 w/c mixtures. With consideration of all test results, the overall average drying shrinkage increase for all ICC mixtures is 24%.

Table 4-26. Drying Shrinkage by Percentage to Standard Control Mixtures

Curing Time	Percentage to standard control mixes (%)					
	0.40 w/c ratio		0.36 w/c ratio		0.32 w/c ratio	
(days)	SM 0.40	LWA 7 0.40	SM 0.36	LWA 7 0.36	SM 0.32	LWA 7 0.32
7	100%	-	100%	-	100%	132%
28	100%	120%	100%	118%	100%	122%
91	100%	115%	100%	114%	100%	132%
182	100%	128%	100%	134%	100%	119%
364	100%	131%	100%	129%	100%	118%
Average	100%	124%	100%	124%	100%	125%

Analysis of CTE test results

Average CTE values of SM and ICC mixtures with w/c ratio 0.36 at 127 days are shown in Table 4-20 in the section 4.3.2.2. As shown in the table, the average CTE of ICC mixtures with w/c ratio of 0.36 is 10% lower than the average CTE of the SM 0.36 at the same ages.

CHAPTER 5
APT EVALUATION OF ICC PAVEMENT SLABS

5.1 Overview

Three test slabs were constructed at the accelerated pavement testing (APT) facility at the Florida Department of Transportation (FDOT) State Materials Office (SMO) to evaluate the performance of internally cured concrete (ICC) in pavement slabs. Three mix designs from the laboratory testing program were selected for use. The three selected mix designs were (1) a standard mixture with 0.40 w/c ratio, (2) an ICC mixture with 0.40 w/c ratio, and (3) an ICC mixture with 0.32 w/c ratio. Samples of the concrete used were collected and evaluated for their fresh concrete properties and hardened concrete properties. All three slabs were instrumented with thermocouples, strain gauges, and LVDTs to monitor the temperature, strain, and deformation of the test slabs during the testing period. The falling weight deflectometer (FWD) tests were performed on the test slabs to characterize their structural behavior. Repetitive wheel loads by the heavy vehicle simulator (HVS) were applied to the test slabs to evaluate their structural performance and to measure the load-induced strains in the concrete slabs. Finally, using the measured properties of the hardened concrete, the measured FWD deflections, and the measured HVS load-induced strains, finite element models were developed and calibrated for the test slabs. The calibrated models were then used to evaluate the structural performance of these test slabs under critical temperature-load conditions.

5.2 Concrete Mixtures Used

5.2.1 Concrete Mix Designs

Three mix designs from the laboratory testing program were selected for use in the APT evaluation of pavement slabs using conventional concrete and ICC. The three selected mix

designs were (1) a standard mixture with 0.40 w/c ratio, (2) an ICC mixture with 0.40 w/c ratio, and (3) an ICC mixture with 0.32 w/c ratio. For ease of reference, these three concrete mixes will be referred to as (1) Control 0.40, (2) ICC-2 0.40, and (3) ICC-1 0.32, respectively. The mix proportions of these three mixtures are shown in Table 5-1.

Table 5-1. Mix Proportions of Concrete for APT Test Slabs

Material	Mix Designs		
	Control 0.40	ICC-2 0.40	ICC-1 0.32
Classification	IV	IV IC	V IC
Cement (lb/yd^3)	549.6	549.6	688.0
Fly ash (lb/yd^3)	137.4	137.4	172.0
Coarse aggregate (lb/yd^3)	1,637.9	1,637.9	1,708.4
Sand (lb/yd^3)	1,174.7	749.9	402.7
Lightweight aggregate (lb/yd^3)	-	248.5	311.1
Air entraining admixture (oz/yd^3)	-	1.3	10.3
Water reducer admixture (oz/yd^3)	27.5	27.5	43.0
High-rage water reducer admixture (oz/yd^3)	7.7	4.4	34.0
Water (lb/yd^3)	274.7	274.7	275.1
w/c	0.40	0.40	0.32

The types and sources of the cement, fly ash, coarse aggregate, conventional fine aggregate, lightweight aggregate, and admixtures used are shown in Table 5-2. The lightweight fine aggregate used was the same lightweight aggregate used in the laboratory study. The properties of the aggregates used are also shown in Table 5-2.

Table 5-2. Types, Sources, and Properties of Materials Used

Materials	Types	Sources	Material Properties
Portland Cement	Type I/II	Florida Rock Company	SG: 3.15
Fly Ash	Class F	Florida Rock Company	SG: 2.40
Coarse Aggregate	#57 limestone	Brooksville, FL	SSD SG: 2.43; Absorption: 5.0%
Sand	Silica	Branford, FL	SSD SG: 2.63; Absorption 0.5%; FM: 2.63
Lightweight Aggregate	LWA [3/16]	Big River Industries Inc.	SSD SG: 1.54; Absorption: 25.2%; FM: 4.29
Air Entraining Admixture	AEA	Euclid AEA 92S	-
Water Reducing Admixture	Type D	Euclid Eucon WR	-
High-range Water Reducing Admixture	Type F	Euclid Eucon HRWR	-

5.2.2 Production of Concrete and Slab Placement

The concretes used in the APT slab test slabs were produced by Argos concrete plant in Gainesville, Florida. They were mixed in a central mix plant and transported to the SMO by a concrete delivery truck. The transit time from the mixing plant to the job site was less than 30 minutes. Once arrived at the site, the fresh concrete was checked for its slump and, if necessary, adjusted by adding water to the concrete on the truck (within limit of w/c ratio).

Upon getting the proper workability of the fresh concrete, the construction crew started placing the concrete slab. Care was taken in placing concrete at and around the instrumentation sensors. To protect the sensors during concrete placement, 12-in. (30.5-cm) diameter PVC buckets with bottoms removed were placed around the gauges. The concrete was placed manually around the strain gauges inside the PVC buckets, and then around the buckets. After the concrete was placed around the PVC buckets, the buckets were removed by pulling them vertically.

After the concrete was placed and finished, a curing compound was sprayed over the top and sides of the slab. Figure 5-1 shows the construction of a concrete test slab. The ICC-1 slab was constructed on December 9, 2014, and the Control and the ICC-2 slabs were both constructed on December 17, 2014.

Figure 5-1. Construction of an APT test slab.

5.2.3 Results of Tests on Fresh Concrete

Before the placement of each test slab, a sample of concrete was taken from the delivery truck to determine its slump, air content, unit weight, and temperature. Description on the procedures for these fresh concrete tests can be found in Section 4.2.3.1 of this report. The properties of the fresh concrete for the three concrete mixtures placed are shown in Table 5-3. The FDOT specification values are also shown in this table. It can be seen that the slumps, air

contents, and concrete temperatures were all within the FDOT specification limits, with the exception of the ICC-2 0.40 mixture which had a slightly higher slump of 6.25 inch.

Table 5-3. Fresh Concrete Properties of the Mixtures from Test Slabs

Mix	Slab	w/c Ratio	Slump (in)	Air Content (%)	Unit Weight (lb/ft^3)	Temperature (°F)
Control 0.40	Control	0.40	5.75	1.00%	142.4	71.0
ICC-2 0.40	ICC-2	0.40	6.25	1.70%	135.8	73.0
ICC-1 0.32	ICC-1	0.32	3.50	3.10%	133.4	78.0
FDOT Spec.	-	-	1 to 6	1 to 6	-	68 to 86

5.2.4 Results of Tests on Hardened Concrete

For each test slab, concrete sample was also obtained from the concrete delivery truck to make a total of nine 4" x 8" concrete cylinders for compressive strength test, elastic modulus test, and splitting tensile strength test; nine 4" x 4" x 14" concrete beams for flexural strength test; and six 3" x 3" x 11.25" concrete prisms for drying shrinkage test for each of the test slabs. Description on the procedures for these tests on hardened concrete can be found in Section 4.2.3.2 of this report. Meanwhile, for the control 0.40 and ICC-2 0.40 concrete mixtures, two additional 4" x 8" concrete cylinders were made from each concrete mixture to be used to estimate the moisture loss of the concrete in the slab. These concrete cylinders were subsequently used for the coefficient of thermal expansion (CTE) test. Figure 5-2 shows the running of fresh concrete tests and the making of the concrete specimens.

Figure 5-2. Fresh concrete properties testing and samples making.

Compressive strength

The average compressive strengths from three 4" x 8" test cylinders for the three concrete mixtures used in the three test slabs are shown in Table 5-4. For comparison purpose, the compressive strengths of similar concretes with the same w/c ratios as obtained in the laboratory testing program, which are presented in Section 4.3 of this report, are shown in parenthesis. It can be seen that the compressive strengths of these concrete mixtures are fairly close to those of similar concretes of the same w/c ratios from the laboratory study. The compressive strength results are plotted against curing days in Figure 5-3.

Table 5-4. Compressive Strengths of the Concrete Mixtures from Test Slabs

Curing Time (Days)	Compressive Strength (psi)		
	Control 0.40	ICC-2 0.40	ICC-1 0.32
7	5,250 (6,170*)	5,090 (5,430*)	6,690 (6,905*)
28	6,830 (7,785*)	6,620 (6,945*)	7,840 (7,870*)

* Compressive strength of similar concrete of the same w/c ratio from laboratory study

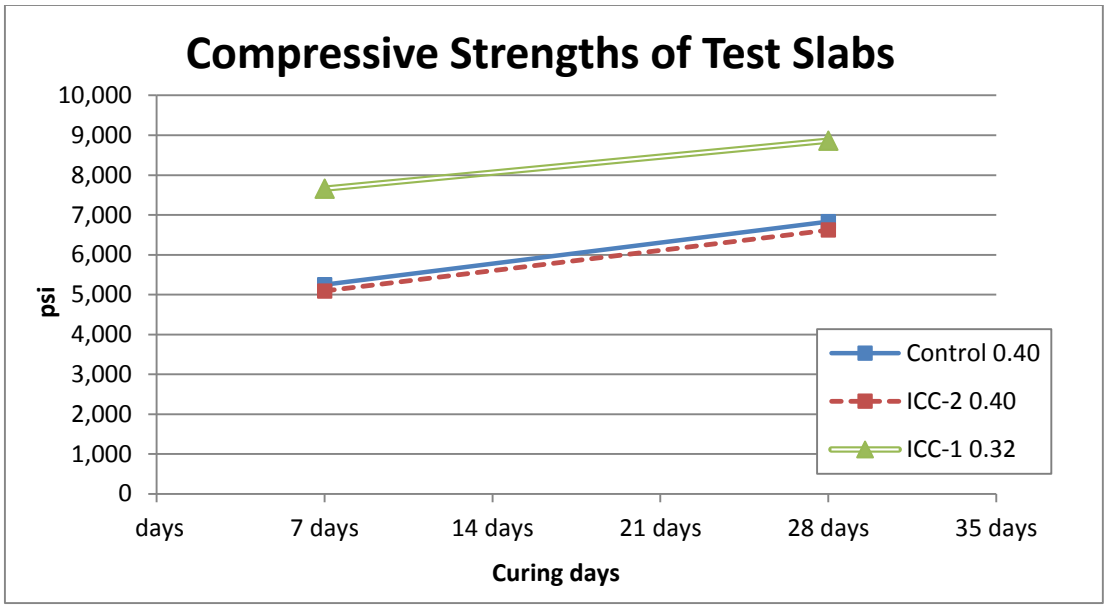

Figure 5-3. Compressive strengths of concrete mixtures from test slabs.

Flexural strength

The average flexural strengths from three 4" x 4" x 14" beams for the three concrete mixtures are shown in Table 5-5. For comparison purpose, the flexural strengths of similar concretes with the same w/c ratios as obtained in the laboratory testing program are shown in parenthesis. It can be seen that the flexural strength of the ICC-1 mixture with w/c ratio of 0.32 was substantially lower than the flexural strength of the corresponding ICC mixture with the same w/c ratio from the laboratory study. It was believed that these low flexural strengths obtained were outliers, and they might be caused by improper fabricating and handling of the concrete beam samples. For this reason, a flexural strength of 820 psi was also used in the calculation of stress-to-strength ratio for the ICC-1 0.32 mixture in the critical stress analysis presented in later section of this report. The flexural strength results are plotted against curing days in Figure 5-4.

Table 5-5. Flexural Strengths of the Concrete Mixtures from Test Slabs

Curing Time (days)	Flexural Strength (psi)		
	Control 0.40	ICC-2 0.40	ICC-1 0.32
7	635 (675*)	655 (673*)	645 (753*)
28	725 (834*)	705 (784*)	662 (820*)

* Flexural strength of similar concrete of the same w/c ratio from laboratory study

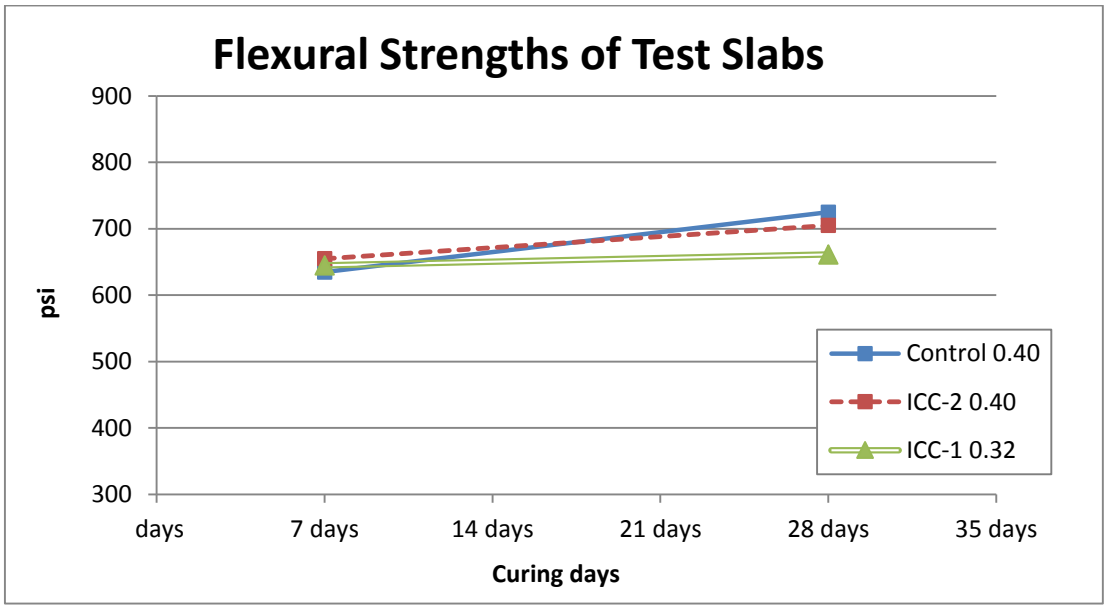

Figure 5-4. Flexural strength of concrete mixtures from test slabs.

Modulus of elasticity

The average moduli of elasticity from three 4" x 8" cylinders for the three concrete mixtures are in Table 5-6. For comparison purpose, the elastic modulus of similar concretes with the same w/c ratios as obtained in the laboratory testing program are shown in parenthesis. It can be seen that the elastic modulus of these concrete mixtures are fairly close to those of similar concretes of the same w/c ratios from the laboratory study.

Table 5-6. Moduli of Elasticity of the Concrete Mixtures from Test Slabs

Curing Time (days)	Modulus of Elasticity ($\times 10^6$ psi)		
	Control 0.40	ICC-2 0.40	ICC-1 0.32
28	4.45 (4.70*)	3.80 (3.90*)	3.90 (4.05*)

* Elastic modulus of similar concrete of the same w/c ratio from laboratory study

Splitting tensile strength

The average splitting tensile strengths from three 4" x 8" cylinders for the three concrete mixtures are shown in Table 5-7. For comparison purpose, the splitting tensile strengths of similar concretes with the same w/c ratios as obtained in the laboratory testing program are shown in parenthesis.

Table 5-7. Splitting Tensile Strength of the Concrete Mixtures form Test Slabs

Curing Time (days)	Splitting Tensile Strength (psi)		
	Control 0.40	ICC-2 0.40	ICC-1 0.32
28	520 (603*)	505 (580*)	460 (605*)

* Splitting tensile strength of similar concrete of the same w/c ratio from laboratory study

Drying shrinkage

The average drying shrinkages from six 3" x 3" x 11.25" prisms for the three concrete mixtures are shown in Table 5-8. For comparison purpose, the drying shrinkage of similar concretes with the same w/c ratios as obtained in the laboratory testing program are shown in parenthesis. Figure 5-5 presents the plot of the drying shrinkage versus curing days.

Table 5-8. Drying Shrinkages of the Concrete Mixtures from Test Slabs

Curing Time (days)	Drying shrinkage strain, X 10^{-6}		
	Control 0.40	ICC-2 0.40	ICC-1 0.32
28	-370 (-250*)	-380 (-300*)	-310 (-355*)
91	-530 (-355*)	-500 (-410*)	-380 (-415*)

* Drying shrinkage of similar concrete of the same w/c ratio from laboratory study

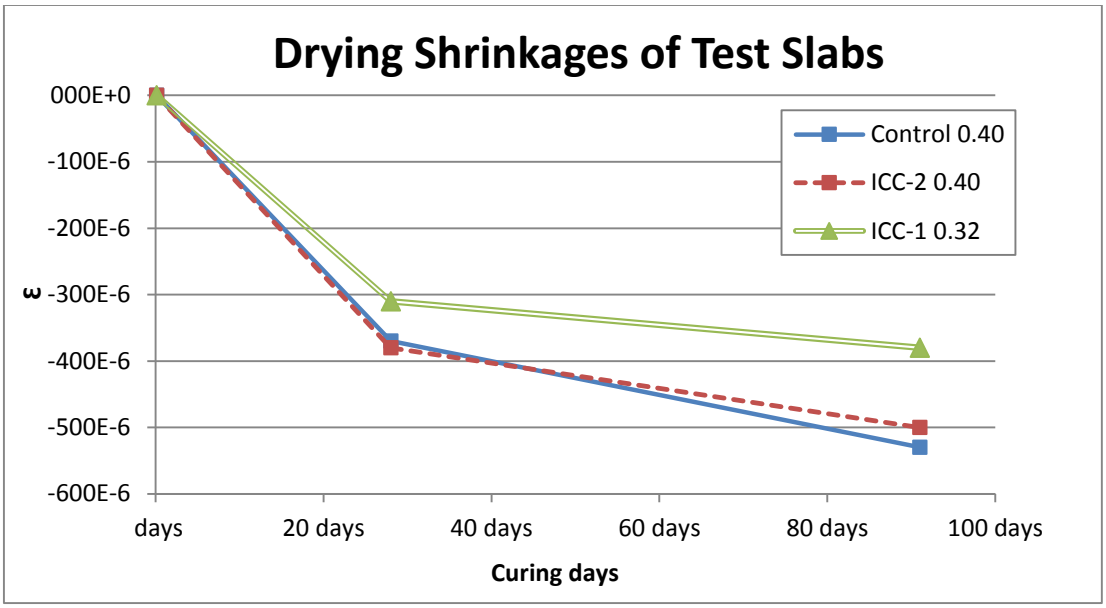

Figure 5-5. Drying shrinkage of concrete mixtures from test slabs.

Estimation of moisture loss

For the control 0.40 and ICC-2 0.40 concrete mixtures, two 4" x 8" concrete cylinders were made from each concrete mixture to be used to estimate the moisture loss of the concrete in the slab. After curing for one day in the molds, which were placed next to the placed slab, the concrete cylinders were de-molded and placed next to the corresponding concrete slab. The weights of these cylinders were taken periodically to determine their weight changes, which would indicate the moisture change of the concrete in the slab. The difference between the initial weight and the measured weight was taken to be the moisture loss of the sample at the particular time. The average weights of the two replicate specimens from each mixture were used in this test. The results of these weight measurements and the calculated moisture loss are shown in Table 5-9. The table also shows the ambient temperature at the location of the test slabs and indicates whether or not it had rained on that day. It can be seen that on the days when it had rained, the weights of the specimens went up slightly. The calculated moisture loss of the two concretes, in terms of % of the weight of the concrete, are plotted versus time in Figure 5-6.

It can be seen that the ICC mixture consistently lost more moisture than the control mixture. At 90 days, the ICC mixture lost about 4% while the control mixture lost about 2.65% of its initial weight.

Table 5-9. Measured Weights of Concrete Specimens for Determination of Moisture Loss

Age (day)	Ambient Temperature (°F)	Rain	Control 0.40			ICC-2 0.40		
			Weight (g)	Moisture Loss (g)	% Change (%)	Weight (g)	Moisture Loss (g)	% Change (%)
1	72.4		3794.00	0.00	0.00%	3617.00	0.00	0.00%
2	66.9		3735.25	-58.75	-1.55%	3542.75	-74.25	-2.05%
5	69.1	Y	3759.75	-34.25	-0.90%	3546.00	-71.00	-1.96%
12	74.8		3715.00	-79.00	-2.08%	3498.50	-118.50	-3.28%
21	62.6		3703.75	-90.25	-2.38%	3486.75	-130.25	-3.60%
22	42.2		3701.50	-92.50	-2.44%	3484.00	-133.00	-3.68%
23	54.9		3702.00	-92.00	-2.42%	3484.50	-132.50	-3.66%
26	69.4	Y	3723.25	-70.75	-1.86%	3503.50	-113.50	-3.14%
27	66.8		3712.75	-81.25	-2.14%	3493.25	-123.75	-3.42%
28	54.1		3708.75	-85.25	-2.25%	3489.75	-127.25	-3.52%
30	56.9		3724.00	-70.00	-1.85%	3503.25	-113.75	-3.14%
35	73.5		3704.00	-90.00	-2.37%	3484.75	-132.25	-3.66%
40	59.4	Y	3725.75	-68.25	-1.80%	3503.50	-113.50	-3.14%
42	54.6		3710.50	-83.50	-2.20%	3489.25	-127.75	-3.53%
43	63.1		3707.50	-86.50	-2.28%	3486.50	-130.50	-3.61%
50	60.5	Y	3727.25	-66.75	-1.76%	3503.75	-113.25	-3.13%
51	58.1		3714.50	-79.50	-2.10%	3492.25	-124.75	-3.45%
56	62.2		3711.25	-82.75	-2.18%	3490.25	-126.75	-3.50%
57	60.7		3706.00	-88.00	-2.32%	3484.75	-132.25	-3.66%
61	71.4		3700.00	-94.00	-2.48%	3478.75	-138.25	-3.82%
70		Y	3716.00	-78.00	-2.06%	3494.25	-122.75	-3.39%
71			3717.00	-77.00	-2.03%	3493.75	-123.25	-3.41%
75		Y	3723.50	-70.50	-1.86%	3499.25	-117.75	-3.26%
82			3705.25	-88.75	-2.34%	3482.50	-134.50	-3.72%
83			3705.25	-88.75	-2.34%	3483.00	-134.00	-3.70%
85			3701.75	-92.25	-2.43%	3479.50	-137.50	-3.80%
90			3696.25	-97.75	-2.58%	3474.25	-142.75	-3.95%
91			3696.25	-97.75	-2.58%	3474.00	-143.00	-3.95%
92			3694.75	-99.25	-2.62%	3472.50	-144.50	-4.00%

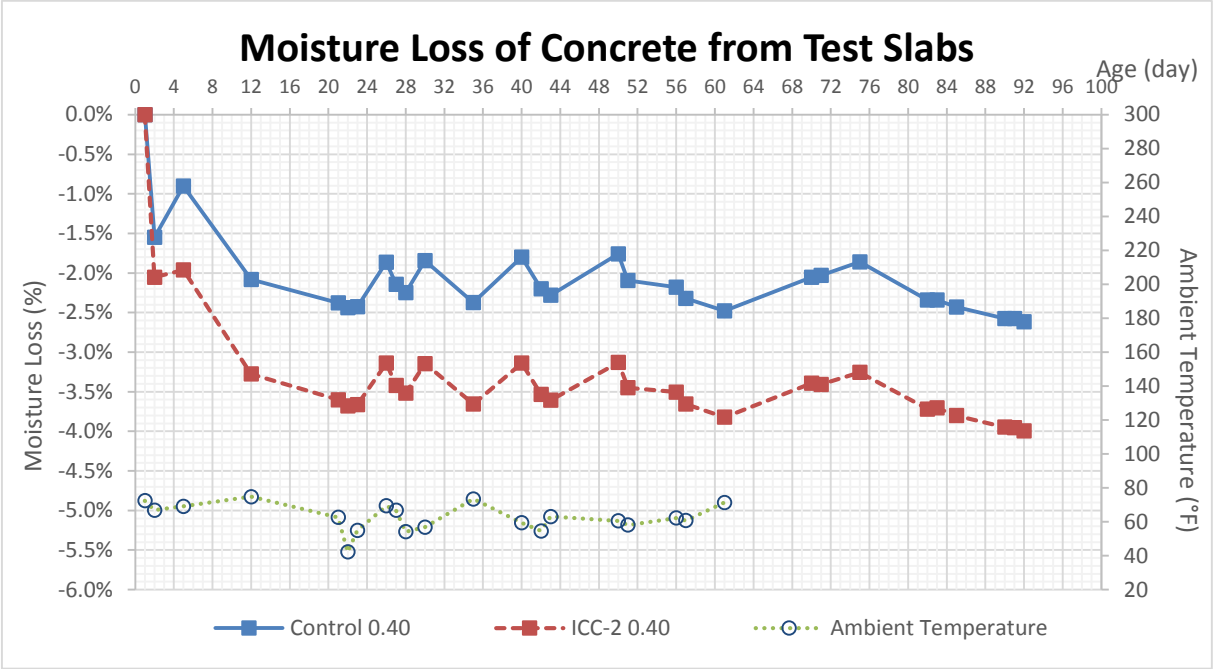

Figure 5-6. Moisture loss of concrete mixtures from test slabs.

Coefficient of thermal expansion (CTE)

The test procedure in accordance with the AASHTO T 336 Standard Method of Test for Coefficient of Thermal Expansion of Hydraulic Cement Concrete was followed in performing the CTE test. The same specimens which were used in the moisture-loss determination test were used in the coefficient of thermal expansion (CTE) test. Each of the 4" x 8" cylindrical concrete specimens was cut to the desired 7-inch height by a grinding machine, and then the specimen was submerged in a lime saturated water tank for at least 48 hours. After the soaking, the specimen was put into a LVDT-mounted frame in a temperature-controlled bath. The LVDT measured the height of the test specimen at various temperature conditions. The bath was connected to a computer, and controlled by the CTE test software. Once all the information about the sample was entered into the software, a CTE test was then started. The CTE testing machine used two spans of temperature, from 10°C to 50°C and from 50°C to 10°C, to determine the CTE value of the specimen. Typically, the sample age of 28 days is required for a CTE test

to give a stable and reliable CTE value. All the samples were tested at age of 100 days and over. The average CTE value from two replicate specimens are shown in Table 5-10.

Table 5-10. CTE of the Concrete Mixtures from Test Slabs

Mixture	Curing Time (days)	CTE (με/°C)
Control 0.40	100	7.9648
ICC-2 0.40	102	7.2929

5.3 Instrumentation of the Test Slabs

5.3.1 Descriptions of the Test Slabs

The three test slabs were constructed at the accelerated pavement testing (APT) facility in the FDOT Materials Research Park in Gainesville, Florida. Each of the three concrete test slabs was 12 ft by 16 ft (3.7 m by 4.9 m) in size and 9 in. in thickness, and was constructed over an existing two-inch (5-cm) thick asphalt layer, which was placed over a 10.5 in. (26.7 cm) limerock base. The asphalt layer acted as a leveling course and provided the concrete slab with a firm and consistent foundation. There was no dowel bar used at the slab joints.

5.3.2 Instrumentation Layout and Installation

Figure 5-7 shows the instrumentation layout for the test slabs. The instrumentation which was installed included (1) electrical resistance strain gauges to measure the dynamic strains in the concrete slabs due to HVS loading, (2) vibrating wire gauges to measure strains in the concrete slabs due to temperature and moisture effects, (3) thermocouple wires to measure temperature distribution in the concrete slabs, and (4) LVDTs to measure the vertical movement of the test slab due to the curling effects of temperature and moisture variation in the slabs.

The locations for the dynamic strain gauges were selected based on the anticipated maximum strain responses in the test slabs from the anticipated HVS loading. They were installed mainly under the anticipated wheel paths of the HVS loading. The vibrating wire

gauges were installed mainly at the slab centers, edges, and corners, where strains due to the slab curling effects of temperature and moisture variations were more pronounced. At each indicated gauge location, two embedded strain gauges were placed at a depth of 1 in. (2.54 cm) from the concrete surface, and 1 in. (2.54 cm) from the bottom of the concrete layer. This was achieved by securing the strain gauges between two nylon rods which were securely driven into the asphalt layer before the pouring of the concrete to form the test slab.

Sets of thermocouple wires were installed at the slab centers, corners, and mid-edges as shown in the layout. Each set of thermocouple wires consisted of seven wires, which were fixed on a PVC rod and placed at depth of 1, 2, 3, 4.5 6, 7, and 8 in. (2.54, 5.08, 7.62, 11.43, 15.24, 17.78, and 20.32 cm) from the surface of the concrete slab, and one thermocouple which was placed in the asphalt layer at a depth of 1 in. (2.54 cm) from the top of the asphalt layer, or at a depth of 10 in. (25.4 cm) from the concrete surface.

LVDTs were installed at the corner of each slab and the center of the longitudinal edge of the control slab and the ICC-2 slab. Invar-bars, which have a uniquely low coefficient of thermal expansion, were secured to the base of the slabs and used to hold the LVDTs so that the LVDT would have a fixed reference which would not be influenced by the fluctuation of temperature. These LVDTs were used to monitor the vertical movement of the slabs at the various locations on the slabs.

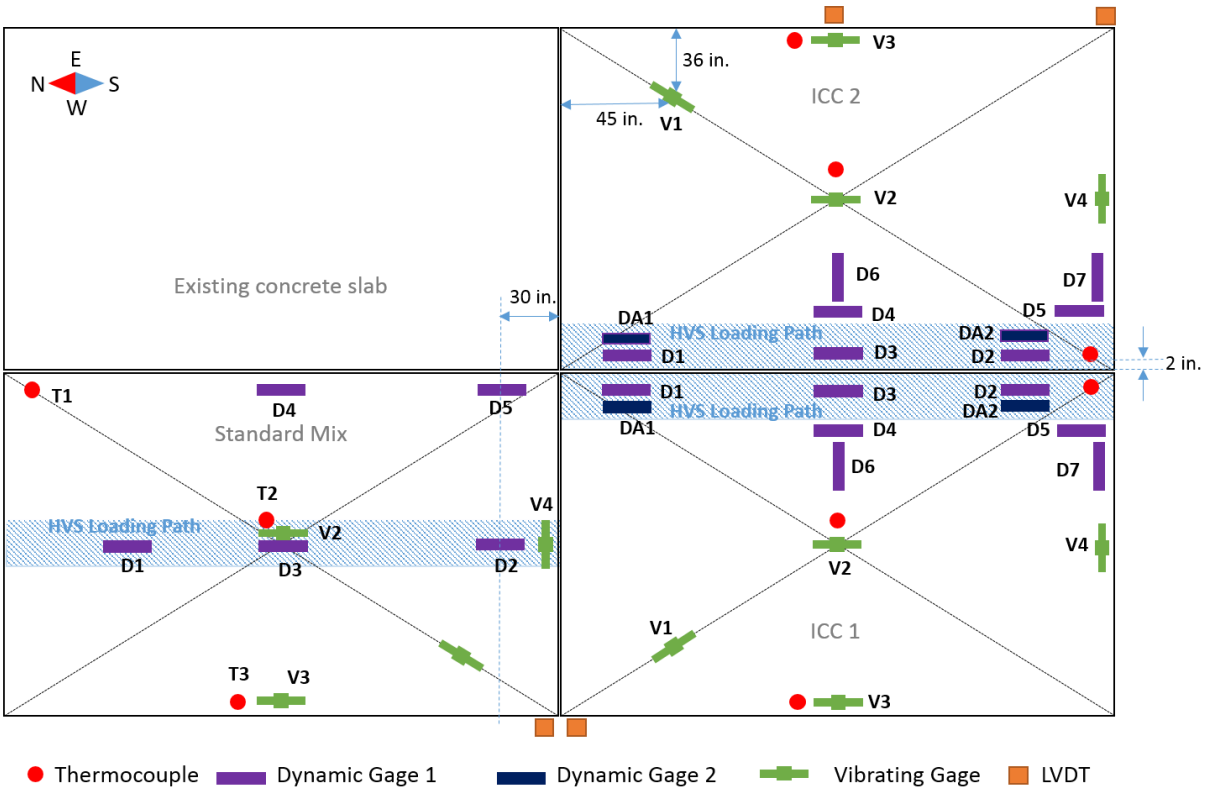

Figure 5-7. Instrumentation layout.

5.3.3 Data Acquisition System

A mobile data acquisition system was set up to read the strains from the vibrating wire gauges and the deformations from the LVDTs at 15-minute intervals. During the HVS testing, dynamic strain data from the tested slab were recorded at every 15-minute interval, for 30 seconds each time, at a rate of 100 values per second for each strain gauge. Temperature data were recorded at five-minute intervals. The AC unit and regulator equipped on the DAQ system cabinet enabled the operation of DAQ system by maintaining a stable condition in terms of temperature, humidity, and electric power.

5.4 Finite Element Modeling of Test Slabs

A 3-D finite element model for analysis of concrete pavement slabs, which was developed for FDOT under another research project, was calibrated and used to analyze the

structural behavior of these three test slabs and to determine their structural responses and performance under critical temperature-load conditions in Florida.

The 3-D finite element model for concrete slabs was developed using the ADINA (version 9) finite element software. Figure 5-8 shows the 3-D finite element model which was developed for the analysis of the three test slabs. A concrete slab is modeled by an assemblage of elastic hexahedron elements. A hexahedron element is defined by eight nodes with each node having three degrees of freedom, i.e., translations in the x-, y-, and z-directions. The effects of temperature changes in the concrete slab can also be considered in the analysis. The concrete is characterized by its elastic modulus, Poisson's ratio, and coefficient of thermal expansion (CTE).

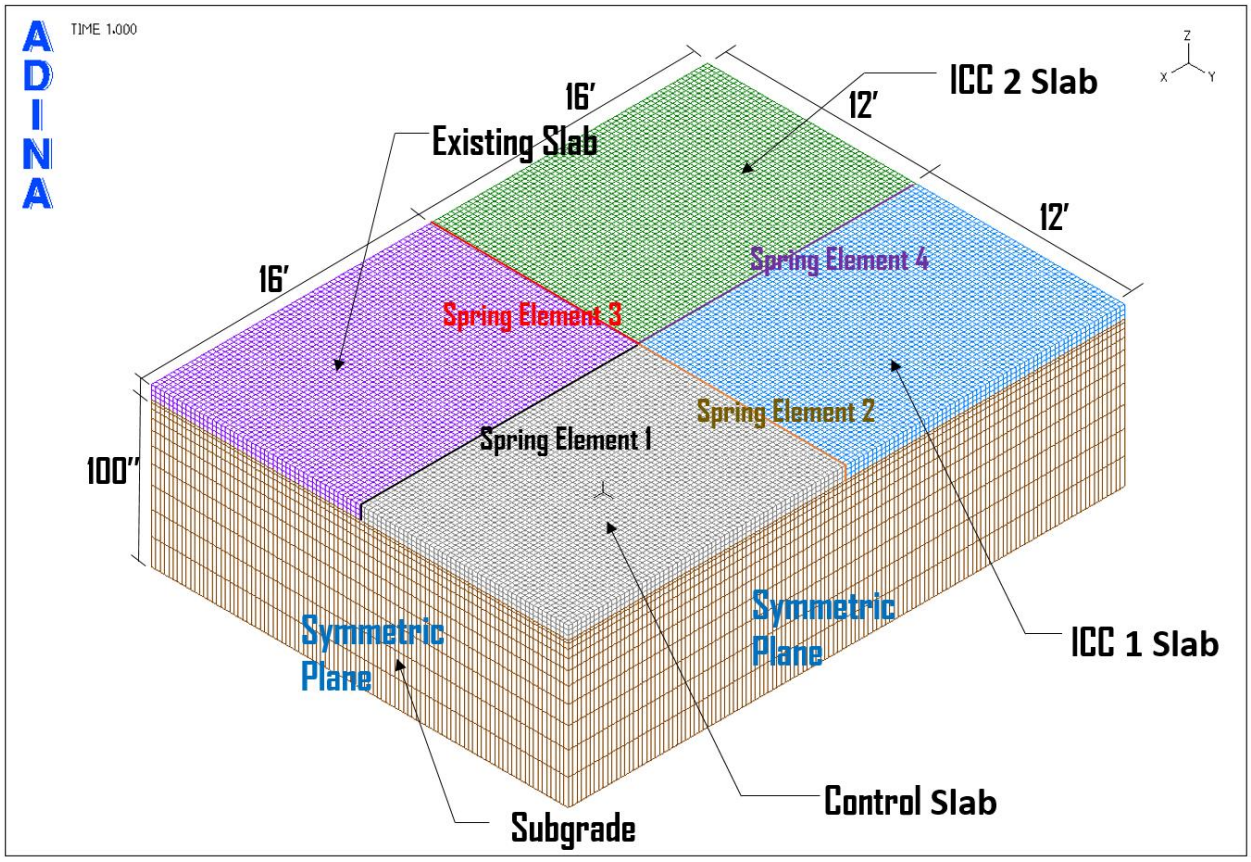

Figure 5-8. 3-D finite element model for test slabs.

The test slabs are modeled as not bonded to the underlying foundation. The pavement foundation is modeled as an isotropic and linearly elastic subgrade material characterized by its elastic modulus and Poisson's ratio. A depth of 100 inches was used to model the subgrade material. The bottom of subgrade layer was modeled as fixed in the z-direction.

The material properties used in this model for the three test slabs are shown in Table 5-11. The properties of the three concretes used in the model were initially obtained from the measured properties of the sampled concrete as presented in Section 5.2. The elastic modulus of the subgrade was obtained through back-calculation method by matching the analytical to the measured FWD deflections of the test slabs, as presented in the next section.

Table 5-11. Material Properties in FEM Model

FEM layers	Modulus of elasticity (psi)	CTE (in/in/°F x 10^{-6})	Poisson's ratio	Density (pcf)
Control Slab	4,450,000	4.425	0.2	138.3
ICC 1	3,900,000	4.239	0.2	129.9
ICC 2	3,800,000	4.239	0.2	130.4
Existing Slab	3,800,000	4.500	0.2	140
Subgrade	115,000	-	0.35	-

Load transfer across the joint between two adjacent slabs is modeled by translational springs connecting the nodes of the finite elements along the joint. Spring elements also have three degrees of freedom. Three values of spring constants are used to represent the stiffnesses along the x-, y-, and z-directions.

5.5 Calibration and Validation of the FE Model

5.5.1 Overview of Calibration and Validation of the FE Model

In order for the 3-D analytical model to accurately analyze the behavior of the test slabs under the HVS loading and critical loading conditions, it needs to have accurate properties of the

test slab materials and the correct values of spring stiffness for modeling the behavior of joints and edges.

The elastic modulus of the concrete material was initially estimated from the results of laboratory tests on the sampled concrete. The elastic modulus of subgrade and the spring stiffnesses of joint and edges were estimated by back-calculation of the FWD deflection data using the ADINA FE model. The elastic moduli of the concrete samples were also adjusted by the back-calculation method.

The results of the FWD tests at the slab center were used to estimate the elastic modulus of the subgrade. The results of the FWD test at the joints and edges were used to calibrate values of spring stiffness at the joints and edges by matching the analytically computed deflections with the measured FWD deflections. This process is referred to as "calibration of model parameters" of the model in this study.

The estimation of the test slab materials properties and parameters was further verified by matching the analytically computed strains with the measured strains in the test slabs caused by HVS wheel loads. This process is referred to as "verification of model parameters" in this study.

5.5.2 Calibration of Model Parameters

Standard-Mix Slab

The standard-mix slab was modeled as a 9-inch concrete slab over a 100-inch subgrade. Pavement surface deflection basins caused by a 9-kip FWD applied load were used to estimate the values of the elastic modulus of the subgrade and the stiffness of the springs used to model the load transfer at the joints.

Figure 5-9 shows the measured and computed deflection basin caused by a 9-kip FWD load at the center of slab. This set of FWD tests was performed in the early morning when the slab would tend to have a negative temperature differential and to have full contact with the

subgrade at the slab center. The measured deflection basins in the transverse direction were very similar to those in the longitudinal direction. The analytical deflection basin was calculated by using an elastic modulus of the subgrade of 115 ksi.

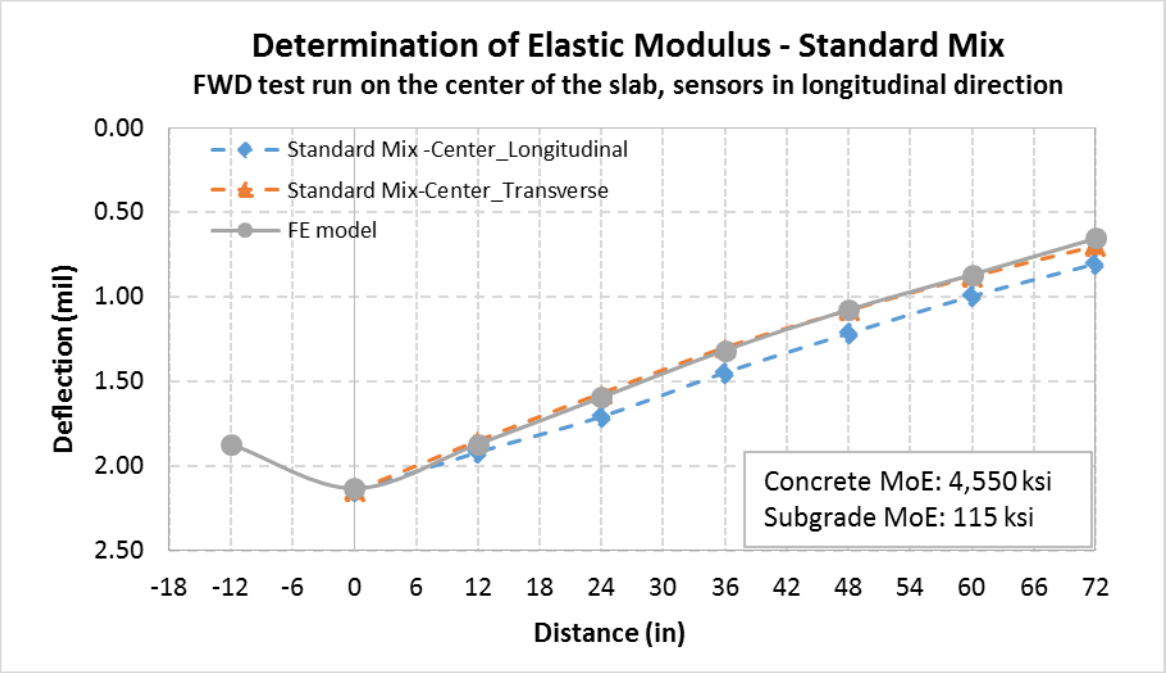

Figure 5-9. Measured and computed deflection basin caused by a 9-kip FWD load at slab center for standard-mix slab.

Deflection basins caused by FWD load applied at the joint were used to estimate the joint spring stiffnesses, which were used to model the load transfer at the joints. This set of FWD tests was performed at midday when the slab would tend to have a positive temperature differential and to have full contact with the subgrade at the joints. The estimated elastic moduli of the slab and subgrade were used in the FE model to compute the deflection basin across the joint.

Figure 5-10 shows the matched deflection basins from the back-calculation process for estimating the joint spring stiffnesses. Using the previous estimated parameters and material properties, a fairly good match between the measured and the calculated deflection basins was

achieved with a vertical stiffness of 100,000 lb/in. and with stiffness of 10,000 lb/in. in the other directions.

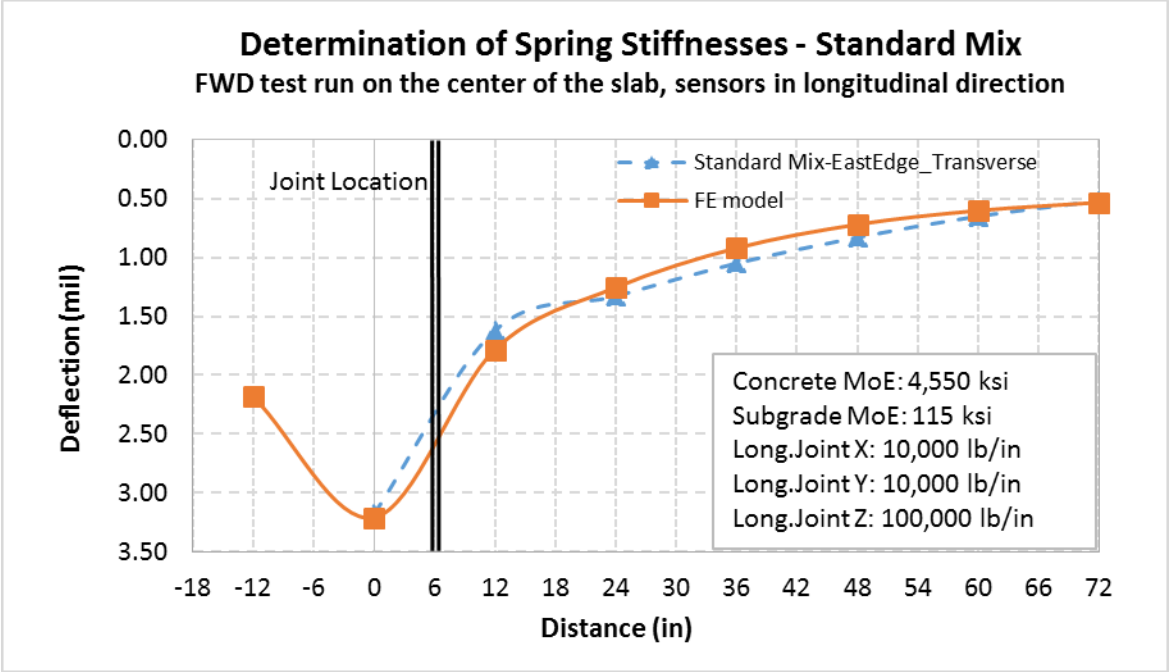

Figure 5-10. Measured and computed deflection basin caused by a 9-kip FWD load across the joint for standard-mix slab.

ICC-1 Slab

The elastic modulus of the ICC-1 slab was initially set to be the laboratory-measured elastic modulus of the sampled concrete (as presented in Section 5.2). The deflection basins caused by a 9-kip FWD load applied to the slab center and at the joint were used to estimate the elastic modulus of subgrade and the joint stiffnesses by the back-calculation method. The analytical deflection basin matched well with the measured deflection basin by using the elastic modulus of the subgrade of 105 ksi, vertical stiffness of 1,000,000 lb/in., and stiffness of 10,000 lb/in. in the other directions. It is to be pointed out that a good match was achieved by using a lower elastic modulus of subgrade and higher vertical spring stiffness in the ICC-1 slab as compared with the standard-mix slab. Figures 5-11 and 5-12 show the matched deflection basins

from the back-calculation process for the estimation of the elastic modulus of subgrade and the joint spring stiffnesses of the ICC-1 slab.

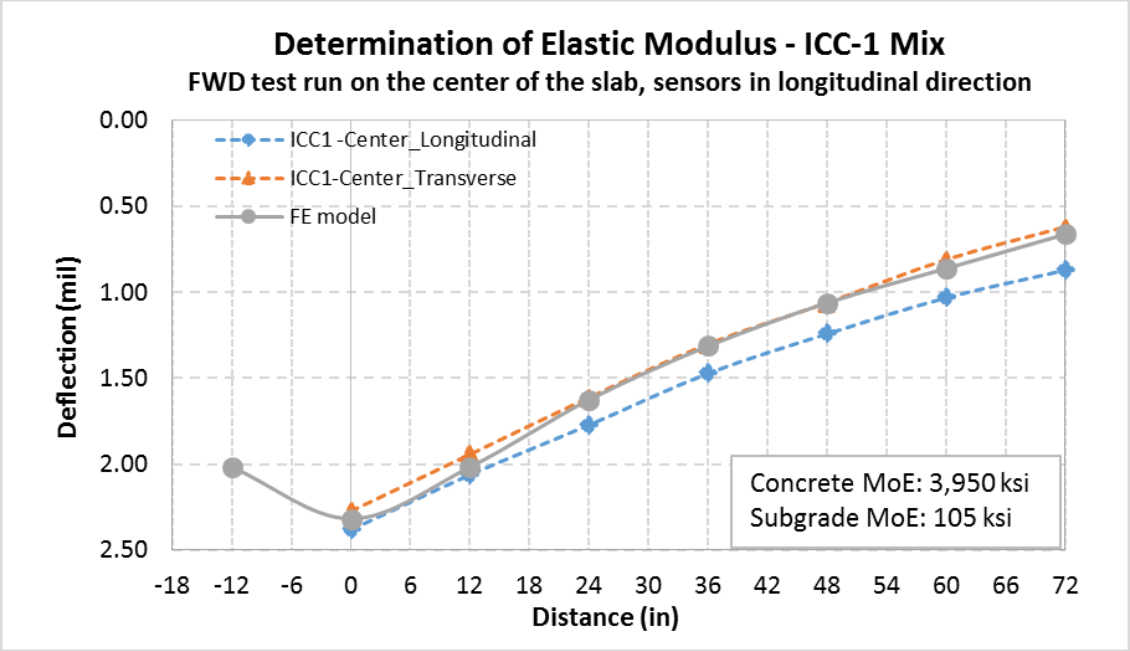

Figure 5-11. Measured and computed deflection basins caused by a 9-kip FWD load at slab center for ICC-1 slab.

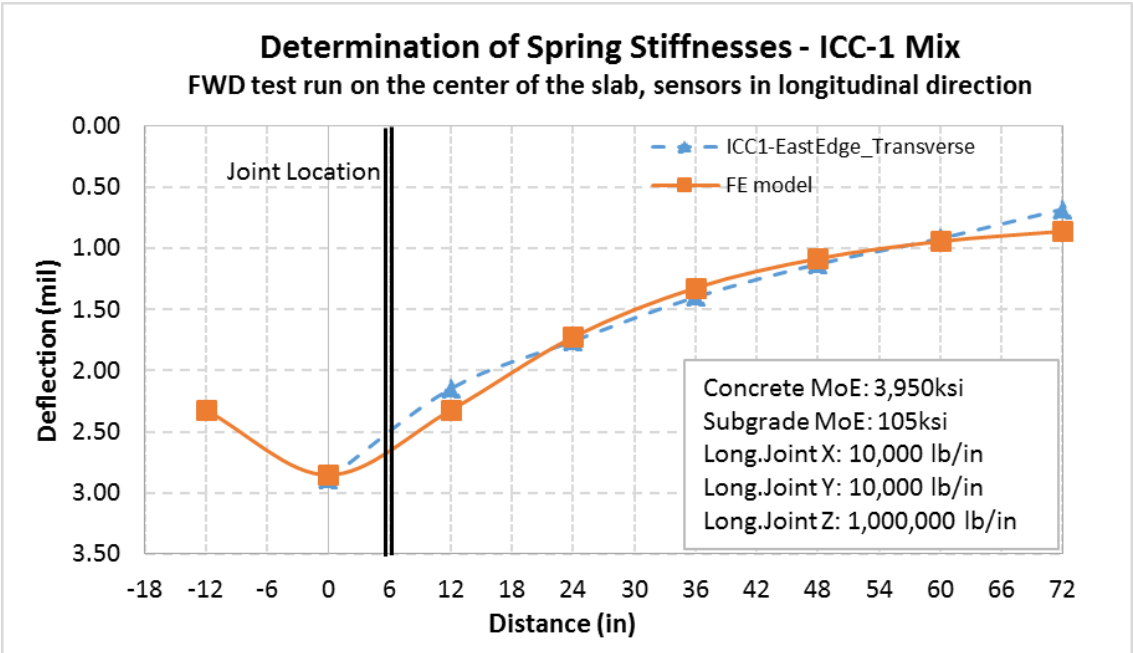

Figure 5-12. Measured and computed deflection basins caused by a 9-kip FWD load across the joint for ICC-1 slab.

ICC-2 Slab

For ICC-2 slab, a 9-kip FWD load was again used as the applied load for calibrating the numerical model. Using a similar process as in the previous step, the analytical deflection basin was matched to the FWD deflection basin by using the elastic modulus of the subgrade of 105 ksi, as shown in Figure 5-13. The analytical and measured deflection across the joint were matched fairly well by using vertical stiffness of 1,000,000 lb/in., and stiffness of 10,000 lb/in. in the other directions, as shown in Figure 5-14.

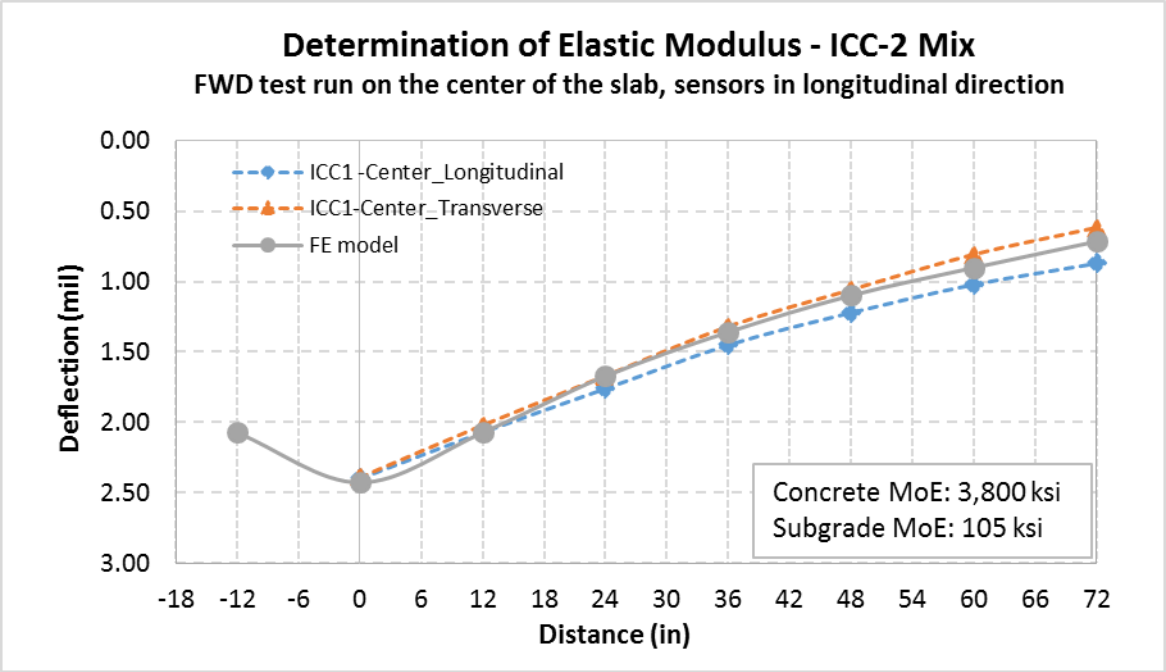

Figure 5-13. Measured and computed deflection basins caused by a 9-kip FWD load at slab center for ICC-2 slab.

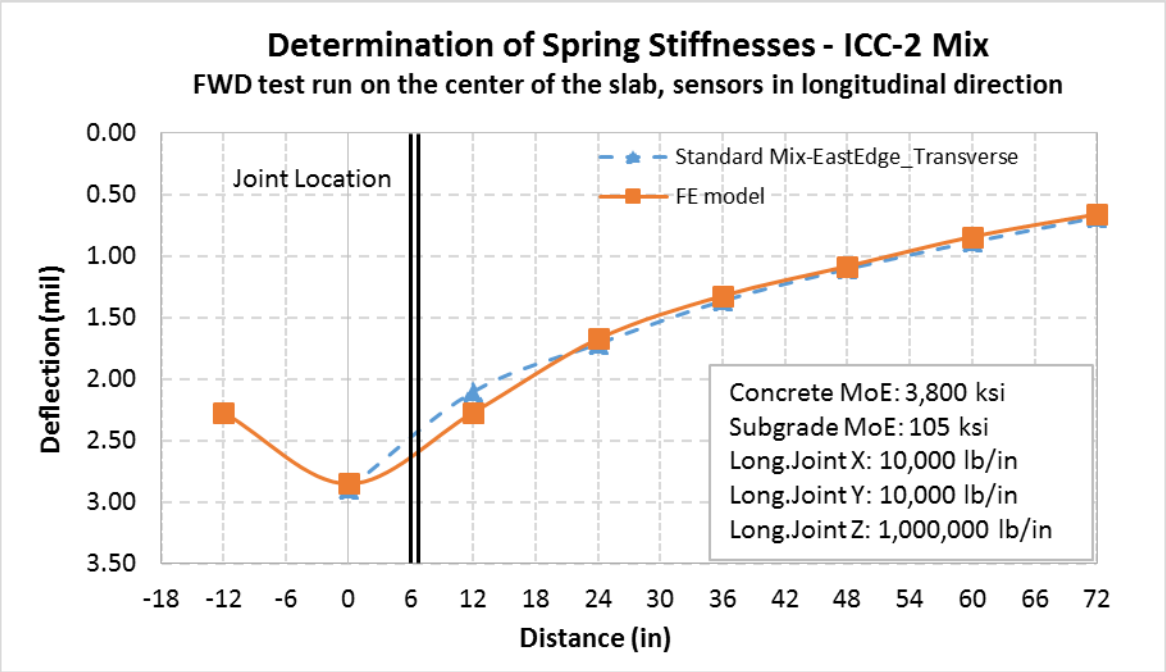

Figure 5-14. Measured and computed deflection basin caused by a 9-kip FWD load across the joint for ICC-2 slab.

5.5.3 Verification of Model Parameters

In order to verify the parameters for ADINA FE models for the test slabs, the measured strains from strain gauges embedded in the test slab were compared with the computed strains. The strain at each gauge location was computed by using ADINA FE model for the case of static load shifted according to the locations of the HVS wheel at different times. A total of 64 shifts of the applied wheel load were used to simulate one pass of the HVS loading with a speed of 7.5 miles per hour. Figures 5-15 through 5-17 show the comparisons of analytical strains using the ADINA FE model with the measured strains on the standard-mix slab.

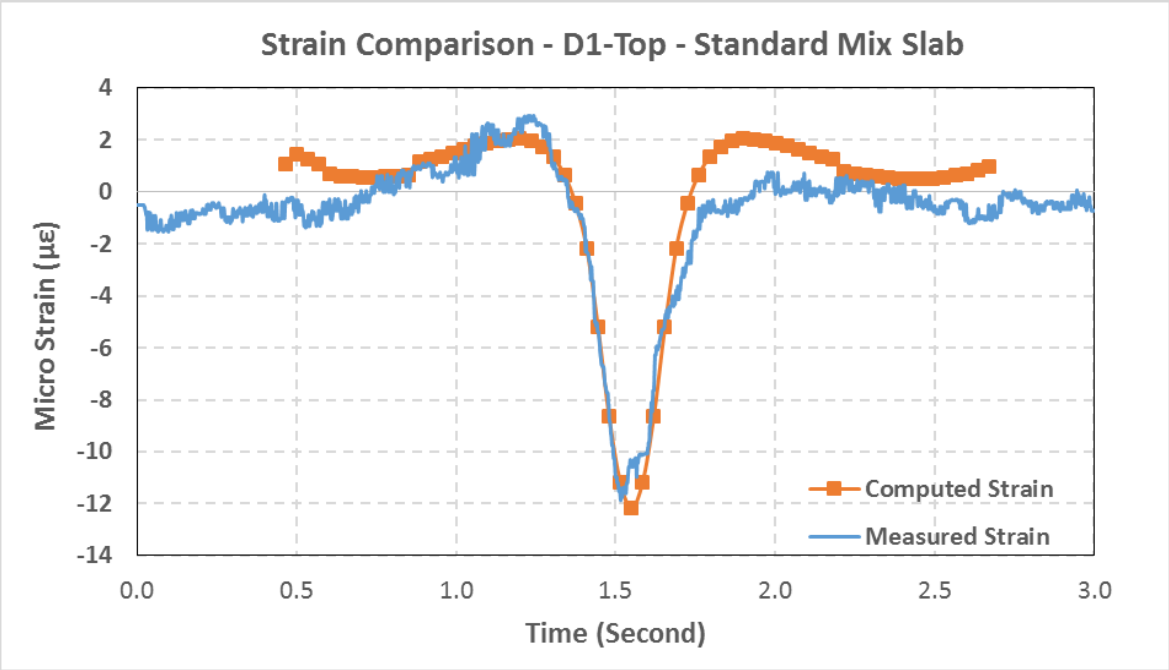

Figure 5-15. Measured and computed strains for gauge D1 top on standard-mix slab

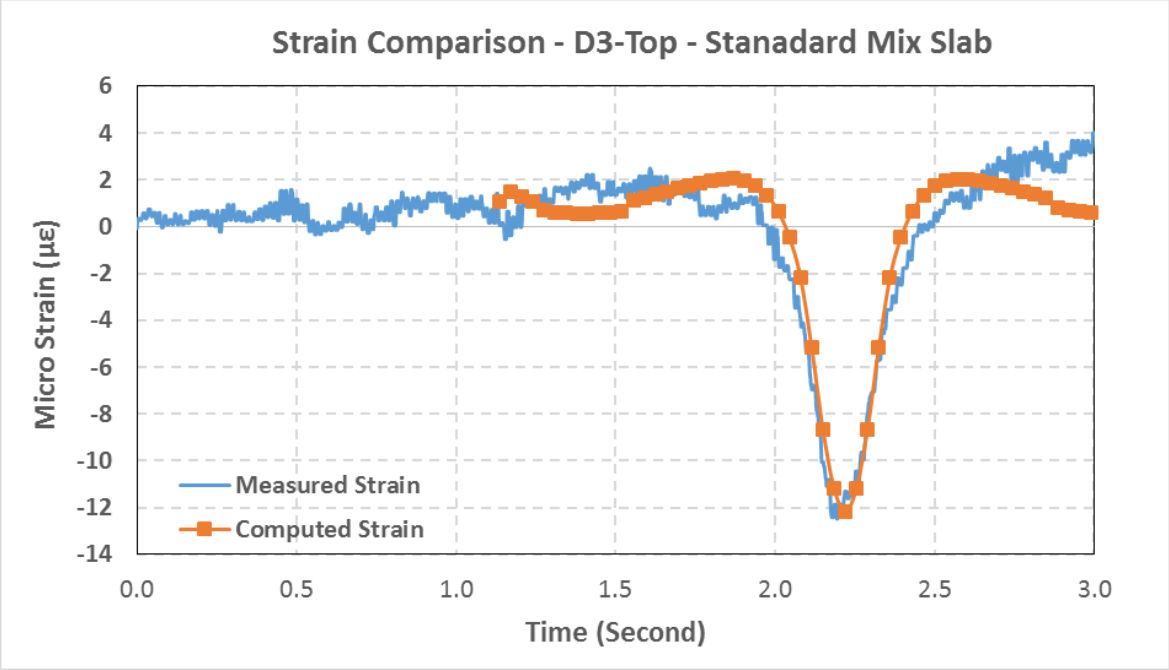

Figure 5-16. Measured and computed strains for gauge D3 top on standard-mix slab

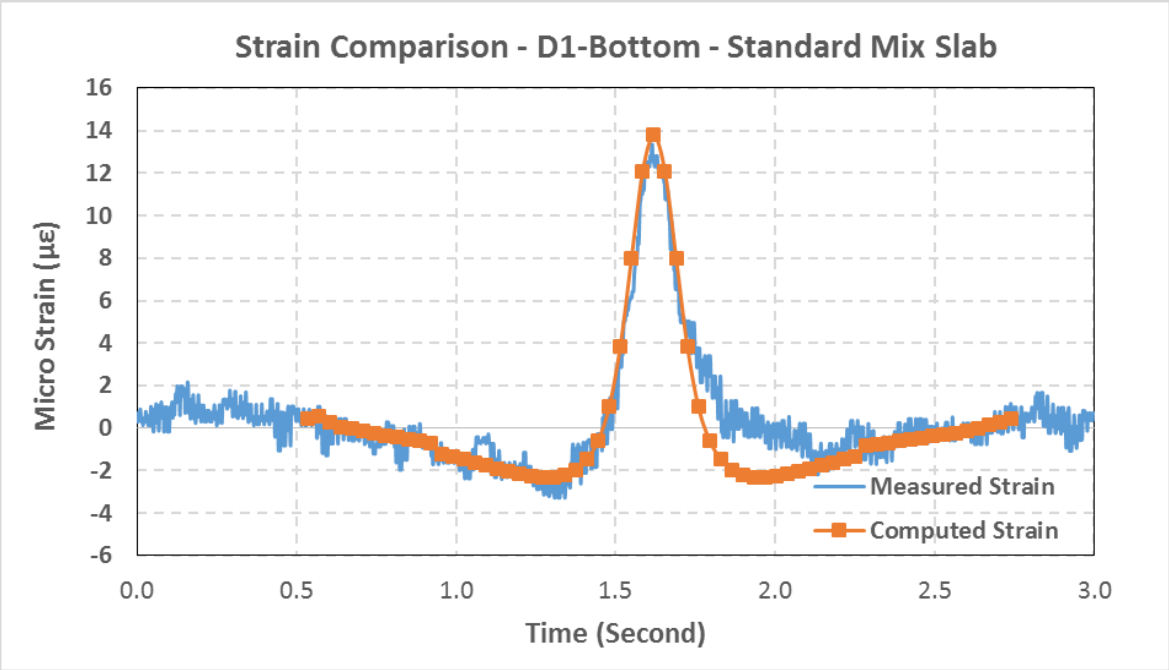

Figure 5-17. Measured and computed strains for gauge D1 bottom on standard-mix slab

The strain-based calibration of the model parameters in ICC-1 slab was also performed in a similar manner as in the standard-mix slab. Figures 5-18 through 5-20 show the comparisons of the computed strains with the measured strains for a few selected gauge locations. It can be seen that, in general, the calculated strains matched well with the measured strain at their maximum values.

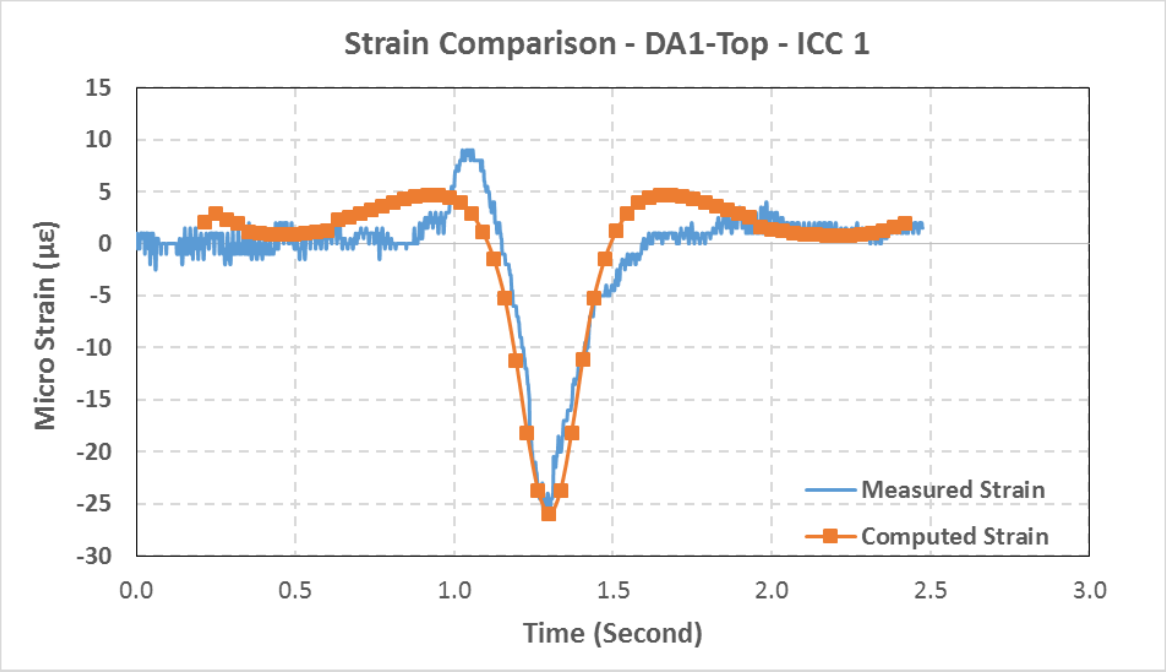

Figure 5-18. Measured and computed strains for gauge DA1 top on ICC-1 slab

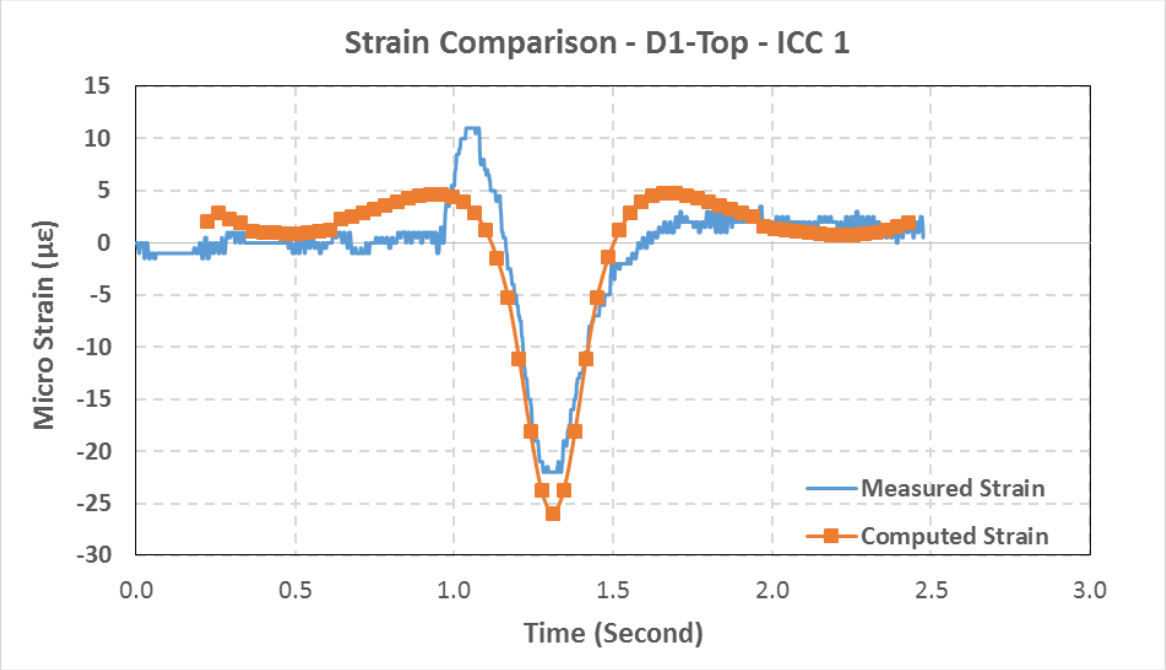

Figure 5-19. Measured and computed strains for gauge D1 top on ICC-1 slab

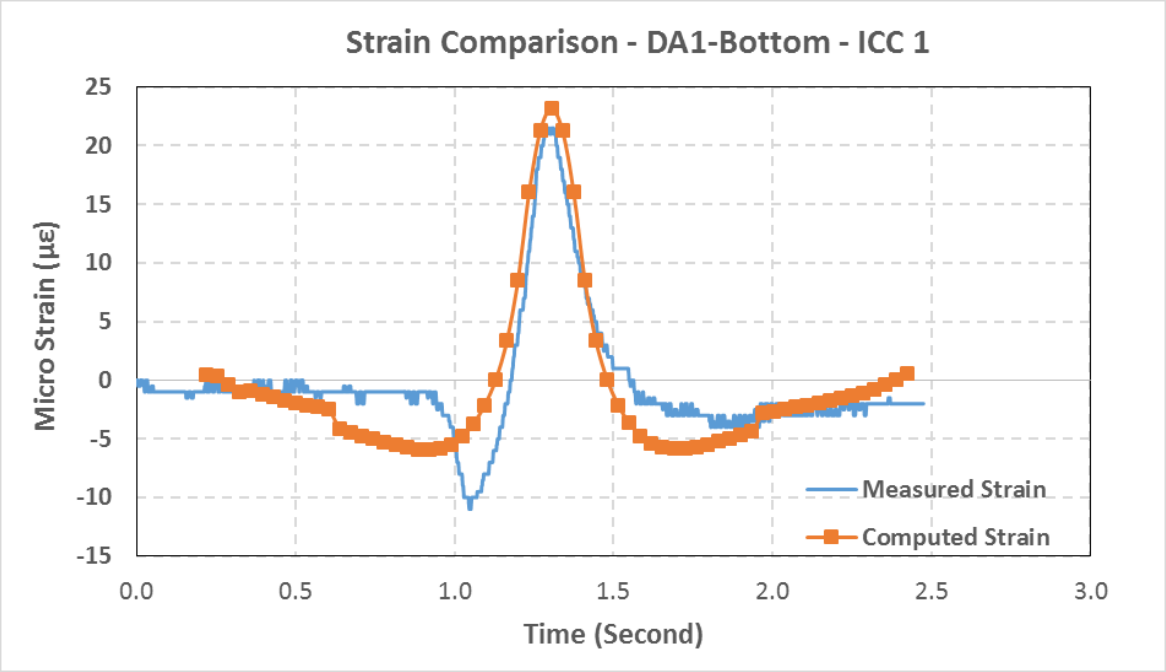

Figure 5-20. Measured and computed strains for gauge DA1 bottom on ICC-1 slab

The model parameters were also verified using measured strain data for ICC-2 slab. Figures 5-21 through 5-23 show the comparisons of analytical strains using the ADINA FE model and measured dynamic strains at gauge locations DA1-Top, D1-Top, and DA1-Bottom, respectively. It can be concluded that reasonable agreement between the simulated results and measured values was found in the strain calibration procedures.

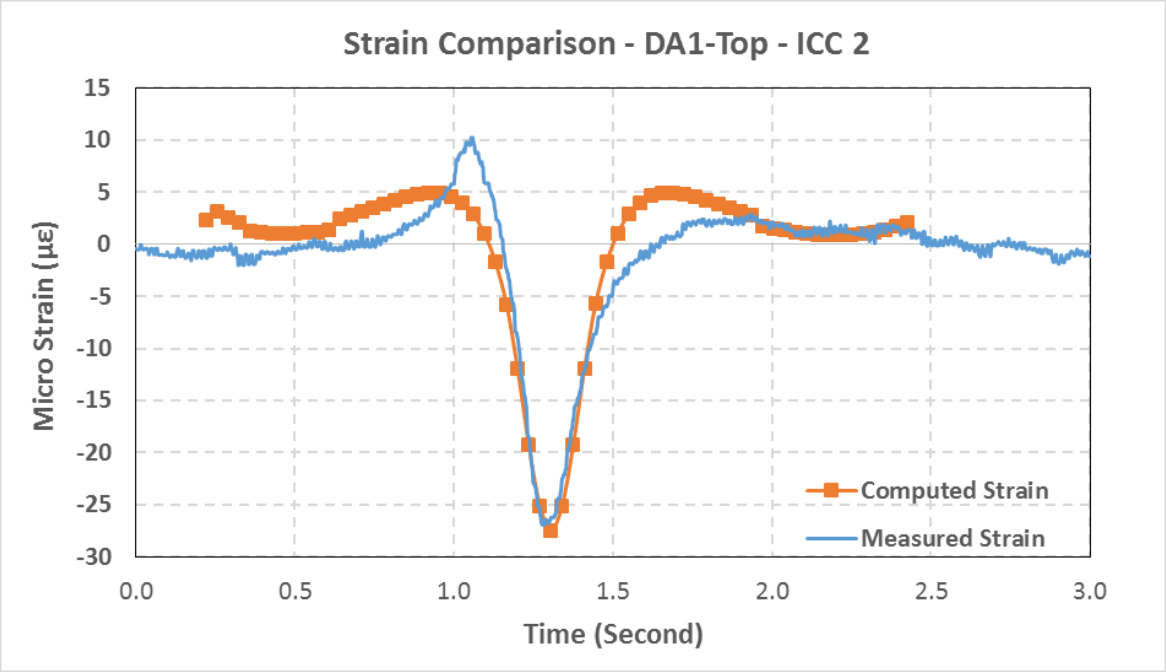

Figure 5-21. Measured and computed strains for gauge DA1 top on ICC-2 slab

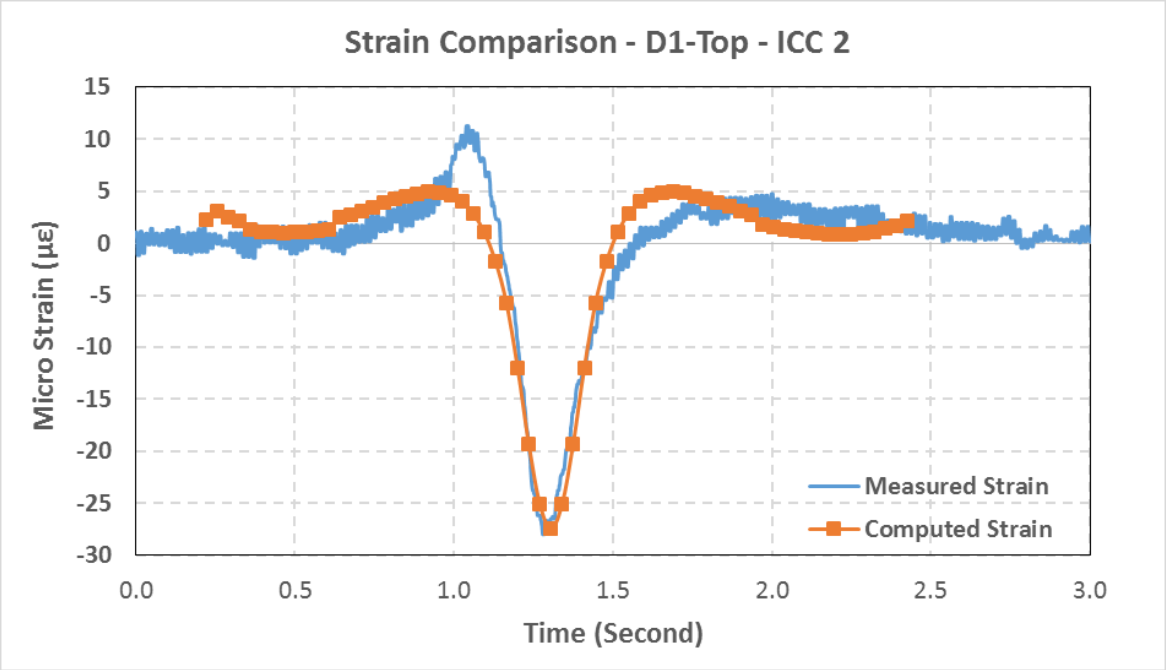

Figure 5-22. Measured and computed strains for gauge D1 top on ICC-2 slab

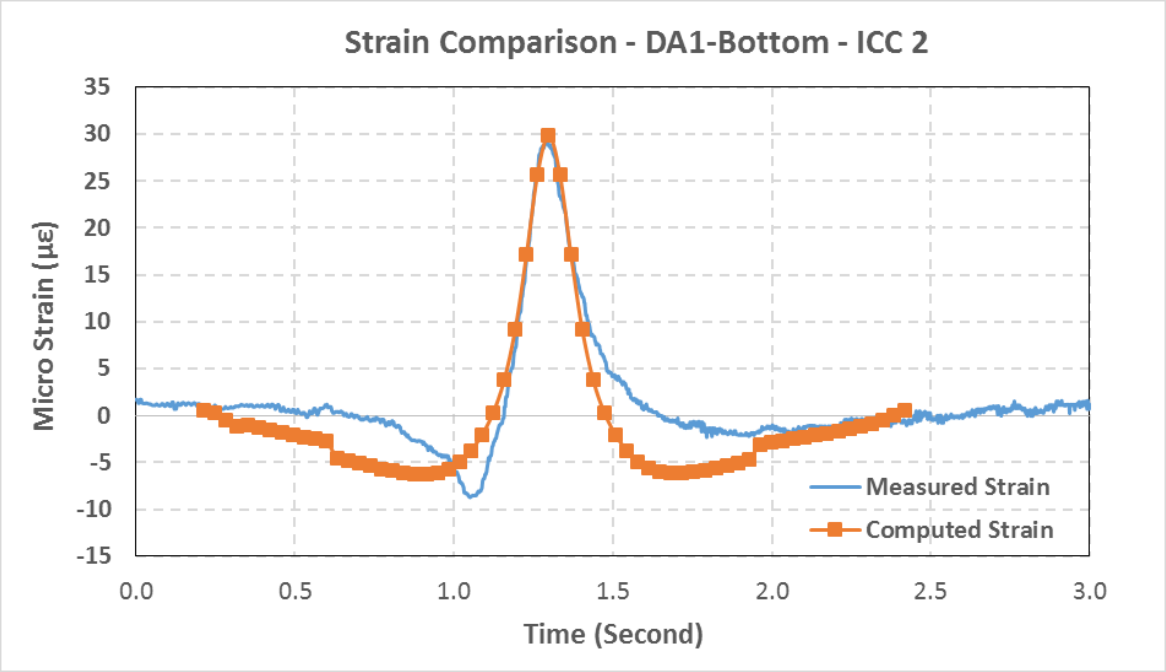

Figure 5-23. Measured and computed strains for gauge DA1 bottom on ICC-2 slab

Table 5-12 presents a summary of model parameters calibrated for the test slabs in this study. The 3-D FE models with the calibrated parameters were used to perform the analysis of stresses under critical loading condition in Florida.

Table 5-12. Summary of Model Parameters Calibrated for the Test Slabs

Parameters used in ADINA		Standard Mix	ICC-1	ICC-2
Elastic Modulus of Concrete (ksi)		4,550	3,950	3,800
Density of Concrete (pcf)		138.3	129.9	130.4
Coefficient of Thermal Expansion (in/in/°F)		4.425E-6	4.239E-6	4.239E-6
Poisson's ratio		0.2	0.2	0.2
Elastic Modulus of Subgrade (ksi)		115	105	105
Spring Constant for Load Transfer (lb/in)	Trans. Joint X	10,000	10,000	-
	Trans. Joint Y	10,000	10,000	-
	Trans. Joint Z	100,000	1,000,000	-
	Long. Joint X	10,000	-	10,000
	Long. Joint Y	10,000	-	10,000
	Long. Joint Z	1,000,000	-	100,000

5.6 Assessment of Performance of ICC Pavement Slabs

5.6.1 Assessment by Critical Stress Analysis

Previous research studies on concrete pavements in Florida have shown that concrete pavement slabs tend to have a positive temperature differential (where the temperature at the top of the slab is higher than the temperature at the bottom) at midday and the slabs tend to curl upward at the slab center. A typical severe temperature differential in the concrete slab at midday has been found to be +20°F. At this temperature condition, the most critical loading position is when the axle load is placed at the mid-edge of the slab.

Conversely, concrete pavement slabs tend to have a negative temperature differential at night, and the slabs tend to curl up at the slab edges and corners. A typical severe temperature differential in the concrete slab at night has been found to be -10°F. At this temperature condition, the most critical loading position is when the axle load is placed at the corner of the slab.

Using the developed 3-D finite element models for the three test slabs, which were calibrated with the measured deflection basins from FWD tests and validated with the measured strains from HVS tests, analysis was performed to determine the maximum stresses in the slabs if they were subject to some critical load and temperature conditions. A 22-kip axle load, which represents the maximum legal load limit for single axle load in Florida, was used as the applied load in the analysis. Analysis for the following two critical load-temperature conditions was performed:

(1) A 22-kip axle load was applied to the mid-edge of the pavement slab with a temperature differential of +20°F.

(2) A 22-kip axle load was applied to the corner of the pavement slab with a temperature differential of -10°F.

These two critical loading conditions are shown in Figure 5-24. For comparison purpose, analysis was also performed for the following load-temperature conditions:

(1) A 22-kip axle load was applied to the mid-edge of the pavement slab with no temperature differential.

(2) A 22-kip axle load was applied to the mid-edge of the pavement slab with a temperature differential of -10°F.

(3) A 22-kip axle load was applied to the corner of the pavement slab with no temperature differential.

(4) A 22-kip axle load was applied to the corner of the pavement slab with a temperature differential of +20°F.

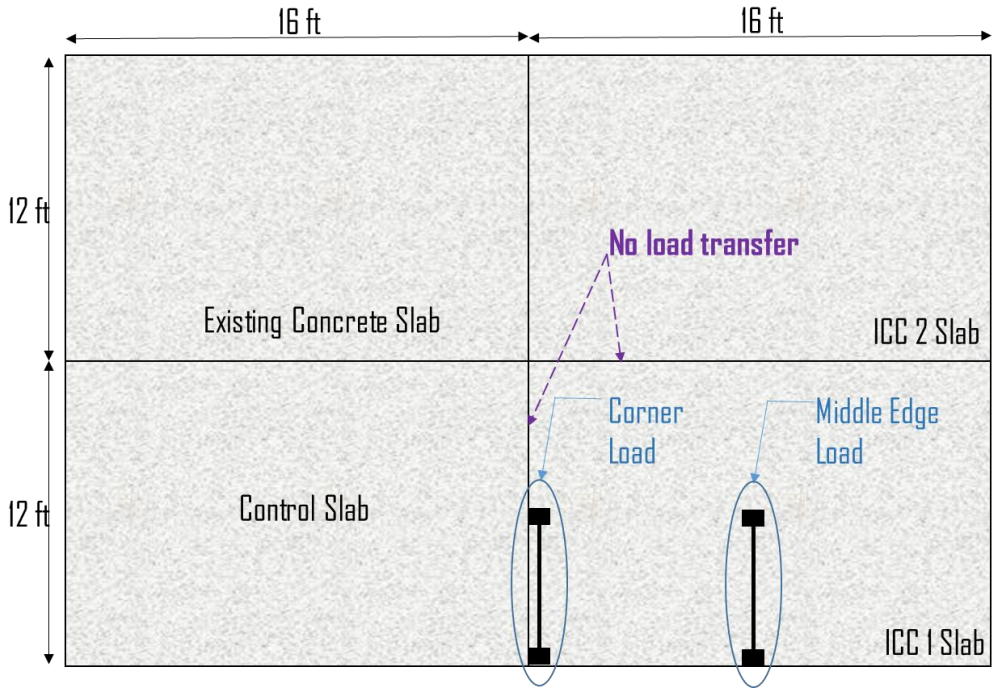

Figure 5-24. Critical loading conditions.

Table 5-13 shows the maximum computed stresses in the three test slabs from the critical stress analysis. In order to assess the potential performance of these test slabs in service, the maximum computed stresses were divided by the flexural strength of the concrete of the test slab

to obtain the stress-to-strength ratios. According to fatigue theory, the number of load repetitions to failure of concrete increases as the stress-to-strength ratio decreases. Thus, a lower computed stress-to-strength ratio would indicate a higher allowable number of load repetitions to failure and a better expected performance in service. The measured 28-day flexural strengths of the concrete sampled from the test slabs as reported in Section 5.2.4 were used to compute the stress-to-strength ratios, which are also shown in Table 5-13. Since the measured flexural strength of ICC-1 with w/c ratio of 0.32 (662 psi) was substantially lower than the flexural strength of the corresponding ICC mixture with the same w/c ratio from the laboratory study (820 psi), the flexural strength value of 820 psi was also used in the calculation of the stress-to-strength ratios for the ICC-1 test slab.

Table 5-13. Computed Maximum Stresses and Stress-to-Strength Ratios for the Test Slabs

Mix	W/C	CTE (in/in/°F)	Modulus of Elasticity (ksi)	Flexural Strength (psi)	Computed Stress (psi)		Stress-to-Strength Ratio	
					Corner	Mid-edge	Corner	Mid-edge
Temperature Differential of +20°F Between Top and Bottom								
SM	0.40	4.425	4,550	725	217.8	451.0	0.30	0.62
ICC-1	0.32	4.239	3,950	662 (820*)	194.3	397.4	0.29 (0.24#)	0.60 (0.48#)
ICC-2	0.40	4.239	3,800	705	190.6	389.7	0.27	0.55
Temperature Differential of -10°F Between Top and Bottom								
SM	0.40	4.425	4,550	725	217.4	154.7	0.30	0.21
ICC-1	0.32	4.239	3,950	662 (820*)	205.2	138.1	0.31 (0.25#)	0.21 (0.17#)
ICC-2	0.40	4.239	3,800	705	204.1	135.8	0.29	0.19
Temperature Differential of 0°F Between Top and Bottom								
SM	0.40	4.425	4,550	725	173.3	235.3	0.24	0.32
ICC-1	0.32	4.239	3,950	662 (820*)	164.9	227.2	0.25 (0.20#)	0.34 (0.28#)
ICC-2	0.40	4.239	3,800	705	163.3	225.7	0.23	0.32

Note: * Flexural strength of similar ICC mix from laboratory study.
Stress-to-strength ratio computed using flexural strength from laboratory study.

From the results presented in Table 5-13, it can be seen that the maximum stresses and the maximum stress-to-strength ratios were obtained at the condition when a 22-kip axle load was applied to the mid-edge of the pavement slab with a temperature differential of +20°F. At this critical loading condition, the computed stress-to-strength ratios for the ICC-2 and ICC-1 slabs (0.55 & 0.60, respectively) were all lower than that for the standard-mix slab (0.62). When the more appropriate flexural strength value of 820 psi was used for the ICC-1 slab, the stress-to-strength ratio was reduced to 0.48, which is substantially lower than that for the standard-mix slab. Thus, based on the results of the critical stress analysis, the two internally cured concrete slabs will likely have better potential performance than the standard-mix slab in service.

5.6.2 Assessment by Visual Observation

Figure 5-25 shows a picture of the surface of the standard-mix slab after it has been loaded by the HVS. Though the standard-mix slab remained in good condition, some hairline cracks could be seen next to the wheel path of the HVS wheel load. These hairline cracks could be caused by micro shrinkage cracks which developed into hairline cracks after the slab was loaded repetitively by the HVS wheel load. Figures 5-26 and 5-27 show the pictures of the surface of the ICC-2 and ICC-1 slabs after they were loaded by the HVS. No visible crack was observed from these two test slabs. From the visual observation of these three test slabs, the ICC slabs appeared to have better performance than the standard-mix slab.

Figure 5-25. Surface of standard-mix slab after HVS loading.

Figure 5-26. Surface of ICC-2 slab after HVS loading.

Figure 5-27. Surface of ICC-1 slab after HVS loading.

5.7 Summary of Findings

Three test slabs were constructed to evaluate the performance of internally cured concrete (ICC) in pavement slabs. They were constructed respectively with (1) a standard-mixture with 0.40 w/c ratio, (2) an ICC mixture with 0.40 w/c ratio, and (3) an ICC mixture with 0.32 w/c ratio. Samples of the concrete used were collected and evaluated for their fresh concrete properties and hardened concrete properties. The falling weight deflectometer (FWD) tests were performed on the test slabs to characterize their structural behavior. Repetitive wheel loads by the heavy vehicle simulator (HVS) were applied to the test slabs to evaluate their structural performance and to measure the load-induced strains in the concrete slabs. Using the measured properties of the hardened concrete, the measured FWD deflections, and the measured HVS load-induced strains, 3-D finite element models were developed and calibrated for the test slabs.

The calibrated models were then used to calculate the maximum stresses in these test slabs under the critical temperature-load condition when a 22-kip axle load was applied to the mid-edge of the pavement slab with a temperature differential of +20°F. The maximum computed stresses for the test slab were divided by the flexural strength of the respective concrete to determine the stress-to-strength ratio, which was used to evaluate the potential performance of the test slabs.

The results of the critical stress analysis showed that, at this critical loading condition, the computed stress-to-strength ratios for the ICC with 0.40 w/c ratio of 0.40 and the ICC with 0.32 w/c ratio were 0.55 & 0.60, respectively, as compared with a stress-to-strength ratio of 0.62 for the standard-mix slab. The flexural strength of the sampled ICC with 0.32 w/c ratio was noted to be much lower than that a similar ICC of the same w/c ratio in the laboratory study. When the flexural strength from the laboratory study was used to compute the stress-to-strength ratio for this ICC slab, the stress-to-strength ratio was reduced to 0.48, which is substantially lower than that for the standard-mix slab.

Visual inspection of the standard-mix slab after HVS loading and at three months after placement showed that some hairline cracks could be seen next to the wheel path. These hairline cracks could be caused by micro shrinkage cracks which developed into hairline cracks after the slab was loaded repetitively by the HVS wheel load. No visible crack was observed from the two ICC test slabs. From the visual observation of these three test slabs, the ICC slabs appeared to have better performance than the standard-mix slab.

Based on the results of the critical stress analysis and the visual inspection of the three test slabs, the ICC test slabs appear to have better performance than the standard-mix slab.

CHAPTER 6
DEVELOPMENT OF FIELD IMPLEMENTATION PLAN

6.1 Introduction

The results from the laboratory testing program on ICC mixes have shown that ICC mixes with w/c ratios of 0.4, 0.36, and 0.32 can be produced with satisfactory workability and satisfactory strength which meet the requirements of Florida Class II (Bridge Deck), IV, and V concretes. The ICC mixes were found to have better resistance to shrinkage cracking than the standard mixes from the results of the restrained shrinkage ring test. The results from the APT evaluation of ICC pavement slabs have shown that the ICC pavement slabs have better resistance to shrinkage cracking and have potentially better performance than the standard-mix slabs from the results of critical stress analysis. Based on the results from the laboratory testing program and the APT evaluation of the ICC test slabs, it is recommended that a field testing program be implemented to further assess the performance and benefits of ICC mixes in bridge deck and pavement applications. This chapter presents the recommended field implementation plan.

6.2 Experimental Bridge Decks and Pavement Slabs

6.2.1 Experimental Bridge Decks

It is recommended that three sets of experimental bridge decks be constructed for evaluation. Each set will consist of two bridge decks at the same location. One bridge deck will use a standard concrete mix and the other bridge deck will use an ICC mix with the same w/c ratio. These three sets of bridge decks will be done in the field on actual FDOT projects with the cooperation of the concrete contractors. It is expected that the selected bridge decks will be reinforced concrete decks with width of no more than 30 feet, length of no more than 45 feet, and thickness of no more than 9 inches. Projects using concrete with three different w/c ratios

ranging from 0.32 to 0.40 are to be identified and selected to be used. The ready-mix plant has to have at least 3 aggregate bins for coarse aggregate, sand, and LWA. Preferably, the concrete producer should have prior experience working with lightweight aggregate.

6.2.2 Experimental Pavement Slabs

It is recommended that three sets of experimental pavement slabs be constructed for evaluation. Each set will consist of two pavement slabs at the same location. One pavement slab will use a standard concrete mix and the other pavement slab will use an ICC mix with the same w/c ratio. One set of pavement slabs will be conducted in the field on actual FDOT project with the cooperation of the concrete contractor. The other two sets of test slabs are to be conducted at the FDOT APT facility in Gainesville. The size of each pavement slab will be 12 feet wide and 16 feet long. The thickness of the concrete test slabs at the FDOT APT facility will be 9 inches, while the thickness of the test slabs in the field will be the same as that of the adjacent slabs. Preferably, the three sets of experimental slabs will use concrete with three different w/c ratios ranging from 0.32 to 0.40.

6.3 Quality Assurance Plan

6.3.1 Design of ICC Mixes

The ICC mixes to be used will have the same w/c ratio as the corresponding standard mixes. They will be designed and evaluated by the procedures as presented in Chapter 4 of this report before they are adopted. The ICC mixes for bridge decks will satisfy the FDOT specification requirements for Florida Class II (Bridge Deck) concrete, while the ICC mixes for pavement slabs will satisfy the FDOT specification requirements for Florida Class I (Pavement) concrete. A target slump of 5 inches is recommended for the ICC mixes for ease of placement and consolidation.

6.3.2 Control of W/C Ratio

It is imperative that the w/c ratios of the concrete to be used on the experimental bridge decks and pavement slabs be strictly controlled to meet the target w/c ratios. If the slump of the fresh concrete is too low, it should be adjusted by the use of a high-range water reducing admixture rather than by adding more water to the mix.

6.3.3 Control of Fresh Concrete Properties

The following tests are to be performed on the fresh concrete before placement:

1) Slump (ASTM C143)

2) Air content (ASTM C231)

3) Unit weight (ASTM C138)

4) Temperature (ASTM C1064)

6.3.4 Special Attention and Care to ICC Mixes

The lightweight aggregate has to be saturated before it is used in a concrete mix. The water content of the lightweight aggregate needs to be accurately determined and the excess water needs to be accurately accounted for in the mix design.

6.4 Testing of Sampled Concrete

For each test bridge deck or test pavement slab, concrete sample is to be obtained from the concrete delivery truck to make specimens for the hardened concrete tests as shown in Table 6-1.

Table 6-1. Hardened Concrete Tests for Bridge Deck and Pavement Slab

Tests	Samples	Days of Testing
Compressive Strength (ASTM C39)	4" x 8" cylinder (6 specimens)	At 7 and 28 days
Modulus of Elasticity (ASTM C469)	4" x 8" cylinder (3 specimens)	At 28 days
Coefficient of Thermal Expansion (AASHTO T 336)	Use the same specimens from MOE test	At 28 days
Flexural Strength (ASTM C78)	4" x 4" x 14" beam (6 specimens)	At 7 and 28 days
Free Drying Shrinkage (ASTM C157)	3" x 3" x 11.25" prism (6 specimens)	At 7 and 28 days
Additional tests for bridge deck		
Rapid Chloride Penetration (ASTM C1202)	4" x 8" cylinder (3 specimens)	At 28 days
Surface Resistivity Test (AASHTO TP95-11)	4" x 8" cylinder (3 specimens)	At 28 days

For each test bridge deck, additional specimens will be made for the following tests on the hardened concrete to characterize its durability quality:

6.5 Instrumentation Plan

6.5.1 Instrumentation Plan for Bridge Decks

Each bridge deck will be instrumented with a total of six moisture sensors, six strain gauges, and nine temperature sensors to monitor the moisture content, strain, and temperature of the concrete. They will be installed at three locations, namely the center, the edge, and the wheel path of the bridge deck. At each of these three locations, one moisture sensor and one strain gauge will be installed near the top and another moisture sensor and another strain gauge will be

installed near the bottom of the concrete deck. At each of these three locations, one temperature sensor will be installed near the top, one near the bottom, and one at the mid-depth of the concrete deck. These sensors will be connected to a data logger in a secure box by the bridge deck, and will be programmed to take readings at one-hour intervals.

6.5.2 Instrumentation Plan for Bridge Decks

Figure 6-1 shows the instrumentation layout for each of the test pavement slabs to be constructed at the FDOT APT facility. The instrumentation will include (1) electrical resistance strain gauges to measure the dynamic strains in the concrete slabs due to HVS loading, (2) thermocouple wires to measure temperature distribution in the concrete slabs, and (3) LVDTs to measure the vertical movement of the test slab due to the curling effects of temperature and moisture variation in the slabs.

The locations for the dynamic strain gauges will be selected based on the anticipated maximum strain responses in the test slabs from the anticipated HVS loading. They will be installed under the anticipated wheel paths of the HVS loading. At each indicated gauge location, two embedded strain gauges will be placed at a depth of 1 in. (2.54 cm) from the concrete surface, and 1 in. (2.54 cm) from the bottom of the concrete layer. This will be achieved by securing the strain gauges between two nylon rods which will be securely driven into the base layer before the pouring of the concrete to form the test slab.

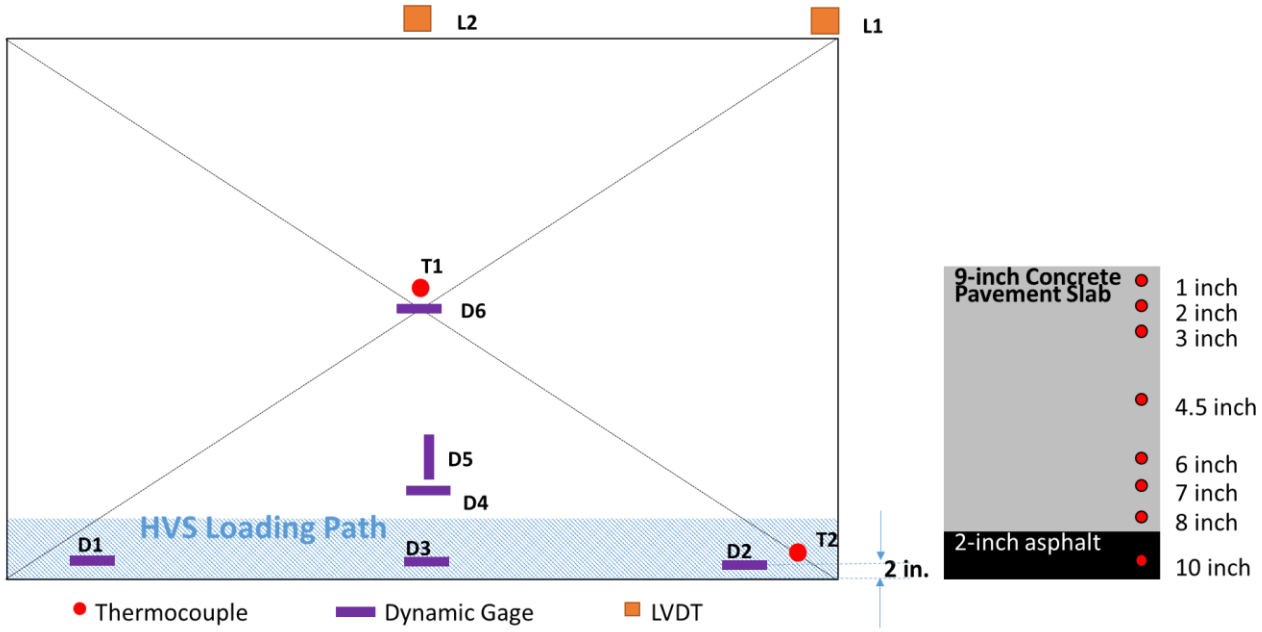

Figure 6-1. Instrumentation layout for test slab at APT facility.

Sets of thermocouple wires will be installed at the slab centers and corners as shown in the layout. Each set of thermocouple wires will consist of eight wires, which will be fixed on a PVC rod and placed at depths of 1, 2, 3, 4.5, 6, 7, and 8 in. (2.54, 5.08, 7.62, 11.43, 15.24, 17.78, and 20.32 cm) from the surface of the concrete slab, and one thermocouple which will be placed in the base layer at a depth of 1 in. (2.54 cm) from the top of the base layer or at a depth of 10 in. (25.4 cm) from the concrete surface.

LVDTs will be installed at the corner of each slab and the center of the longitudinal edge of the control slab and the ICC slab. Invar-bars, which have a uniquely low coefficient of thermal expansion, will be secured to the base of the slabs and used to hold the LVDTs so that the LVDT will have a fixed reference which will not be influenced by the fluctuation of temperature. These LVDTs will be used to monitor the vertical movement of the slabs at the various locations on the slabs.

A mobile data acquisition system will be used to read the LVDTs and the temperature data at 15-minute intervals. During the HVS testing, dynamic strain data from the tested slab will be recorded at every15-minute interval, for 30 seconds each time, at a rate of 100 values per second for each strain gauge.

When the test slabs are constructed in the field, the electronic dynamic strain gauges will be installed under the wheel path where the slab is going to be loaded. Additional dynamic strain gauges will also be installed at the mid-edge and corner. The instrumentation layout for each test slab in the field is shown in Figure 6-2.

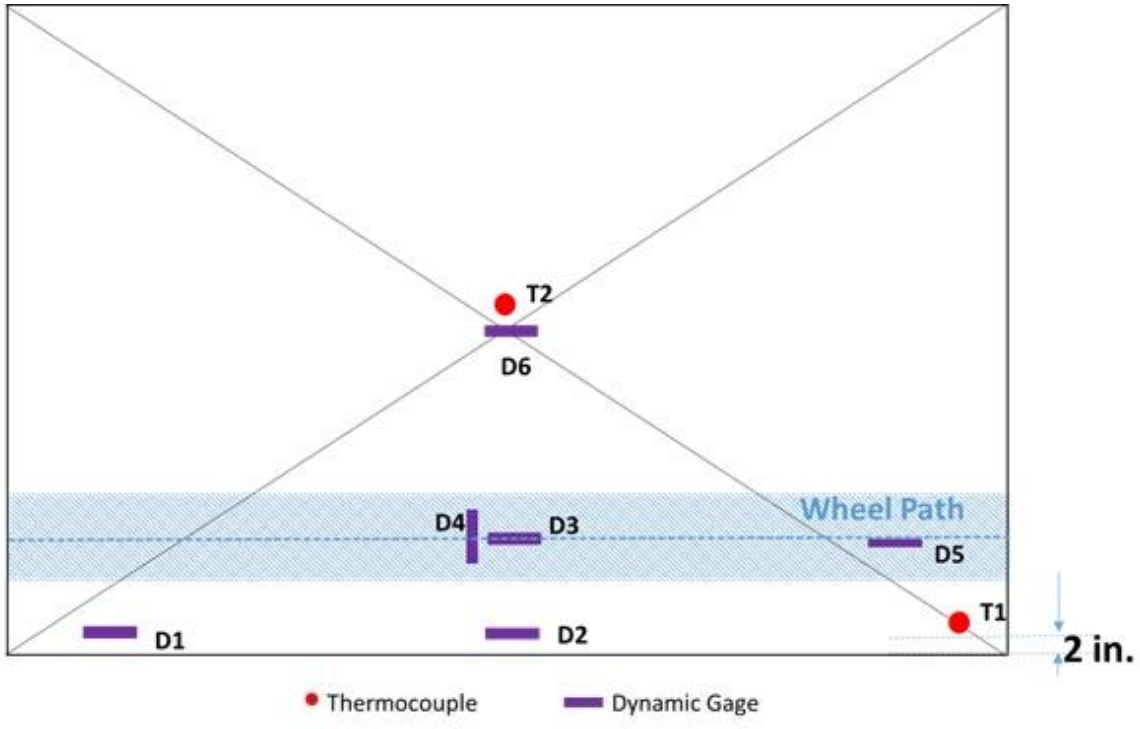

Figure 6-2. Instrumentation layout for test slab in the field.

Prior to installation of gauges, the gauges should be checked for proper operation and calibration. Thermocouple wires and strain gauge lead wires must be fitted with a nylon sheath to protect them from abrasion and unexpected damage during the construction and testing period.

If concrete is to be placed over an aggregate base, the lead wires should be routed in a shallow trench and then covered with sand. The lead wires are to be routed from the paved lane to the DAQ cabinet through a conduit installed in a trench as shown in Figure 6-3.

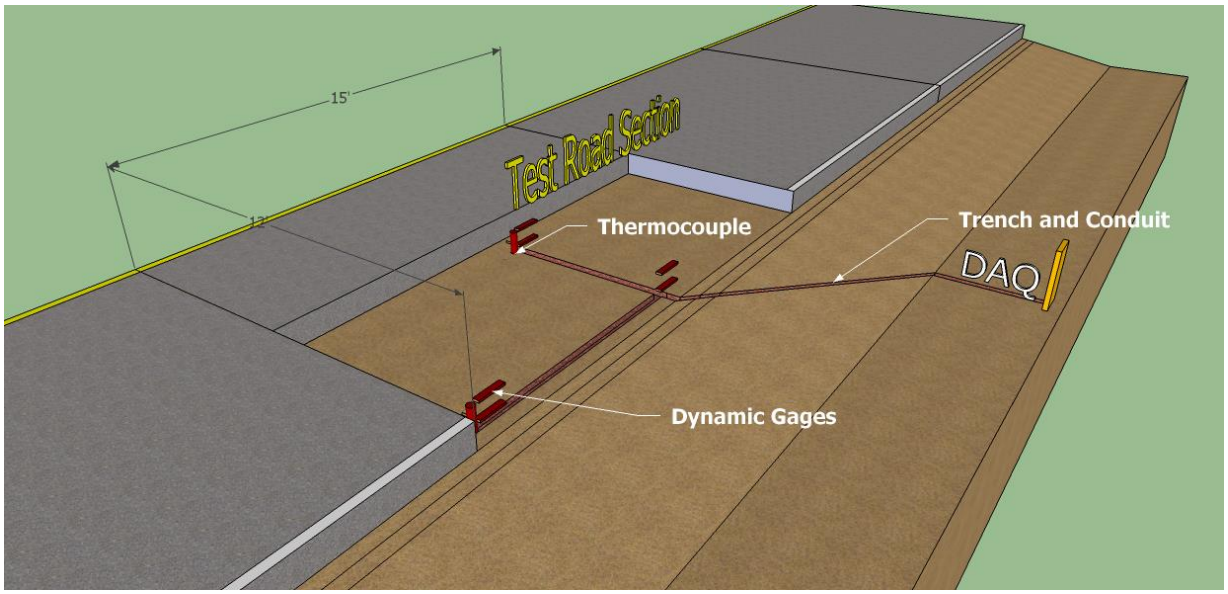

Figure 6-3. Schematics of trench and conduit to protect lead wires.

6.6 Monitoring and Evaluation Plan

6.6.1 Monitoring and Evaluation Plan for Bridge Decks

Thermal imaging of the test bridge decks will be taken after concrete placement to compare the temperature distribution on the surface of the ICC decks with that on the standard-mix decks. The monitored moisture content and temperature variations in the ICC decks will be compared with those in the corresponding standard-mix decks. The test bridge decks will be evaluated by periodic visual inspection for distresses to compare the performance of the ICC bridge decks with the corresponding standard-mix bridge decks. Visual inspection will be performed once a month in the first three months, and once every three months thereafter until one year after concrete placement.

The results of tests on the sampled concrete as listed in Section 6.4 will be evaluated to compare the strength, elastic modulus, CTE, drying shrinkage, and durability quality of the ICC mixes with those of the corresponding standard mixes.

Using the measured properties of the hardened concrete as input parameters, a finite element model will be developed to analyze the strain response of the concrete bridge deck. The calculated strains at various temperature conditions will be compared to the measured strains, and the developed model will be refined as needed. The validated finite element model for analysis of concrete bridge decks will be used to compare the performance of ICC bridge decks with that of the standard mix bridge decks under various critical temperature and load conditions.

6.6.2 Monitoring and Evaluation Plan for Pavement Slabs

Thermal imaging of the test pavement slabs will be taken after concrete placement to compare the temperature distribution on the surface of the ICC slabs with that on the standard mix decks. The monitored moisture content and temperature variations in the ICC slabs will be compared with those in the corresponding standard-mix slabs. The test slabs will be evaluated by periodic visual inspection for distresses. The falling weight deflectometer (FWD) tests will be performed on the test slabs to characterize their structural behavior. Repetitive wheel loads by the heavy vehicle simulator (HVS) will be applied to the test slabs at the FDOT APT facility to evaluate their structural performance and to measure the load-induced strains in the concrete slabs. Dynamic strains caused by the HVS loads will be collected during HVS loading. For the test slabs constructed in the field, HVS loads will not be applied. Using the measured properties of the hardened concrete, the measured FWD deflections, and the measured HVS load-induced strains, finite element models will be developed and calibrated for the test slabs. The calibrated models will then be used to evaluate the structural performance of these test slabs under critical

temperature-load conditions. The recommended method of structural analysis as presented in Chapter 5 of this report will be used.

CHAPTER 7
SUMMARY OF FINDINGS AND RECOMMENDATIONS

7.1 Summary of Findings

7.1.1 Findings from Laboratory Testing Program

A laboratory testing program was conducted to evaluate the properties of three standard concrete mixes and three corresponding internally cured concrete (ICC) mixes with the same w/c ratios and cementitious materials contents. These three concrete mixes met the requirements for Florida Class II (Bridge Deck), IV, and V concretes, had w/c ratios of 0.40, 0.36, and 0.32, and had total cementitious materials contents of 687, 780, and 860 lb/yd^3, respectively. The cementitious materials consisted of 80% Type I/II Portland cement and 20% Class F fly ash. The ICC mixes were produced by replacing a part of the fine aggregate with a pre-wetted lightweight aggregate (LWA). The quantity of LWA used was an amount that would supply 7 lbs of absorbed water per 100 lb of cement used. The LWA used was a manufactured expanded clay with a dry bulk specific gravity of 1.23 and water absorption of 25.2%.

The main findings from the laboratory testing program can be summarized as follows:

(1) The amounts of water reducing admixtures needed for the ICC mixes to achieve the same workability of the fresh concrete are less than those for the standard mixes with the same w/c ratios.

(2) The average compressive strength of the ICC mixes was lower than that of the standard mixes with the same w/c ratio by about 11%.

(3) The average flexural strength of the ICC mixes was lower than that of the standard mixes with the same w/c ratio by about 6%.

(4) The average elastic modulus of the ICC mixes was lower than that of the standard mixes with the same w/c ratio by about 18%.

(5) The splitting tensile strength of the ICC mixes was lower than that of the standard mixes with the same w/c ratio by about 10%.

(6) The ICC mixes showed substantially greater resistance to shrinkage cracking than the standard mixes. The average cracking age of all ICC mixes, as measured by the restrained shrinkage ring test, was 2.7 times that of the standard mixes.

(7) The average drying shrinkage of the ICC mixes was higher than that of the standard mixes by about 24%.

(8) The average coefficient of thermal expansion of the ICC mixes was lower than that of the standard mixes with the same w/c ratios by 10%

7.1.2 Findings from Evaluation of Test Slabs

Three test slabs were constructed to evaluate the performance of ICC in pavement slabs. They were constructed respectively with (1) a standard mixture with 0.40 w/c ratio, (2) an ICC mixture with 0.40 w/c ratio, and (3) an ICC mixture with 0.32 w/c ratio. Samples of the concrete used were collected and evaluated for their fresh concrete properties and hardened concrete properties. The test slabs were evaluated by the falling weight deflectometer (FWD) tests and repetitive wheel loads by the heavy vehicle simulator (HVS). Critical stress analysis was performed on the test slabs to evaluate their performance under a typical critical combination of load and temperature condition in Florida.

The results of the critical stress analysis showed that, at a typical critical loading condition in Florida, the computed stress-to-strength ratios for the ICC slab with 0.40 w/c ratio and the ICC slab with 0.32 w/c ratio were 0.55 & 0.60, respectively, as compared with a stress-to-strength ratio of 0.62 for the standard-mix slab.

The flexural strength of the sampled ICC with 0.32 w/c ratio was noted to be much lower than that of a similar ICC with the same w/c ratio in the laboratory study. When the flexural

strength from the laboratory study was used to compute the stress-to-strength ratio for this ICC slab, the stress-to-strength ratio was reduced to 0.48, which is substantially lower than that for the standard-mix slab.

Visual inspection of the standard-mix slab after HVS loading and at about three months after placement showed that some hairline cracks could be seen next to the wheel path. These hairline cracks could be caused by micro shrinkage cracks which developed into hairline cracks after the slab was loaded repetitively by the HVS wheel load. No visible crack was observed from the two ICC test slabs. From the visual observation of these three test slabs, the ICC slabs appeared to have better performance than the standard-mix slab.

Based on the results of the critical stress analysis and the visual inspection of the three test slabs, the ICC test slabs appear to have better performance than the standard-mix slab.

7.2 Recommendations

Based on the results from the laboratory testing program and the evaluation of the ICC test slabs, it is recommended that a field testing program be implemented to further assess the performance and benefits of ICC mixes in bridge deck and pavement application. It is recommended that three sets of experimental bridge decks and three sets of pavement test slabs be constructed for evaluation. The recommended plans for concrete mix designs, quality control, instrumentation, monitoring, and evaluation of these experimental bridge decks and pavement test slabs are presented in Chapter 6 of this report.

LIST OF REFERENCES

Abell, A. B., Willis, K. L., and Lange, D. A. [1998]. "Mercury Intrusion Porosimetry and Image Analysis of Cement-Based Materials". Journal of Colloid and Interface Science, Vol. 211, pp 39-44.

ASTM International. [2014]. ASTM C1702-14 Standard Test Method for Measurement of Heat of Hydration of Hydraulic Cementitious Materials Using Isothermal Conduction Calorimetry. West Conshohocken: ASTM International.

Bentz, D. [2009]. "Influence of Internal Curing using Lightweight Aggregates on Interfacial Transition Zone Percolation and Chloride Ingress in Mortars". *Cement and Concrete Composites*, Vol. 31 [5], pp 285-289.

Bentz, D., Bognacki, C., Riding, K., and Villarreal, V. [2011]. "Hotter Cements, Cooler Concretes". Concrete International, Vol. 33 [1], pp 41-48.

Bentz, D.P. and Weiss, W.J. [2011]. *Internal Curing: A. State-of-the-Art Review*. National Institute of Standards and Technology [NIST], February 2011.

Bentz, D. and Stutzman, P. [2008]. "Internal Curing and Microstructure of High Performance Mortars". *ACI SP-256, Internal Curing of High Performance Concretes: Laboratory and Field Experiences*, American Concrete Institute, Farmington Hills, pp 81-90.

Byard B., Schindler A.K. [2010]. *Cracking tendency of lightweight concrete*. The Expanded Shale, Clay, and Slate Institute. December 2010.

Cardoso, A. V., Oliveira, W. J., and Vaz, G.J.O. [2007]. "Cortical Bone Porosity Visualization Using Mercury Porosimetry Intrusion Data". *Revista Materia*, Vol. 12, No 4, pp 612-617.

Cook, R. A. and Hover, K. C. [1999]. "Mercury Porosimetry of Hardened Cement Pastes". *Journal of Cement and Concrete Research*, Vol. 29, pp 933-943.

Cusson, D., & Hoogeveen, T. [2005]. "Internally-Cured High-Performance Concrete under Restrained Shrinkage and Creep". *CONCREEP 7 Workshop on Creep, Shrinkage, and Durability of Concrete and Concrete Structures*, Nantes, pp 579-584.

Delatte, N., E. Mack, J. Cleary. [2007]. *Evaluation of High Absorptive Materials to Improve Internal Curing of Low Permeability Concrete*. Ohio Department of Transportation, Final Report.

El-Dieb, A. S. and Hooton, R. D. [1994]. "Evaluation of the Katz-Thompson Model for Estimating the Water Permeability of Cement-Based Materials from Mercury Intrusion Porosimetry Data." *Journal of Cement and Concrete Research*, Vol. 24, No 3, pp 443-455.

Espinoza-Hijazin, G. and Lopez, M. [2010]. “Extending Internal Curing to Concrete Mixtures with W/C Higher than 0.42“. *Construction and Building Materials*.

Geiker, M., Bentz, D., and Jensen, O. [2004]. “Mitigating Autogenous Shrinkage by Internal Curing”. *ACI SP-218, High-Performance Structural Lightweight Concrete*, American Concrete Institute, Farmington Hills, pp 143-154.

Ghezal, A. F., G. J. Assaf. [2014]. “Restrained Shrinkage Cracking of Self-Consolidating Concrete”. *Journal of Materials in Civil Engineering*.

Halamickova, P., Detwiler, R., Bentz, D., and Garboczi, E. [1995]. “Water Permeability and Chloride Ion Diffusion in Portland Cement Mortars: Relationship to Sand Content and Critical Pore Diameter”. *Cement and Concrete Research*, Vol. 25, pp 790-802.

Henkensiefken, R., Bentz, D., Nantung, T., and Weiss J. [2009]. “Volume Change and Cracking in internally cured mixtures made with Saturated Lightweight Aggregate under sealed and unsealed conditions”. *Cement and Concrete Composites*, Vol. 31, Issue 7, pp 427-437.

Henkensiefken, R., Briatka, P., Bentz, D., Nantung, T., and Weiss J. [2010]. “Plastic Shrinkage Cracking in Internally Cured Mixtures Made with Pre-wetted Lightweight Aggregate”. *Concrete International*, Vol. 32 [2], pp 49-54.

Ji, T., Zhang, B., Zhuang, Y., Wu, H. [2015]. “Effect of Lightweight Aggregate on Early-Age Autogenous Shrinkage of Concrete“. *ACI Materials Journal*, Vol. 112, No. 1-6, January-December 2015.

Kosmatka S.H., Kerkhoff B., and Panarese W.C. [2003]. *Design and Control of Concrete Mixtures*. Portland Cement Association [PCA].

Li, Z., Qi, M., Li, Z., and Ma, B. [1999]. “Crack Width of High-Performance Concrete Due to Restrained Shrinkage”. *Journal of Materials in Civil Engineering*, Vol. 11, pp 214-223.

Lopez, M., Kahn, L., and Kurtis, K. [2008]. “Effect of Internally Stored Water on Creep of High Performance Concrete.” *ACI Materials Journal*, Vol. 105 [3], pp 265-273.

Lura, P., Pease, B., Mazzotta, G., Rajabipour, F., and Weiss, J. [2007]. “Influence of ShrinkageReducing Admixtures on Development of Plastic Shrinkage Cracks”. *ACI Materials Journal*, Vol. 104, pp 187-194.

Ma, H. [2014]. “Mercury Intrusion Porosimetry in Concrete Technology: Tips in Measurement, Pore Structure Parameter Acquisition and Application”. *Journal of Porous Matter*, Vol. 21, pp 207-215.

Mehta, P.K. and Monteiro, P.J. [2013]. *Concrete: Microstructure, Properties and Materials*, McGraw Hill, New York.

Mindess, S., Young, J.F., Darwin,D. [2002]. *Concrete*, Second Edition, Prentice Hall PTR.

Moura, M. J., P. J. Ferreira, and M. M. Figueiredo. [2005]. "Mercury Intrusion Porosimetry in Pulp and Paper Technology". *Journal of Power Technology*, Vol. 160, pp 61-66.

Pease, B., Hossain, A., and Weiss, W. [2004]. "Quantifying Volume Change, Stress Development, and Cracking Due to Self-Desiccation," *Autogenous Deformation of Concrete* (ACI Special Publication SP-220). American Concrete Institute, Farmington Hills, pp 23-39.

Powers, T., Copeland, L., & Mann, H. [1959]. "Capillary Continuity or Discontinuity in Cement Pastes". *The Research Bulletin of the Portland Cement Association*, Vol. 1 [2], pp38-48.

Schlitter, J., Henkensiefken, R., Castro, J., Raoufi, K., Weiss, J., and Nantung, T. [2010]. "Development of Internally Cured Concrete for Increased Service Life". *Joint Transportation Research Program*, No. FHWA/IN/JTRP-2010/10.

Schlitter, J., Senter, A., Bentz, D., Nantung, T., and Weiss, J. [2010]. "Development of a Dual Ring Test for Evaluating Residual Stress Development of Restrained Volume Change". *Journal of ASTM International*, (7), 13.

Shin, K., Castro, J., Schlitter, J., Golias, M., Pour-Ghaz, M., Henkensiefken, R., et al. [2010]. "The Role of Internal Curing as a Method to Improve Durability". *Handbook of Concrete Durability*, pp 379-428.

Shuhui, D., Z. Baosheng, G. Yong, Y. Jie. [2009]. "Effect of Lightweight Aggregate with Different Moisture on Autogenous Shrinkage and Stress under Partially Restrained Condition". *Ninth International Conference of Chinese Transportation Professionals.*

Suksawang, N., A. Mirmiran, V. H. Surti, D. Yohannes. [2014]. *Use of Fiber Reinforced Concrete for Concrete Pavement Slab Replacement*. Florida Department of Transportation, Final Report.

Sun, X., Zhang, B., Dai, Q., and Yu, X. [2015]. "Investigation of internal curing effects on microstructure and permeability of interface transition zones in cement mortar with SEM imaging, transport simulation and hydration modeling techniques". *Construction and Building Materials*, pp 366–379

TRB. [2006]. *Control of Cracking in Concrete – State of the Art*. Transportation Research Circular, Number E-C107.

Wei, Y. and Hansen, W. [2008]. “Pre-soaked Lightweight Fine Aggregates as Additives for Internal Curing in Concrete”. *Internal Curing of HighPerformance Concretes: Laboratory and Field Experiences*, American Concrete Institute, Farmington Hills, pp. 35-44.

Weiss, W., Borischevsky, B., and Shah, S. [1999]. “The Influence of a Shrinkage Reducing Admixture on the Early-Age Behavior of High Performance Concrete”. *Fifth International Symposium on the Utilization of High Strength/High performance Concrete*, Sandefjord, pp 1418- 1428.

Weiss, W., Yang, W., and Shah, S. [1999]. “Factors Influencing Durability and Early-Age Cracking in High Strength Concrete Structures”. *SP-189-22 High Performance Concrete: Research to Practice*, Farmington Hills: American Concrete Institute, pp 387-409.

Volzone, C. and Zagorodny, N. [2014]. “Mercury Intrusion Porosimetry (MIP) Study of Archaeological Pottery from Hualfin Valley, Catamarca, Argentina”. *Journal of Applied Clay Science*, Vol. 91-92, pp 12-15.

Zou D. amd Weiss J., [2014]. “Early age cracking behavior of internally cured mortar restrained by dual rings with different thickness”. *Construction and Building Materials*, Vol.66, pp146–153.

APPENDIX A
TEST RESULTS FROM LABORATORY TESTING PROGRAM

Table A-1. Compressive Strengths of the Concrete Mixtures Tested

Mix Number	Classification	Compressive Strength (psi)					
		Curing Time (days)					
		1	3	7	28	91	182
#1	II (Bridge Deck) w/c 0.40	3,120	5,360	6,330	8,070	7,860	8,500
#2		2,890	5,030	6,010	7,500	8,320	7,220
#3	II (Bridge Deck) IC w/c 0.40	2,750	4,730	5,550	7,460	6,690	7,560
#4		2,490	4,360	5,310	6,430	7,190	6,040
#5	IV w/c 0.36	4,100	6,010	6,480	8,190	8,320	8,220
#6		4,170	5,960	6,940	8,270	8,730	7,620
#7	IV IC w/c 0.36	3,620	5,580	6,370	7,670	7,560	7,460
#8		3,730	5,380	6,240	7,600	8,110	6,740
#9	V w/c 0.32	4,550	6,900	7,970	9,650	9,010	9,860
#10		4,410	6,170	7,350	8,070	9,290	7,690
#11	V IC w/c 0.32	3,580	5,740	6,920	8,040	7,520	8,850
#12		4,180	6,040	6,890	7,700	8,630	7,290

Table A-2. Flexural Strengths of the Concrete Mixtures Tested

Mix Number	Classification	Flexural Strength (psi)			
		Curing Time (days)			
		7	28	91	182
#1	II (Bridge Deck) w/c 0.40	630	875	875	775
#2		720	792	815	745
#3	II (Bridge Deck) IC w/c 0.40	685	795	790	640
#4		660	772	755	655
#5	IV w/c 0.36	635	892	980	-
#6		730	905	915	895
#7	IV IC w/c 0.36	680	838	895	-
#8		755	820	865	875
#9	V w/c 0.32	800	1,005	1,040	1,015
#10		780	900	995	905
#11	V IC w/c 0.32	735	820	995	945
#12		770	820	895	840

Table A-3. Modulus of Elasticity of the Concrete Mixtures Tested

Mix Number	Classification	Modulus of Elasticity (Mpsi)			
		Curing Time (days)			
		7	28	91	182
#1	II (Bridge Deck) w/c 0.40	4.70	4.75	4.50	4.55
#2		4.65	4.65	4.55	4.50
#3	II (Bridge Deck) IC w/c 0.40	3.80	4.00	3.80	3.75
#4		3.75	3.80	3.80	3.70
#5	IV w/c 0.36	4.65	4.75	4.55	4.35
#6		4.65	4.80	4.75	4.40
#7	IV IC w/c 0.36	3.85	4.00	3.75	3.55
#8		3.80	3.85	3.85	3.75
#9	V w/c 0.32	5.00	5.10	5.00	5.15
#10		4.75	4.70	4.70	4.60
#11	V IC w/c 0.32	3.95	4.00	4.05	4.00
#12		3.85	4.10	4.05	3.80

Table A-4. Splitting Tensile Strengths of the Concrete Mixtures Tested

Mix Number	Classification	Splitting Tensile Strength (psi)			
		Curing Time (days)			
		7	28	91	182
#1	II (Bridge Deck) w/c 0.40	565	630	590	525
#2		590	575	610	565
#3	II (Bridge Deck) IC w/c 0.40	395	575	560	550
#4		450	585	560	500
#5	IV w/c 0.36	620	670	660	565
#6		520	635	570	550
#7	IV IC w/c 0.36	505	620	575	455
#8		420	590	470	500
#9	V w/c 0.32	705	715	555	620
#10		640	620	590	545
#11	V IC w/c 0.32	610	665	595	525
#12		600	595	580	550

Table A-5. Drying Shrinkages of the Concrete Mixtures Tested

Mix Number	Classification	Drying Shrinkage (Ɛ)				
		Curing Time (days)				
		7	28	91	182	364
#1	II (Bridge Deck) w/c 0.40	400E-6	-270E-6	-470E-6	-390E-6	-390E-6
#2		-40E-6	-230E-6	-240E-6	-210E-6	-160E-6
#3	II (Bridge Deck) IC w/c 0.40	-400E-6	-340E-6	-560E-6	-470E-6	-480E-6
#4		-70E-6	-260E-6	-260E-6	-300E-6	-240E-6
#5	IV w/c 0.36	-	-270E-6	-390E-6	-350E-6	-270E-6
#6		-10E-6	-350E-6	-330E-6	-350E-6	-310E-6
#7	IV IC w/c 0.36	-	-320E-6	-480E-6	-510E-6	-400E-6
#8		-90E-6	-410E-6	-340E-6	-430E-6	-350E-6
#9	V w/c 0.32	-60E-6	-390E-6	-440E-6	-420E-6	-390E-6
#10		-30E-6	-190E-6	-190E-6	-280E-6	-280E-6
#11	V IC w/c 0.32	-120E-6	-480E-6	-560E-6	-520E-6	-500E-6
#12		1E-6	-230E-6	-270E-6	-310E-6	-290E-6

APPENDIX B
TEST RESULTS FROM MIP TEST

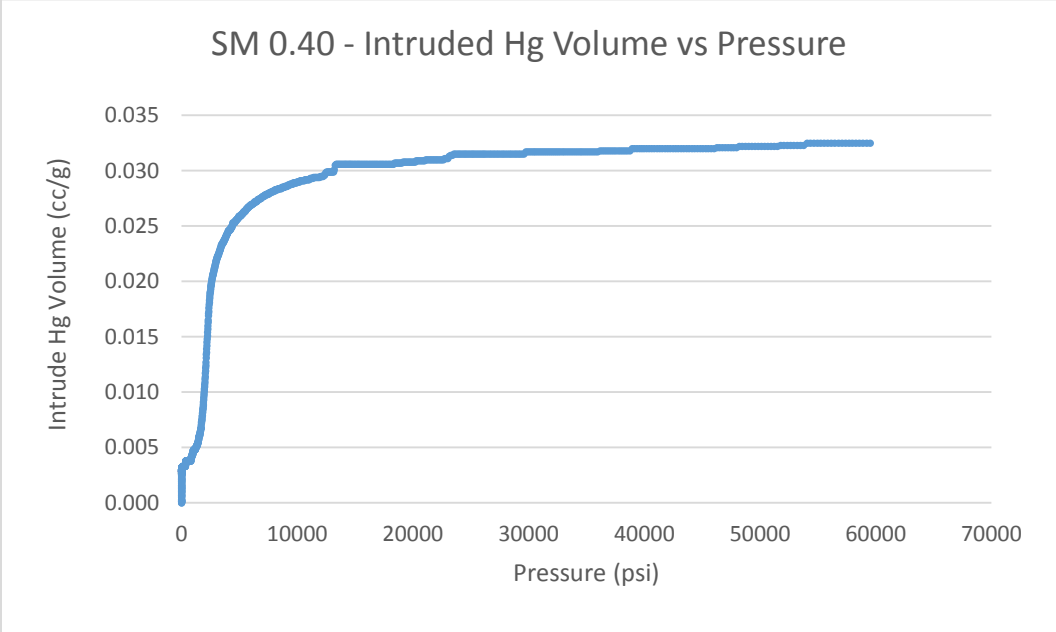

Figure B-1. Intruded Hg volume vs pressure for SM 0.40 mix.

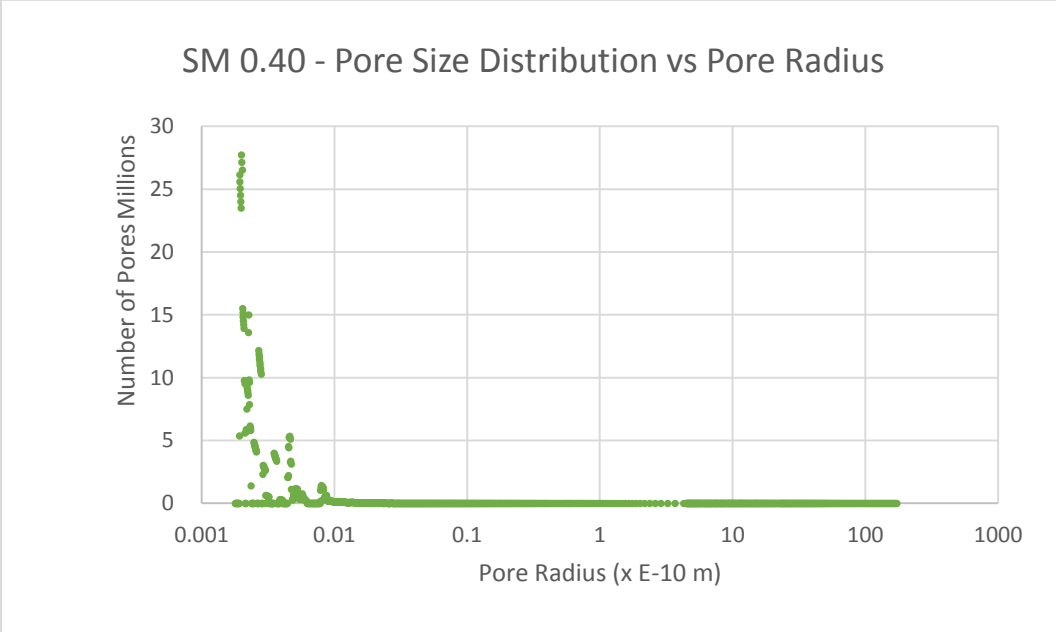

Figure B-2. Pore size distribution vs pore radius for SM 0.40 mix.

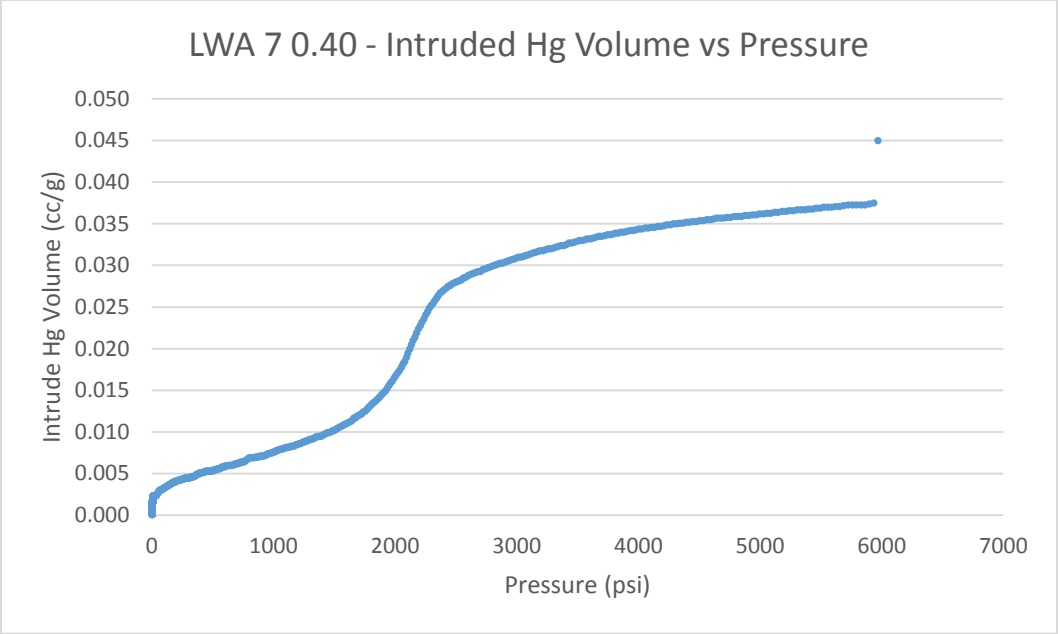

Figure B-3. Intruded Hg volume vs pressure for LWA7 0.40 mix.

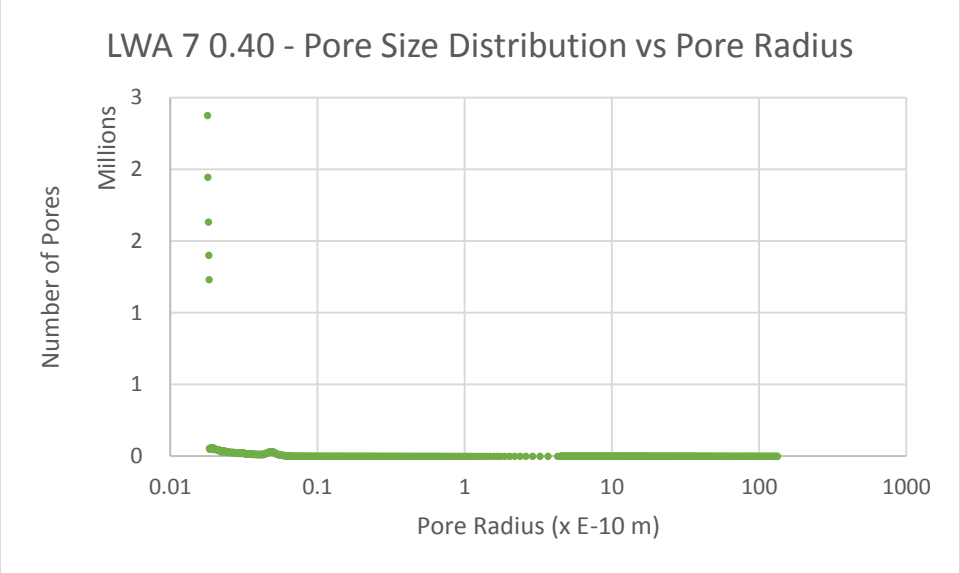

Figure B-4. Pore size distribution vs pore radius for LWA7 0.40 mix.

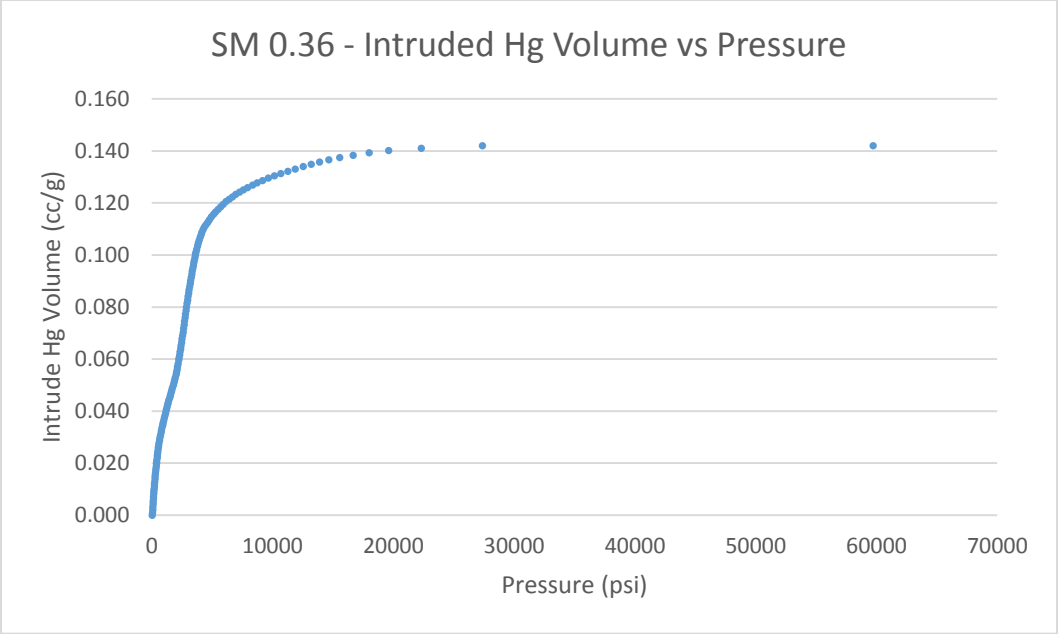

Figure B-5. Intruded Hg volume vs pressure for SM 0.36 mix.

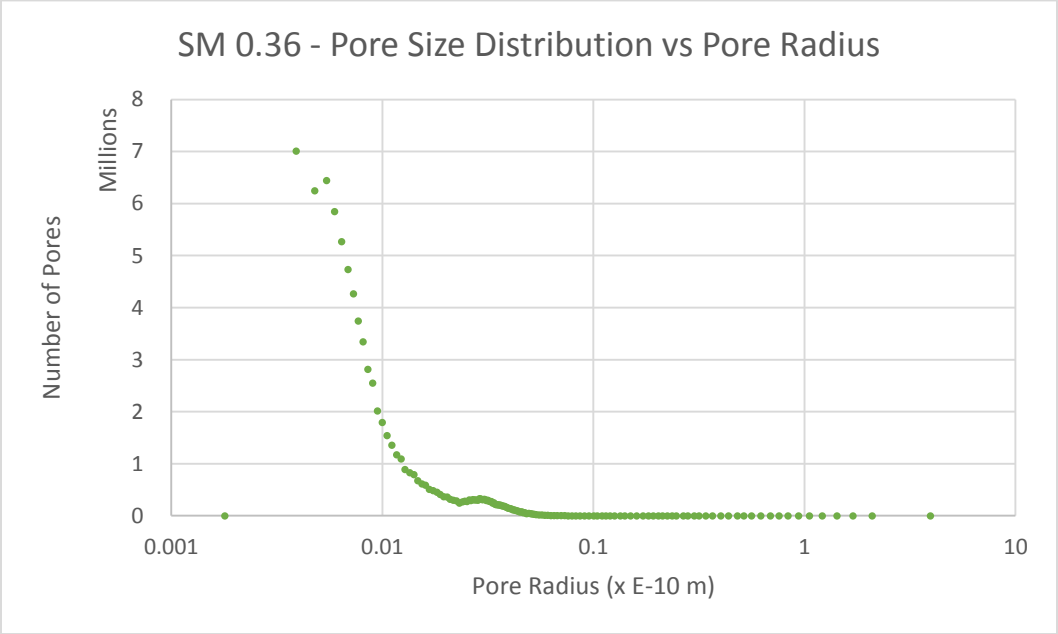

Figure B-6. Pore size distribution vs pore radius for SM 0.36 mix.

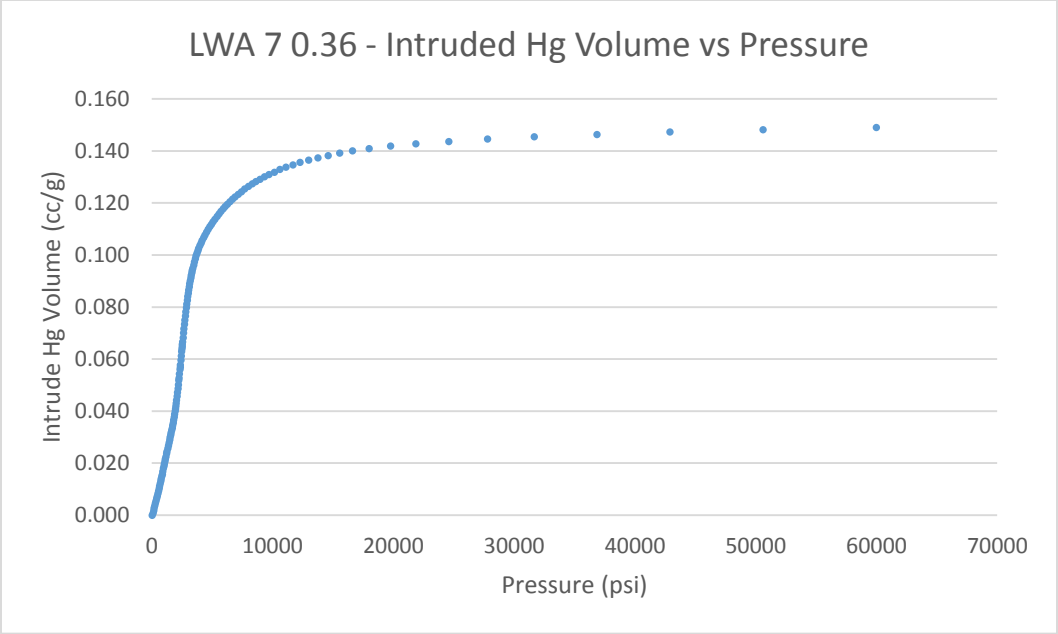

Figure B-7. Intruded Hg volume vs pressure for LWA7 0.36 mix.

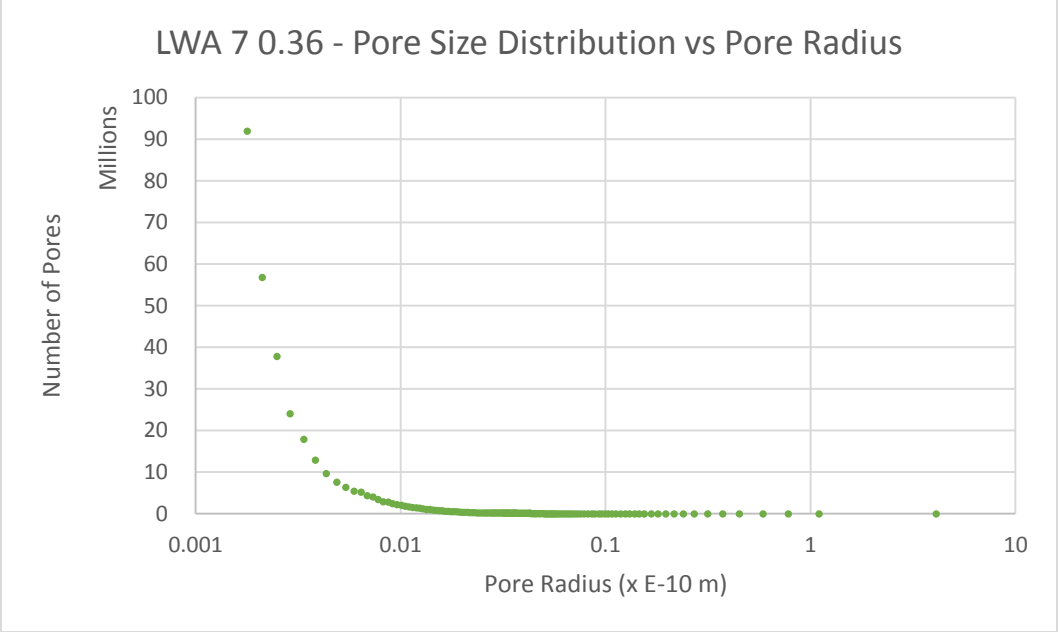

Figure B-8. Pore size distribution vs pore radius for LWA7 0.36 mix.

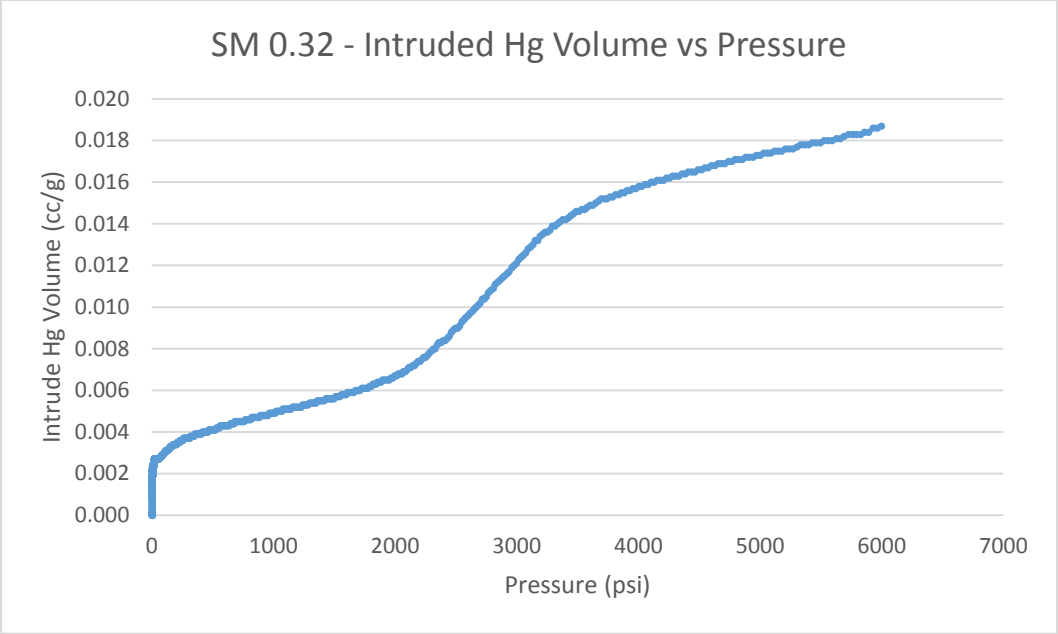

Figure B-9. Intruded Hg volume vs pressure for SM 0.32 mix.

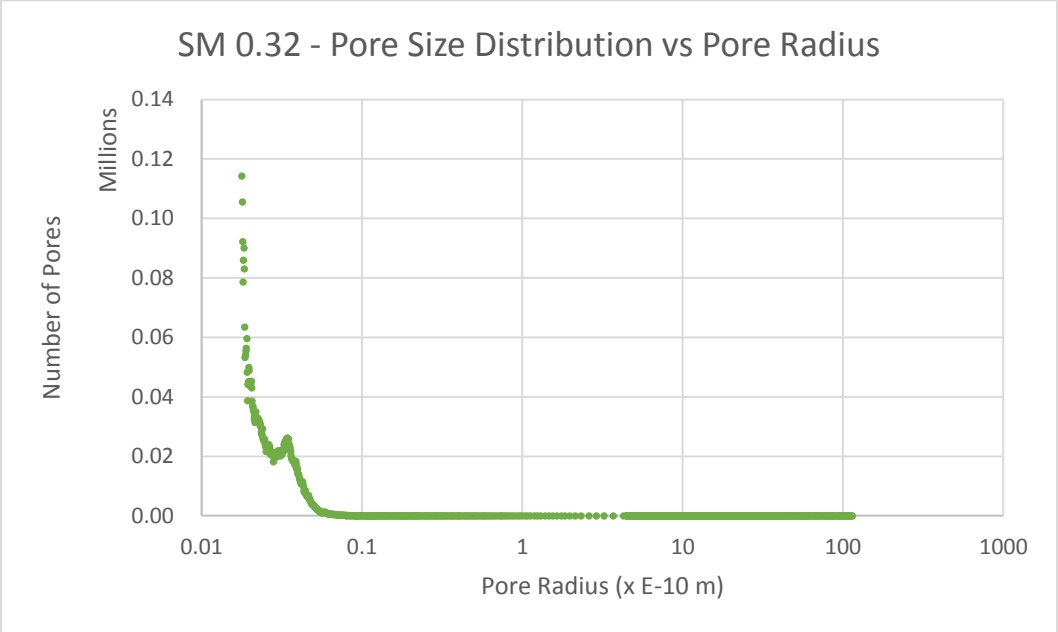

Figure B-10. Pore size distribution vs pore radius for SM 0.32 mix.

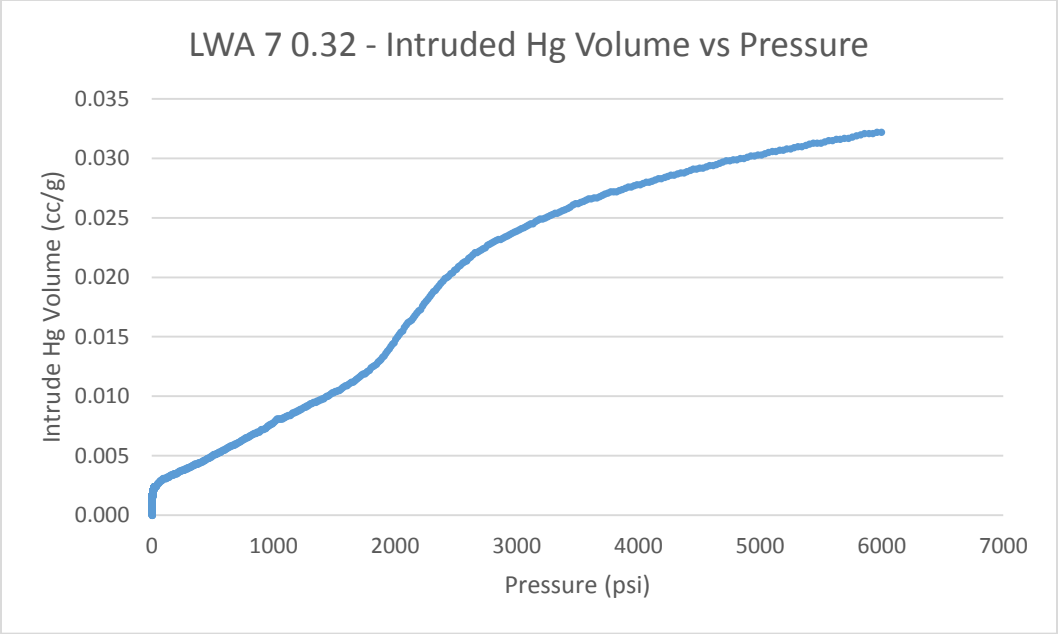

Figure B-11. Intruded Hg volume vs pressure for LWA7 0.32 mix.

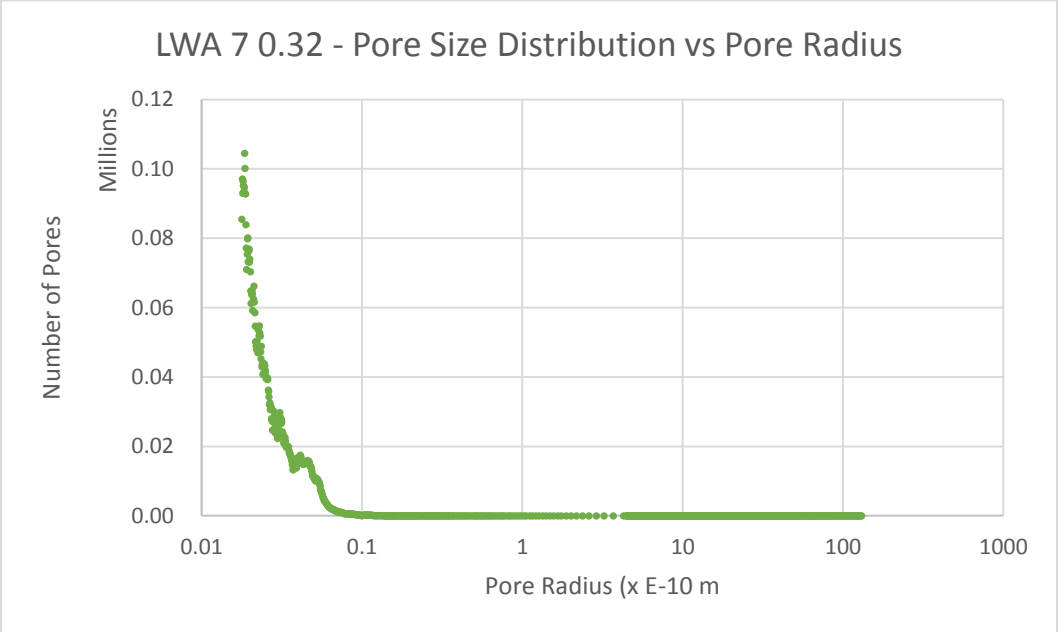

Figure B-12. Pore size distribution vs pore radius for LWA7 0.32 mix.